Atomic Energy Control Board
P.O. Box 1046
Ottawa, Canada
K1P 5S9

Commission de contrôle de l'énergie atomique
C.P. 1046
Ottawa, Canada
K1P 5S9

INFO-0216

IMPACT OF RADIATION ON CONTAINMENT OF RADIOACTIVE WASTE IN DEEP DISPOSAL SITES

by

P.G. Mallory, R.A. Stairs, T.G. Carter
Spectrum Engineering Corp. Ltd.

A research report prepared for the
Atomic Energy Control Board
Ottawa, Canada

August 1986

Canada

Research report

IMPACT OF RADIATION ON CONTAINMENT OF
RADIOACTIVE WASTE IN DEEP DISPOSAL SITES

ABSTRACT

This report describes the current conceptual designs of the waste repository and evaluates the effects of nuclear radiation from the waste on the engineered and natural components in and near the repository based on the information acquired from Canadian and international sources.

RÉSUMÉ

Le présent rapport décrit les différents modèles actuels de conception de dépôt souterrain de déchets et évalue les effets des rayonnements provenant des déchets sur les composants naturels et artificiels dans le dépôt et dans son voisinage, d'après les renseignements obtenus à partir de sources canadiennes et internationales.

DISCLAIMER

The Atomic Energy Control Board is not responsible for the accuracy of the statements made or opinions expressed in this publication and neither the Board nor the authors assume liability with respect to any damage or loss incurred as a result of the use made of the information contained in this publication.

IMPACT OF RADIATION ON CONTAINMENT OF

RADIOACTIVE WASTE IN DEEP DISPOSAL SITES

Table of Contents

		Page
	List of Figures	v
	List of Tables	vii
1.	Introduction	1
2.	Scope	2
3.	Literature Search	4
4.	Repository Design	5
4.1	Design Concept	5
4.2	Used Fuel Disposal Activities	6
5.	Thermal Environment	8
6.	Nuclear Radiation Environment	10
7.	Properties of Engineered Components	12
7.1	Waste Containers	12
7.2	Buffer and Backfill	13
8.	Properties of Rock, Minerals and Groundwater	16
8.1	Rock Material	16
8.1.1	Mode of Origin	16
8.1.2	Composition	18
8.2	Fractures	18
8.2.1	Fracture Systems	18
8.2.2	Fracture Filling	20
8.2.3	Weathering and Hydrothermal Alteration	21
8.3	Rock Mass Condition	23
8.3.1	Thermomechanical Properties	23
8.3.2	Hydrogeological Characteristics	24
8.4	Groundwater	24
9.	Construction Perturbations	27
10.	Effects of Radiation on Solid Materials	29
10.1	Waste Containers	29
10.1.1	Direct Effects	29
10.2.2	Chemical and Electrochemical Corrosion	29
10.2	Radiation Effects on Waste Form	31
10.2.1	Direct Effects	31
10.2.2	Indirect Effects	31
10.3	Mineral Components	33
10.3.1	Buffer	33
10.3.2	Backfill and Host Rock	34

		Page
11.	Radiation and the Groundwater	36
11.1	Transport of Radionuclides by Groundwater	36
11.2	Breached Container Scenario	39
11.3	Radiation Chemical Effects	40
12.	Thermal Effects	43
12.1	Effect on Groundwater	43
12.2	Effect on Groundwater Movement	43
12.3	Effect on Engineered Barrier Materials	44
12.4	Effect on Rock Mass	45
12.5	Thermo-Chemical Effects on Rock Mass Mineralogy	46
13.	Natural Analogues	48
13.1	Key Processes	48
13.1.1	Thermal/Chemical Breakdown of Buffer and Seal	48
13.1.2	Waste Package Corrosion	49
13.1.3	Waste Forms	49
13.1.3.1	Borosilicate Glass Forms	49
13.1.3.2	Spent Fuel	49
13.1.4	Solution and Speciation	50
13.1.5	Mineralogical Fixation at High Temperatures	51
13.1.6	Radiolysis	51
13.1.7	Redox Equilibration	51
13.1.8	Retardation	52
13.1.9	Matrix Diffusion	52
13.2	Natural Analogues - Reassurances and Questions	53
14.	Conclusions	54
14.1	Summary of Findings	54
14.2	Recommendations	58
References		ix
Appendix A	AECB Statement of Work	xvii
Appendix B	Physical Properties of Granitic Rocks	xx
Appendix C	Glossary of Geological Terms	xxvii

List Of Figures

		Page
Figure 4.1	Waste Disposal Vault Emplacement Room Dimensions	5a
Figure 4.2	Container Emplacement and Backfilling	5b
Figure 4.3	Alternate Concepts of Waste Emplacement in the Vaults	5c
Figure 4.4	Components of the Vault Sealing Program	7a
Figure 5.1	Backfill Temperature Rise (UF)	8c
Figure 5.2	Backfill Temperature Rise (FRW)	8d
Figure 5.3	Borehole Heater Tests: Stress and Cracking	8f
Figure 5.4	Temperature History: Effect of Vault Dimensions	9a
Figure 5.5	Temperature Rise in Two-Level UF Vault	9b
Figure 5.6	Contribution of Each Radionuclide to Temperature Rise	9c
Figure 6.1	Radioactivity of Pickering Used Fuel	10d
Figure 6.2	Radioactivity of Fuel Recycle Waste	10e
Figure 6.3	External Dose Equivalent Rate from a Pickering Fuel Bundle	10h
Figure 6.4	Integrated Dose at Container Surface	11a
Figure 6.5	Total Attenuation for UF Container	11b
Figure 6.6	Total Attenuation for FRW Container	11c
Figure 7.1	TEC-II Used Fuel Basket and Packed-Particulate Container	12a
Figure 7.2	Prototype Titanium-Shell Structurally-Supported Container for Used Fuel	12b
Figure 7.3	TEC-IIR Fuel Recycle Waste Canister and Packed Particulate Container	12c
Figure 8.1	Classification of Plutonic Rocks	18a
Figure 8.2	Isotope Data for Strontium and Lead	18d
Figure 8.3	Cooling Diagram, Lac du Bonnet Granite	19a
Figure 8.4	Borehole Log: Coloration and Fractures, Lac du Bonnet Batholith	19b
Figure 8.5	Fracture Zones, Lac du Bonnet Batholith	19c
Figure 8.6	Acoustic Televiewer Log	20a
Figure 8.7	Fracture Filling Materials Age and Temperature of Crystallization	20b
Figure 8.8	Correlation between Filling Type and Width of Fractures, Eye-Dashwa Pluton	21b
Figure 8.9	Geomechanical Properties for Typical Plutonic Rock	24a
Figure 8.10	Fracture Aperture Distribution, Lac du Bonnet Granites	24b
Figure 8.11	Hydrogeological Characteristics for Typical Plutonic Rocks	24d
Figure 10.1	Variation in Accumulated Dose with Distance (Granite)	34a
Figure 10.2	Variation in Accumulated Dose with Distance (Salt)	34b
Figure 11.1	Radionuclide Concentrations in Granite Groundwater in Contact with Irradiated Fuel at 150°C	38a

		Page
Figure 11.2	Concept of a Vault Isolated from Major Fracture Zones Showing Principal Radionuclide Transport Path Mechanisms	38b
Figure 11.3	Radionuclide Transport Modes	40a
Figure 11.4	Flow Distances in Fractures, with and without Matrix Diffusion	40b
Figure 11.5	Redox Front	41a
Figure 12.1	Effect of Temperature on Total Dissolved Ions from Groundwater/Granodiorite Reaction	43a
Figure 12.2	Thermal Conductivity vs. Temperature of Stripa Granite	46b
Figure 12.3	Comparison of Thermal Diffusivities of Four Granodiorites	46c
Figure 12.4	Simulation: Ionic Composition with Time in Flow Through a Fracture	47a

List of Tables

		Page
Table 5.1	Used Fuel Bundle Characteristics	8a
Table 5.2	Radionuclides: Empirical Constants for Heat Generation Equations	8a
Table 5.3	Waste Container Heat Production Rates	8b
Table 5.4	Specified Thermal and Mechanical Constraints for FRW and UF Vaults	8e
Table 6.1	Composition of a Typical Pickering Fuel Bundle	10a
Table 6.2	Initial Inventory of Selected Radionuclides (UF)	10b
Table 6.3	Initial Inventory of Selected Radionuclides (FRW)	10c
Table 6.4	Container Surface Photon Flux and Dose Rate	10f
Table 6.5	Container Surface Neutron Flux and Dose Rate	10g
Table 7.1	Typical Material Properties of Geological Materials Relevant to Buffer and Backfill Use	13a
Table 7.2	Thermal Conductivity of Candidate Buffer/ Backfills	13b
Table 7.3	Some Possible Buffer Materials	13c
Table 7.4	Specifications for Reference Buffer Material	14a
Table 7.5	Specifications for Reference Backfill Materials	14b
Table 8.1	Common Minerals in Granitic Rocks	18b
Table 8.2	Common Minerals in Gabbroic Rocks	18b
Table 8.3	Compositions of Common Plutonic Rocks	18c
Table 8.4	Veins and Heterogeneous Zones from Borehole Core, Eye-Dashwa Pluton	21a
Table 8.5	Alteration of Major Minerals in Granitoids During Weathering	22a
Table 8.6	Alteration of Major Minerals in Gabbroids During Weathering	22b
Table 8.7	Properties of Unaltered and Altered Granite Rock	23a
Table 8.8	Relative Resistance of Igneous Minerals to Weathering	23b
Table 8.9	Material Properties for Intact Plutonic Rocks	23b
Table 8.10	Material Properties of Granitic Gneiss at Room Temperature	23c
Table 8.11	Summary of Hydrogeological Measurements in the URL Boreholes	24c
Table 8.12	Sorption Coefficient of ^{238}U on Four Representative Rock Types	24e
Table 8.13	Sorption of Strontium on Representative Plutonic Rocks as a Function of Groundwater Composition	24e
Table 8.14	Sorption Coefficients for Selected Minerals	24f
Table 8.15	Groundwater Composition from Granite and Gabbro Terrains (Selected Analyses)	25a
Table 8.16	Mean Chemical Composition of Waters Collected on Granitic Massifs and on Basic Rocks	25b
Table 8.17	Representative Brine Chemistries from Sites on the Canadian Shield	25c

		Page
Table 8.18	Concentration of Various Ions in Brine	25d
Table 8.19	Summary of Groundwater Chemistry (Whiteshell)	25e
Table 8.20	Ionic Composition of Synthetic Groundwaters	26a
Table 10.1	Influence of Temperature and Radiation Dose on Rock Mass Properties	33a
Table 11.1	Important Radionuclide Properties	37a
Table 11.2	Potential Aqueous Species of Key Radionuclides in Natural Groundwaters	37b
Table 11.3	Predominant Solution Species of Radioelements	37c
Table 11.4	Some Reactions in the Radiolysis of Water	40c
Table 12.1	Variations of Rock Properties with Temperature	46a
Table 12.2	Comparative Ultimate Strength of High-Silica and Low-Silica Rocks	46a

IMPACT OF RADIATION ON CONTAINMENT OF RADIOACTIVE WASTE IN DEEP DISPOSAL SITES

1. Introduction

The Canadian concept for the disposal of radioactive waste arising from the nuclear power program is deep burial of the waste in plutonic rock in the Canadian Shield.

This report describes the current conceptual design of the waste repository and evaluates the effects of nuclear radiation from the waste on the engineered and natural components in and near the repository.

The study is based on information acquired from Canadian and international sources, through personal communications, direct references and searches of international databases.

The study was done at the request of the Atomic Energy Control Board (AECB #E1103452560) under contract with Supply and Services Canada, D.S.S. File No. 55SS.87055-4-4058.

The Atomic Energy Control Board is not responsible for the accuracy of the statements made or opinions expressed in this publication and neither the Board nor the authors assume liability with respect to damage or loss incurred as a result of the use made of the information contained in this publication.

2. Scope

The scope of work was directed to investigation of the effects of nuclear radiation from irradiated fuel and fuel recycle wastes on the near-field components of the waste repository.

The work was carried out in three phases:

Phase I - Investigation

The investigation phase encompassed the following tasks:

a) Acquire information on the repository design (including engineered components design) proposed for the Canadian Nuclear Fuel Waste Management Program (CNFWMP).

b) Identify materials and relevant component designs being considered for the CNFWMP, which may be affected by radiation.

c) Acquire information on radiation effects on above materials from Canadian libraries and data banks, from Spectrum files and from personal and AECB sources.

d) Identify characteristics of nuclear radiation fields and thermal effects produced by the irradiated fuel in storage, including their decay with time.

e) Acquire information on physical and chemical properties of the common plutonic rocks, vein-filling minerals and groundwater prevalent in the plutonic structures in the Canadian Shield.

f) Acquire information on radiation effects on the plutonic rock and related materials identified in e) above from Canadian and international libraries and data banks. Data on historic naturally occurring nuclear fission sites were sought as part of this task.

Phase II - Evaluation

The evaluation phase generally followed the investigation phase with evaluations of the data obtained as follows:

a) The effects of alpha, beta and gamma radiation on the components and materials identified in Phase I.

b) The effects of the applied radiation and temperature on the plutonic rocks and related materials.

c) The length of time required for significant effects, such as fracturing and dissolution, to take place.

d) The consequences of the alteration of the oxidation potential of the groundwater on the surrounding materials.

Phase III - Report

This document comprises the final report which documents the results of the investigation, Phase I, and the evaluation, Phase II.

The scope of work is defined in detail in Appendix A, "AECB Statement of Work".

3. Literature Search

A comprehensive search and subsequent review of literature relevant to the effects of radiation on near field components being considered for the Canadian Nuclear Fuel Waste Management Program has been carried out, as follows:

(a) Technical Records, reports and publications of Atomic Energy of Canada Limited

(b) In-house technical reference material available within the libraries of Golder Associates, Spectrum Engineering and R&R Laboratories, accumulated in the course of numerous projects on nuclear waste management and radiation effects on materials and components. Access to this extensive reference data base of relevant material greatly broadened the acquisition of published information.

(c) Holdings of the Thomas J. Bata Library of Trent University.

(d) Materials from Canadian and international sources found by extensive computer searches conducted with the assistance of the Canadian Institute for Scientific and Technical Information, and obtained through the Interlibrary Loan service of the Bata Library.

In the last category, the databases GEOREF and INIS, from their earliest entries up to September 1985, have been searched using the keywords, "radiation, effects on: granite, gabbro, feldspar, quartz, plagioclase, orthoclase, clay, bentonite, illite, kaolinite, concrete, aggregate, ilmenite". The search elicited nearly 600 titles, of which about 10 percent were deemed relevant to the present study, and were ordered. Four or five were not available through North American libraries, and have not been seen. A number of the items received were in the form of chapters or articles in symposium or other collected volumes, and a number of other related articles were found in this way.

The many relevant items which have been examined represent work done in Canada, the United States, Sweden, Great Britain, France, Holland, the Federal German Republic, The Soviet Union, Japan and the Republic of Gabon.

4. Repository Design

4.1 Design Concept

The Canadian Nuclear Fuel Waste Management Program has proposed that suitably immobilized nuclear fuel waste be placed deep underground in stable rock within the Canadian Shield (Ref. 1). Plutonic rock masses are favoured as the optimum geological environment for deep disposal of either used fuel (UF - irradiated CANDU fuel) or fuel recycle waste (FRW - vitrified or immobilized waste resulting from the reprocessing of used fuel as well as transuranic contaminated medium-level waste (TRUW) generated at the reprocessing plant).

The current design concept proposes excavation of a vault composed of arrays of rooms, emplacement of the packaged waste in holes drilled in the room floors, backfilling of the holes and then backfilling and sealing the rooms, tunnels and access shafts. At the Fuel Recycle Waste Disposal Centre, two vaults are envisaged. One vault will contain the FRW. A second vault, which is anticipated to be constructed at the same elevation as the FRW vault but spatially separated, is to be provided for disposal of the TRUW.

Design studies are ongoing to develop the reference disposal system for deep burial of wastes arising from the Canadian Candu-PHW reactors up to the year 2035.

It is currently proposed that each UF and FRW disposal vault be located in a Precambrian granite or gabbroic plutonic rock body on a single level at a depth of 1000 m. The layout of each vault, which consists of shafts, access tunnels, haulage ways and waste emplacement rooms, consistent with the concept of an underground container-handling system for both UF and FRW is shown in Figure 4.1 (Ref. 2). Details of container and waste placement concepts which have been considered are shown on Figures 4.2 and 4.3 (Refs. 3 and 4).

It is envisaged that each UF and FRW vault will be square in plan with a maximum room extraction ratio of 25% for overall vault dimensions of 2000 m x 2000 m. Access to the TRUW vault, which will be at the same depth as the FRW vault, will be common to both facilities. The vault will then have the same extraction ratio and be sized according to the amount of waste requiring disposal.

The current disposal concept assumes borehole emplacement of TEC-II containers in the UF vault and TEC-IIR containers in the FRW disposal vault. In-room emplacement of industrial drums is the concept for disposal of the TRUW material. The containers are described in Section 7.

Excavations in the vault and accessways are being sized to accommodate the equipment necessary for borehole drilling, buffer emplacement, buffer borehole augering, waste handling

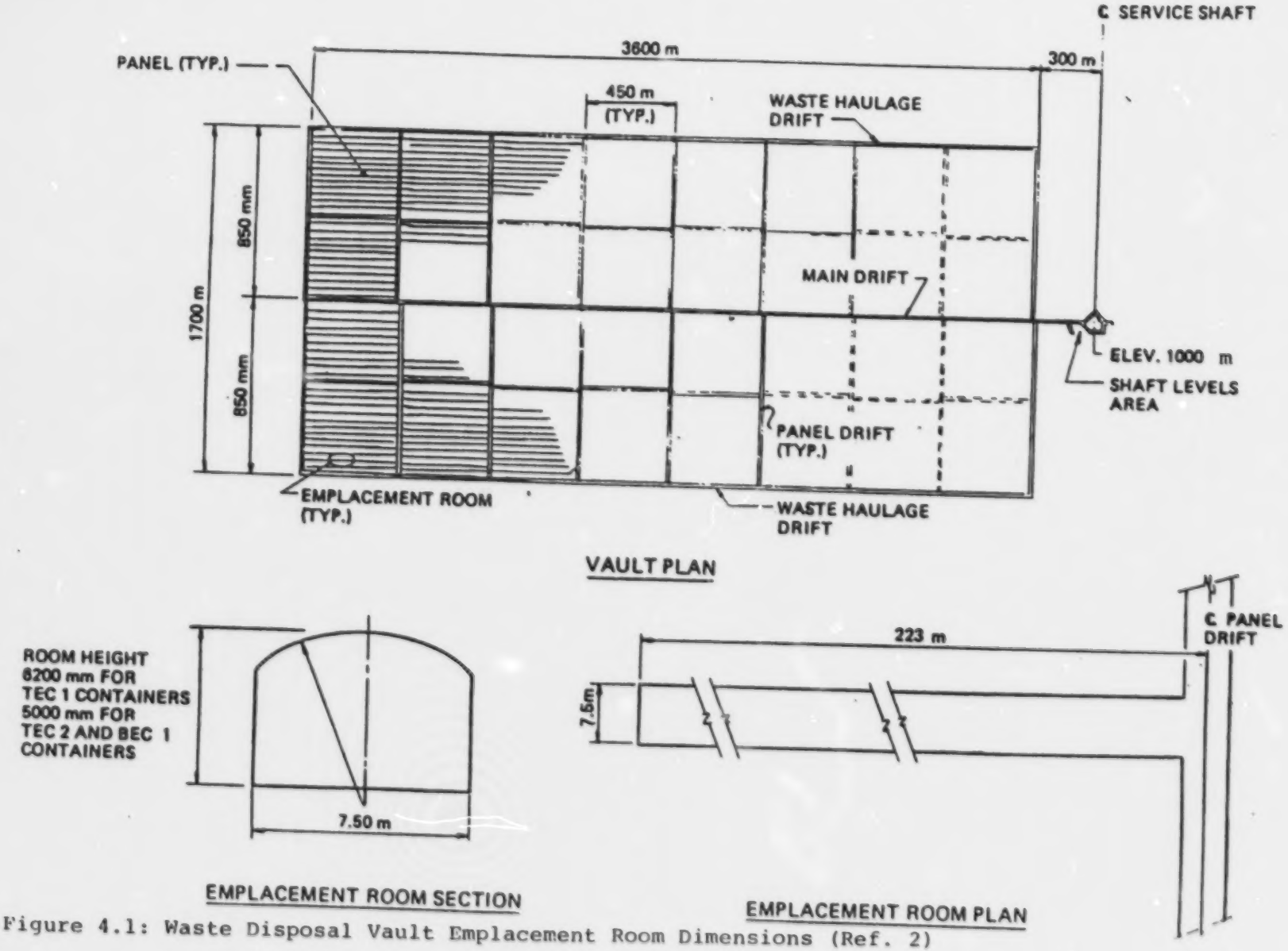

Figure 4.1: Waste Disposal Vault Emplacement Room Dimensions (Ref. 2)

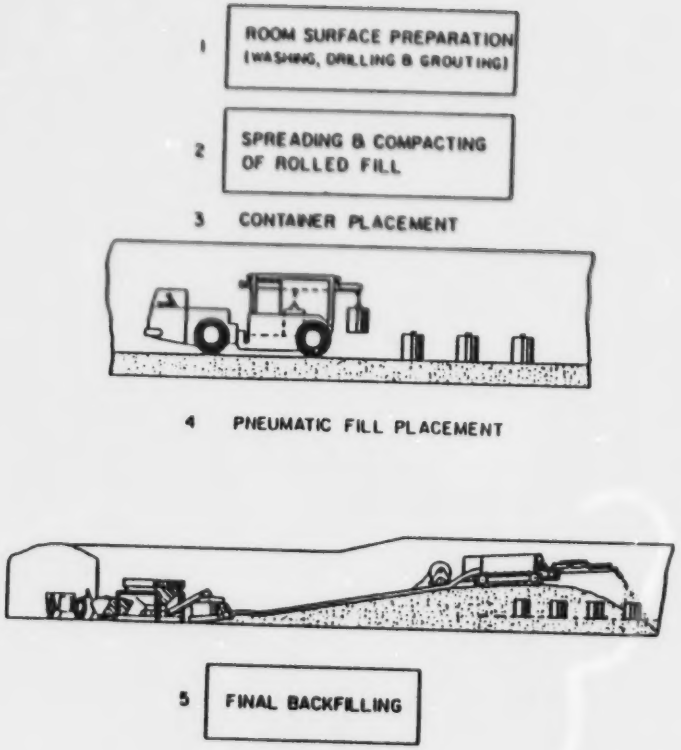
1 ROOM SURFACE PREPARATION (WASHING, DRILLING & GROUTING)
2 SPREADING & COMPACTING OF ROLLED FILL
3 CONTAINER PLACEMENT
4 PNEUMATIC FILL PLACEMENT
5 FINAL BACKFILLING

Figure 4.2(a): TECI Container Emplacement and Backfilling (Ref. 3)

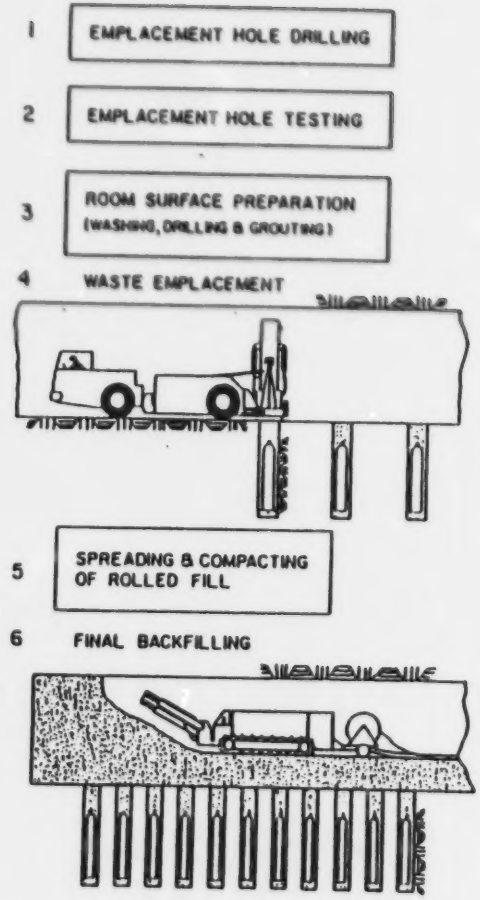
1 EMPLACEMENT HOLE DRILLING
2 EMPLACEMENT HOLE TESTING
3 ROOM SURFACE PREPARATION (WASHING, DRILLING & GROUTING)
4 WASTE EMPLACEMENT
5 SPREADING & COMPACTING OF ROLLED FILL
6 FINAL BACKFILLING

Figure 4.2(b): TECII and TECIIR Container Emplacement and Backfilling (Ref. 3)

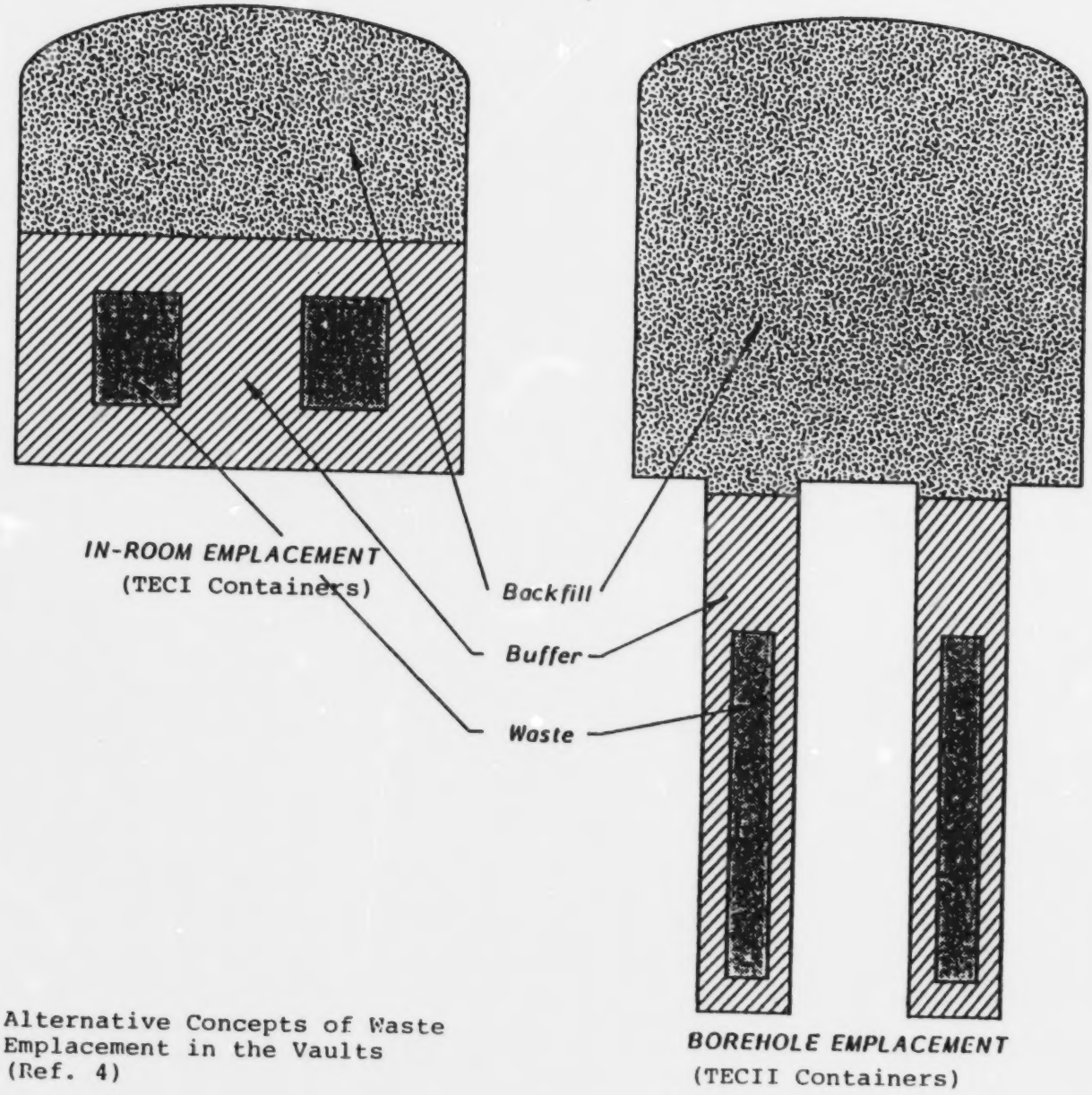

Figure 4.3: Alternative Concepts of Waste Emplacement in the Vaults (Ref. 4)

and emplacement and backfill emplacement. Similarly, the equipment is also being custom designed to be readily transportable along the smaller access tunnels and haulage ways. All construction and development of the vaults will be required to conform with standard accepted mining industry practises under the Mining Act and Regulations of the Province of Ontario (as guidelines).

4.2 Used Fuel Disposal Activities

The current design concept for disposal of the containerized UF waste is as follows:

provide access to 1000 m depth via bored or drill and blast excavated shaft or shafts

develop main access tunnels and haulage ways by drill and blast methods (grades of 0.5% sloped to ensure that all drainage occurs back to main sumps at access shaft)

develop room and pillar layout (also by drill and blast excavation procedures) to suit rate of supply of waste for disposal; grades of 2% sloped to ensure drainage out of rooms to access tunnels

drill out arrays of boreholes in the rooms typically three rows of containers spaced across the room, in 5 m deep holes, 1.2 m diameter

compact buffer material into holes to achieve dry density of 1.67 T/m^3 at 18% moisture content (containerized delivery from surface)

auger out hole in clay buffer of 680 mm dia. and 4200 mm length to receive container

install temporary stainless steel liner into clay buffer material

replace liner with TEC-II container (weight 3 tonnes approximately)

fill 25 mm wide annular gap between container and buffer with well graded or single sized fine sand

fill remaining space above and around container with buffer material and compact to achieve near homogeneity with original material (to achieve 95% AASHO* density as for original placement)

[*AASHO = American Association of State Highway Officials - Modification of the standard Proctor density test for compaction of soils for highway and other uses]

on completion of borehole filling or in sequence with the filling, backfill the rooms. Backfill to be placed in horizontal 150 mm lifts compacted to achieve a near homogeneous mass at a dry density of 2.1 T/m^3 at 6-8% moisture content

with only 1 m left in crown of drifts - ram vertically, compact to 1.75 T/m^3 or better using coal mining type machinery

cast pressure-resistant concrete bulkhead keyed into rock mass at end of each room

sequentially backfill rooms, tunnels and drifts with clay-gravel mix back to main shafts

dispose of all contaminated surface machinery, structures and facilities in controlled manner in drifts and at base of shaft prior to final shaft backfilling

place compacted clay and concrete pressure seals in shafts at geologically controlled locations

grout seals and specific fracture zones

cement seal all surface emplacement boreholes through areas of encountered fractured ground

place clay seals in boreholes (using perforated copper containerized cylinders to place clay)

grout surface seals on shafts and boreholes

The concept for the FRW vault is essentially similar except that only one row of containers would be placed per room. It should be noted that throughout many of these operations, surface water will be introduced into the underground environment. Initially, water will be introduced during drilling for blast holes and subsequently as trapped moisture in the engineered buffer and backfill materials. Bleed water from concreting and grouting will also enter the groundwater system.

In consequence, after the Disposal Centre Vault has been filled to capacity and the remaining access shafts, haulage ways and ancillary excavations have been backfilled and sealed as illustrated on Figure 4.4 (Ref. 5), considerable perturbations will have been introduced into the natural rock environment. However, on completion, the surface facilities will be returned to as natural a state as possible prior to site release.

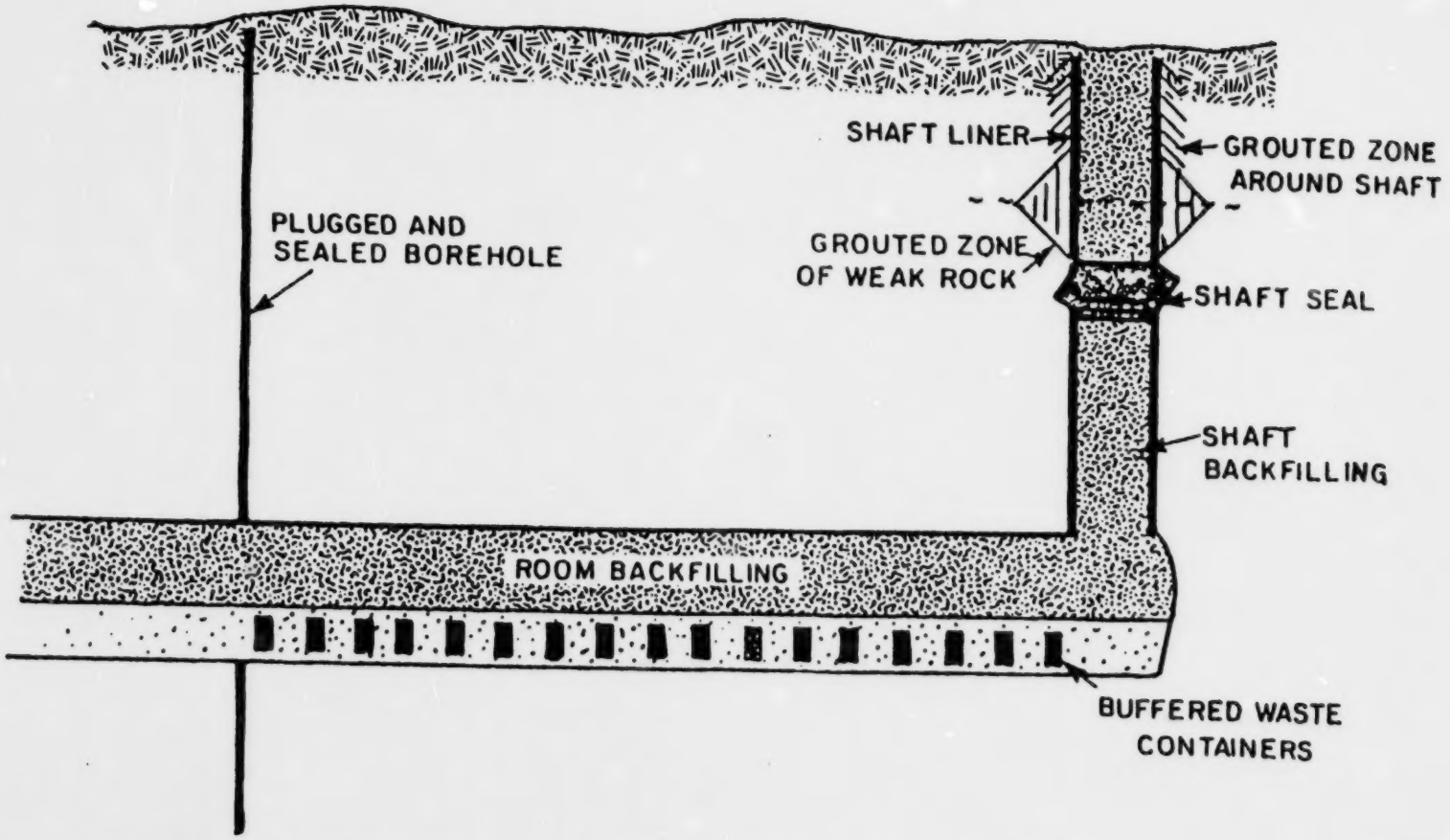

Figure 4.4: Components of the Vault Sealing Program (not to scale)
(Ref. 5)

5. Thermal Environment

Heat will be generated by the various waste forms dependent on the rate of fission product and actinide radioactive decay. This heat will be superimposed on the natural geothermal gradient existing within the plutonic body selected for vault location. The typical geothermal gradient assumed for vault concept assessment is 12°C/1000 m with the earth's surface temperature at 5°C (Ref. 1).

Each TEC-II container of UF waste on disposal will contain 72 CANDU used fuel bundles at a reference heat output of 4.13W per bundle. The thermal characteristics for each bundle are presented on Table 5.1 based on the decay of the fission products and actinides listed on Table 5.2 (Ref. 1).

For the two types of reference container, it is anticipated that heat output per container (at the container) will follow the decay characteristics given on Table 5.3 (Ref. 1). This gives an initial reference heat generation per container for UF containers of 300W and for FRW containers of 950W. The maximum design temperature on the container surface and also in the backfill is 100°C (Ref. 1). Backfill temperature analysis based on heat outputs of 269W per container and earlier container and placement concepts for UF and FRW containers show that for the UF containers the peak backfill temperature is reached 70 years after emplacement and is sustained for 10,000 years as shown in Figure 5.1 (Ref. 6). For the FRW containers the peak backfill temperature is reached 70 years after emplacement. For the case studied, the peak temperature rise was 100°C, dropping to 30°C after 1,000 years as shown in Figure 5.2 (Ref. 6).

Table 5.4 (Ref. 3) presents the thermal and mechanical constraints that have been considered in the conceptual vault planning design work.

Experimental and analytical studies of both near-field and far-field thermal effects have been conducted as part of the US, Canadian and Swedish Programs. Data on thermal stresses and rock mass behaviour under thermal loadings have been gained both experimentally and analytically. Figure 5.3 from the Stripa work in Sweden (Ref. 7) illustrates the extent of spalling and rock damage adjacent to a borehole that can be caused by thermal distress due to 3.5 kw and 5 kw heaters placed in open boreholes in granite.

The temperature fields at the container surface for these experiments, although considerably higher (up to 455°C) than temperatures in the Canadian concept (100°C), illustrate graphically the local borehole wall damage that can be induced by high temperatures.

Similar crack development resulting in fragmentation of the borehole wall and a 25% increase in hole diameter was recorded

Table 5.1: Used Fuel Bundle Characteristics (Ref. 1)

Reference Mass	23.74 kg
Reference Burnup For Thermal Calcs. (avg. Bruce GS)	684 GJ/kgU
For Radiation Calcs. (max. bundle)	1008 GJ/kgU
Reference Cooling Time	10 a
Reference Contact Gamma-ray Flux	35 Gy/hr at 50 cm
Reference Heat Output	4.13 W

Table 5.2: Primary Heat Producting Radionuclides in Used Fuel or Fuel Recycle Waste and Empirical Constants for Heat Generation Equations (Ref. 1)

	i	B_i (W/kgU)	λ_i (a^{-1})
Actinides			
^{240}Pu	1	8.066×10^{-3}	1.06×10^{-4}
^{239}Pu	2	5.189×10^{-3}	2.86×10^{-5}
^{238}Pu	3	2.694×10^{-3}	7.89×10^{-3}
^{241}Pu	4	-2.374×10^{-2}	4.71×10^{-2}
^{241}Am	5	2.479×10^{-2}	1.60×10^{-3}
Fission Products			
$^{90}Sr,Y$ $^{137}Cs,Ba$	6	2.233×10^{-1}	2.34×10^{-2}
$^{125}Sb,Te$ $^{134}Cs,^{147}Pa$	7	2.123×10^{-1}	3.19×10^{-1}
$^{106}Ru,Rh$ $^{144}Ce,Pr$	8	4.099×10^{0}	7.22×10^{-1}
^{154}Eu	9	1.016×10^{-2}	8.44×10^{-2}

Note: With the exception of ^{241}Am, the rate of heat production in nuclear fuel waste from the listed radionuclides or radionuclide chains may be estimated from the following equation:

$$q_i(t) = B_i e^{-\lambda_i t}$$

where $q_i(t)$ = heat output at time t for radionuclide group i (W/kgU)

t = time since t = 0 (a)

B_i = decay heat output constant for radionuclide group i (Wkg/U)

λ_i = radioactive decay constant for radionuclide group i (a^{-1}) = $0.693/t_{1/2}$

$t_{1/2}$ = half-life of radionuclide group i (a)

Table 5.3: Waste Container Heat Production Rates (from Ref. 1)

Years after Emplacement	UF Age = 10a (W/Container)	FRW Age = 20a @ 6.0% FPO (W/Container)
0	297.3	950.1
1	286.7	928.8
2	278.2	908.3
3	271.1	868.4
4	264.7	869.1
5	259.0	850.3
6	253.6	832.1
7	248.6	814.3
8	243.9	797.0
9	239.3	780.2
10	234.9	763.6
20	197.2	619.7
30	167.3	506.6
40	143.2	417.2
50	123.9	346.4
60	108.3	290.2
70	95.7	245.5
80	85.6	209.9
90	77.4	181.4
100	70.8	158.7
125	59.2	119.5
150	52.2	96.5
200	44.9	73.6
500	32.4	40.8
1 000	23.5	18.5
1 500	19.2	8.5
2 000	16.9	4.0
5 000	12.6	0.3
10 000	9.1	0.2
20 000	5.3	0.1
50 000	1.7	0.0
100 000	0.4	0.0

UF = Used Fuel Container

FRW = Fuel Recycle Waste Container

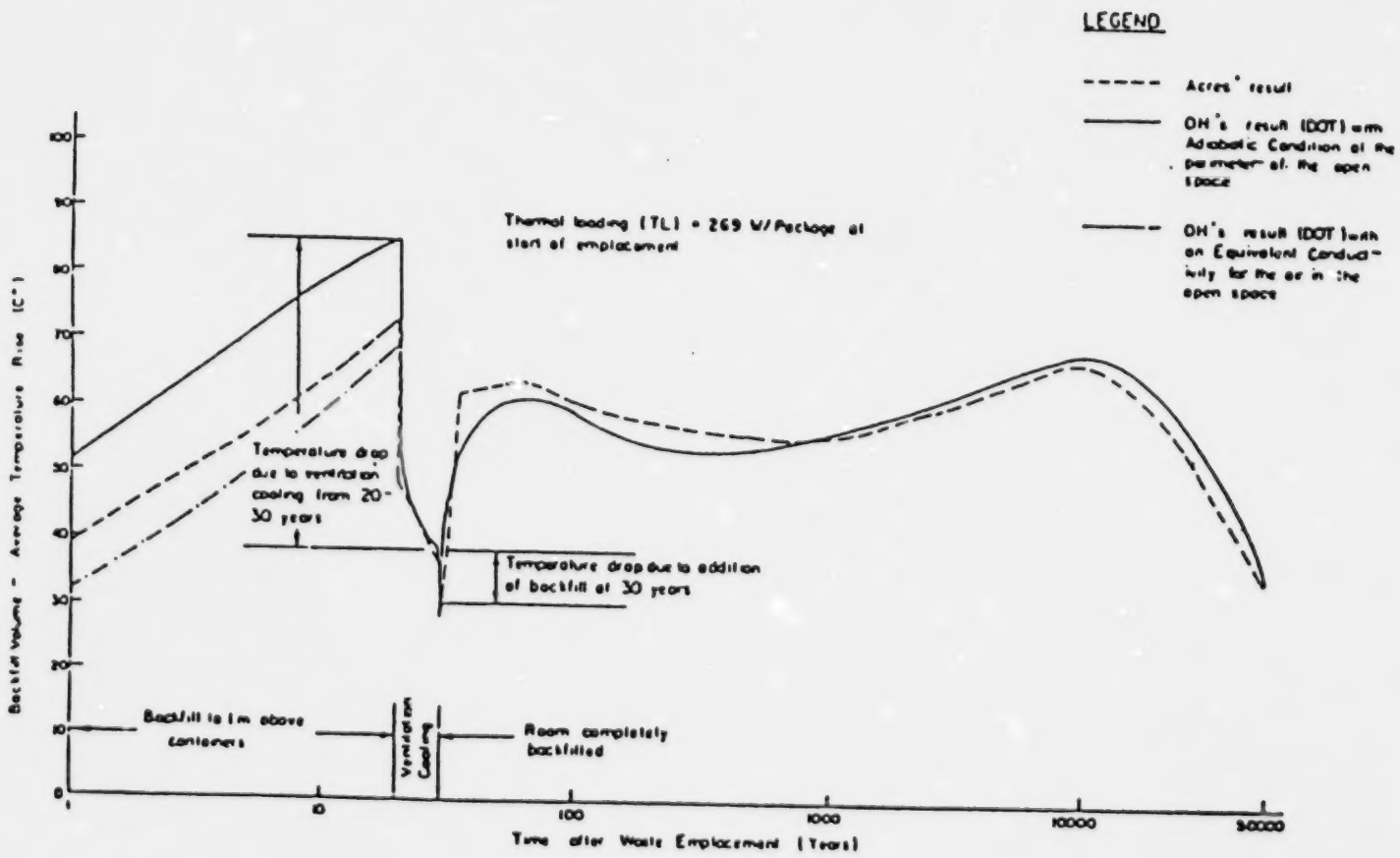
LEGEND
Acres' result
OH's result (DOT) with Adiabatic Condition at the perimeter of the open space
OH's result (DOT) with an Equivalent Conductivity for the air in the open space
Thermal loading (TL) = 269 W/Package at start of emplacement
Temperature drop due to ventilation cooling from 20-30 years
Temperature drop due to addition of backfill at 30 years
Backfill is 1m above containers
Ventilation Cooling
Room completely backfilled
Backfill Volume - Average Temperature Rise (C°)
Time after Waste Emplacement (Years)
1
10
100
1000
10000
50000

Figure 5.1: Backfill Temperature Rise in Granite UF Room as a Function of Time With Ventilation Cooling From 2-30Years After Waste Emplacement (Ref. 6)

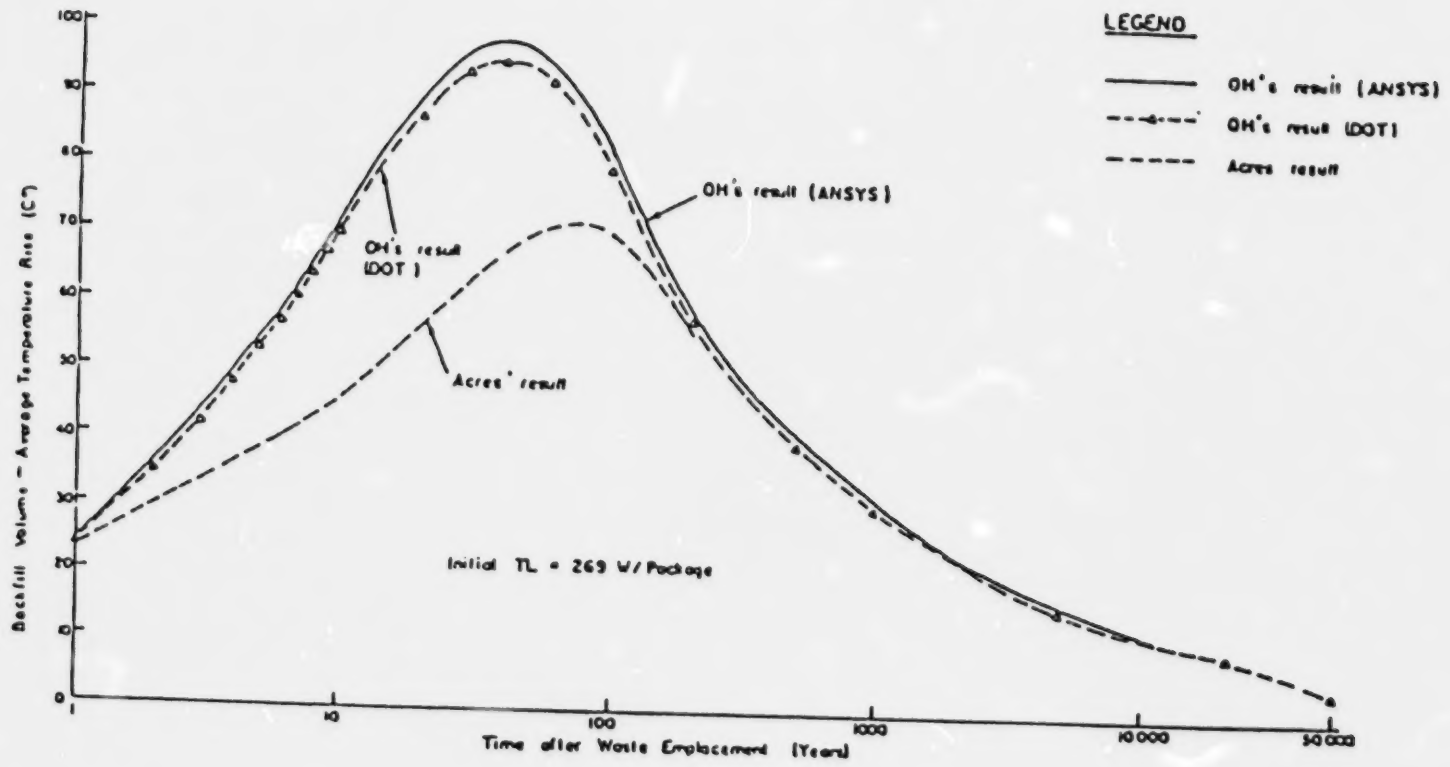

Figure 5.2: Backfill Temperature Rise in Granite FRW Room as a Function of Time (Ref. 6)

Table 5.4: Specified Thermal and Mechanical Constraints for FRW and UF Vaults (modified from Ref. 3)

Geometric Region of Vault	Thermomechanical Constraint	IW(FRW) Vault	IF(UF) Vault
Container near field	Container skin maximum temperature	100°C	100°C
	Container cavity stability	Open and stable hole	Not applicable
	Near-field rock mass stability	Not supported	Not supported
Room and pillar	Buffer/backfill maximum temperature	100°C	100°C
	Roof and rib failure/support	Conventional rock-bolting requirements	Conventional rock-bolting requirements
	Integrated average of strength-stress ratio in pillar	>2	>2
Far-field	*Sustained long-term temperature	Not applicable	75°C to 125°C (60 to 110 K rise)
	*Rock mass stability and deformation	Negligible irreversible deformation and perturbed fissure zone <100 m deep	Negligible irreversible deformation and perturbed fissure zone <100 m deep
	Ground surface movement	Comparable to long-term regional movements	Comparable to long-term regional movements

*The "restrictions" of sustained long-term temperature (75°C, etc.) and depth of perturbed fissure zone (<100 m) were not initially specified as constraints; these restrictions evolved during the course of the investigations for establishing acceptable ranges of thermal loadings

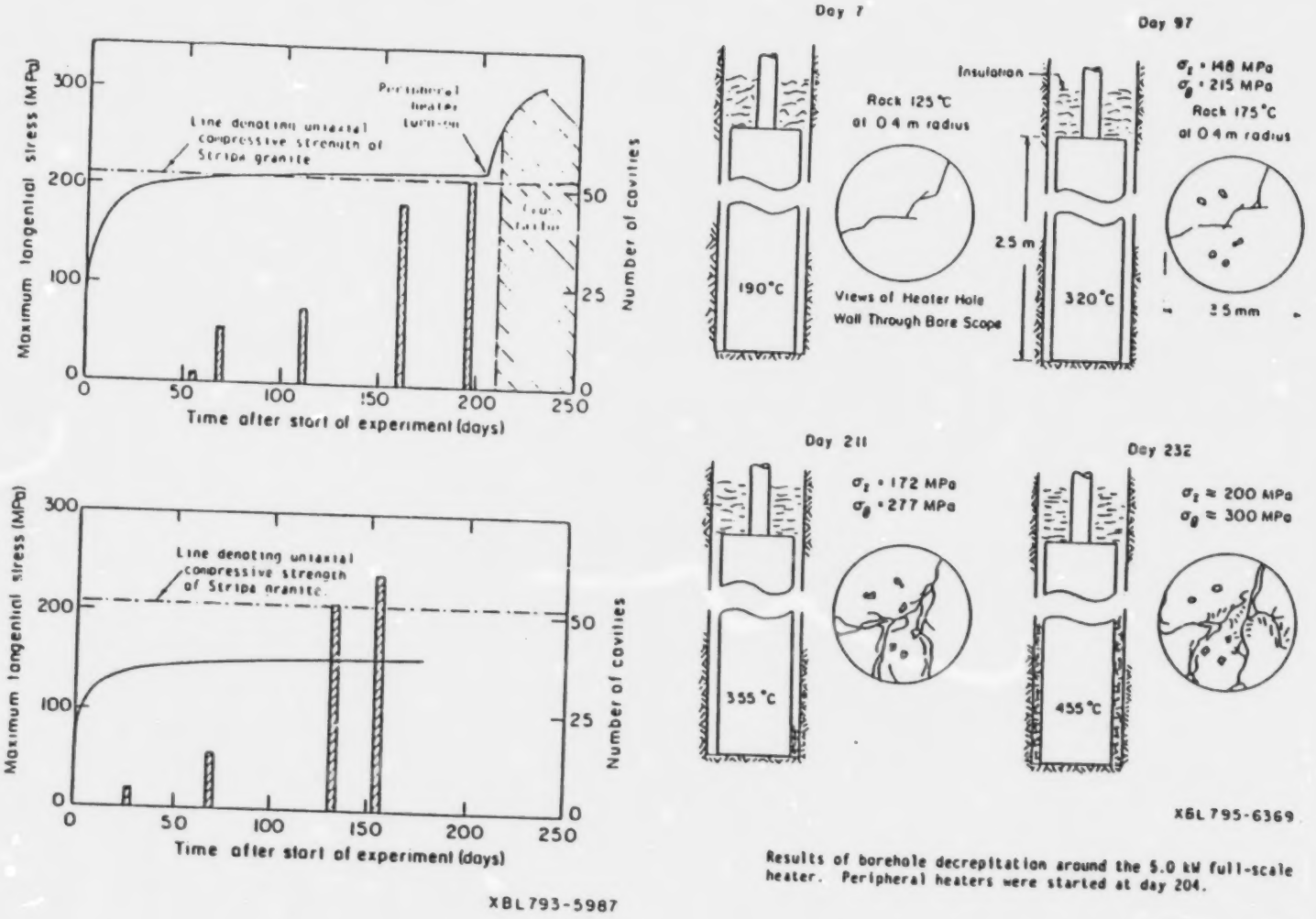

Results of borehole decrepitation around the 5.0 kW full-scale heater. Peripheral heaters were started at day 204.

Figure 5.3: Results of Borehole Heater Tests Showing Crack Patterns and Maximum Induced Compressive Stress at the Walls of Both the 5 kW (Upper Graph) and the 3.6 kW (Lower Graph) Heater Boreholes Plotted as a Function of Time (Ref. 7)
Note: Histograms of the Number of Cavities Induced in the Borehole Wall as a Result of Thermal Spalling are Shown on the Graph
(Data for Stripa Granite)

from smaller scale tests carried out in the UK (Ref. 8). For the Canadian concept, even without the mitigating effect of the buffer material, it appears unlikely that container temperature levels will be sufficiently high to initiate appreciable cracking of the rock mass adjacent to the holes.

Considerable variations in the thermal field created around the vault occur with variations in finite vault size and with single and multiple vault levels at different elevations in the rock mass. The time-dependent temperature changes that can be induced for various vault dimensions are shown on Figure 5.4 (Ref. 9). Figure 5.5 (Ref.6) shows the effects of the interaction of two vault levels. Currently, however, concept assessment design is going ahead for one level only. Thermal rock mechanics analyses are being directed to determine the magnitude of induced thermal stresses around the vault in order to ensure that they do not exceed the yield strength of the rock mass even in the pillars between the various rooms, (i.e. it is a design requirement that no general failure occur of the rock mass). However, some localized, but very minor temperature induced cracking is to be expected.

The temperature curves shown on these diagrams result from the decay history of the various radionuclides responsible for generating the heat within the rock mass. The contribution of each of the various important radionuclides to the time-dependent generation of heat is illustrated on Figure 5.6 (Ref. 9).

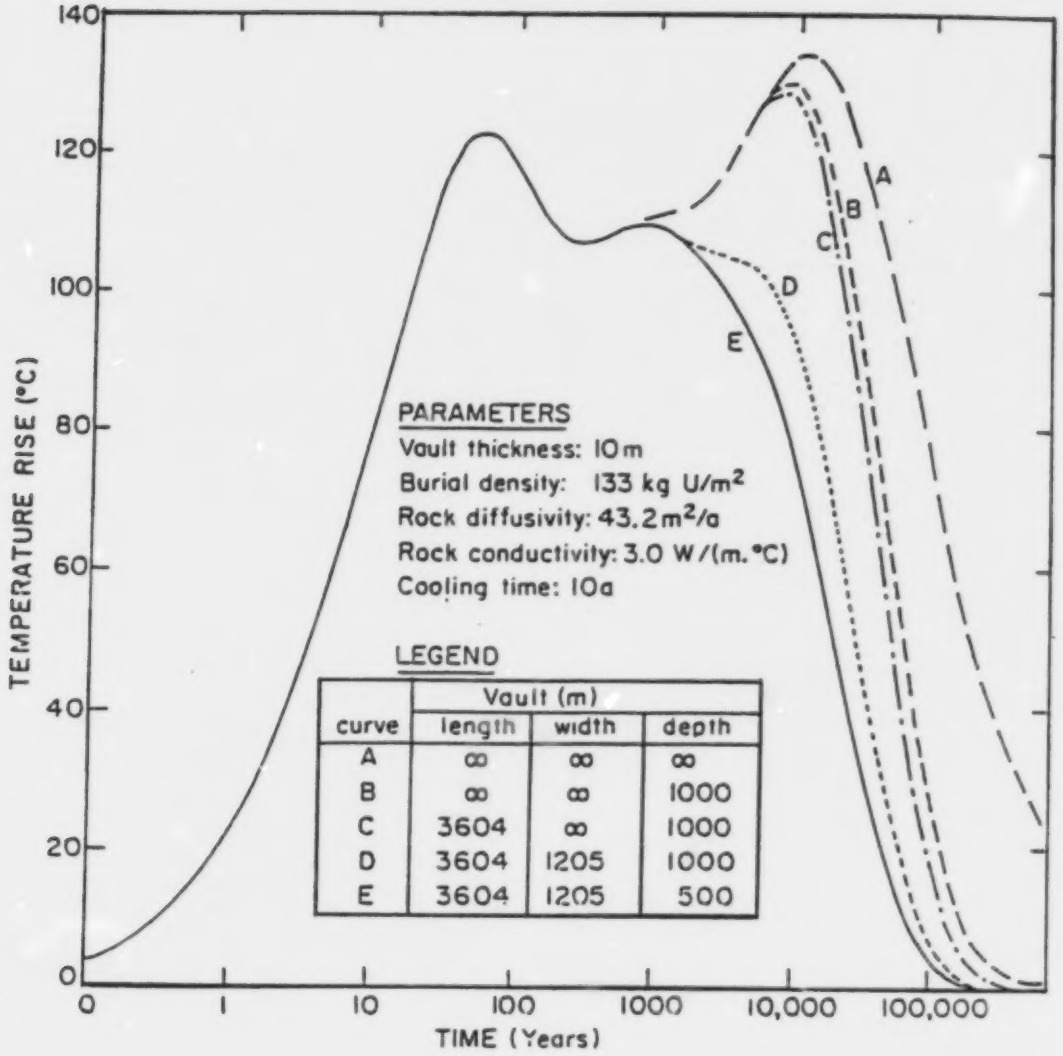

Figure 5.4: The Effect of Finite Vault Dimensions on Long-Term Temperature History (Ref. 9)

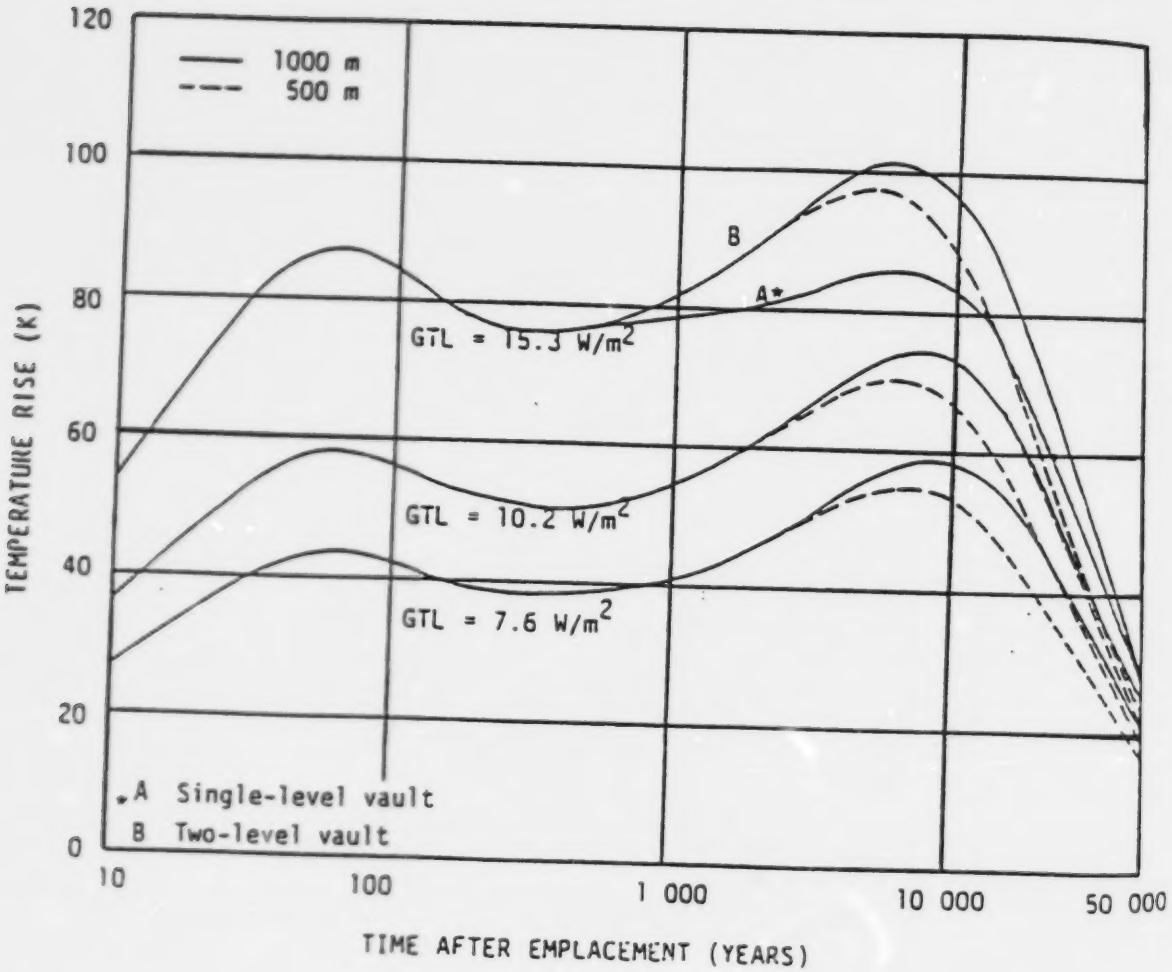

Figure 5.5: Midpoint Temperature Rise in Two-Level UF Vault in Gabbro (Square-Vault Geometry) (Ref. 6)

NOTE: GTL = Gross Thermal Loading

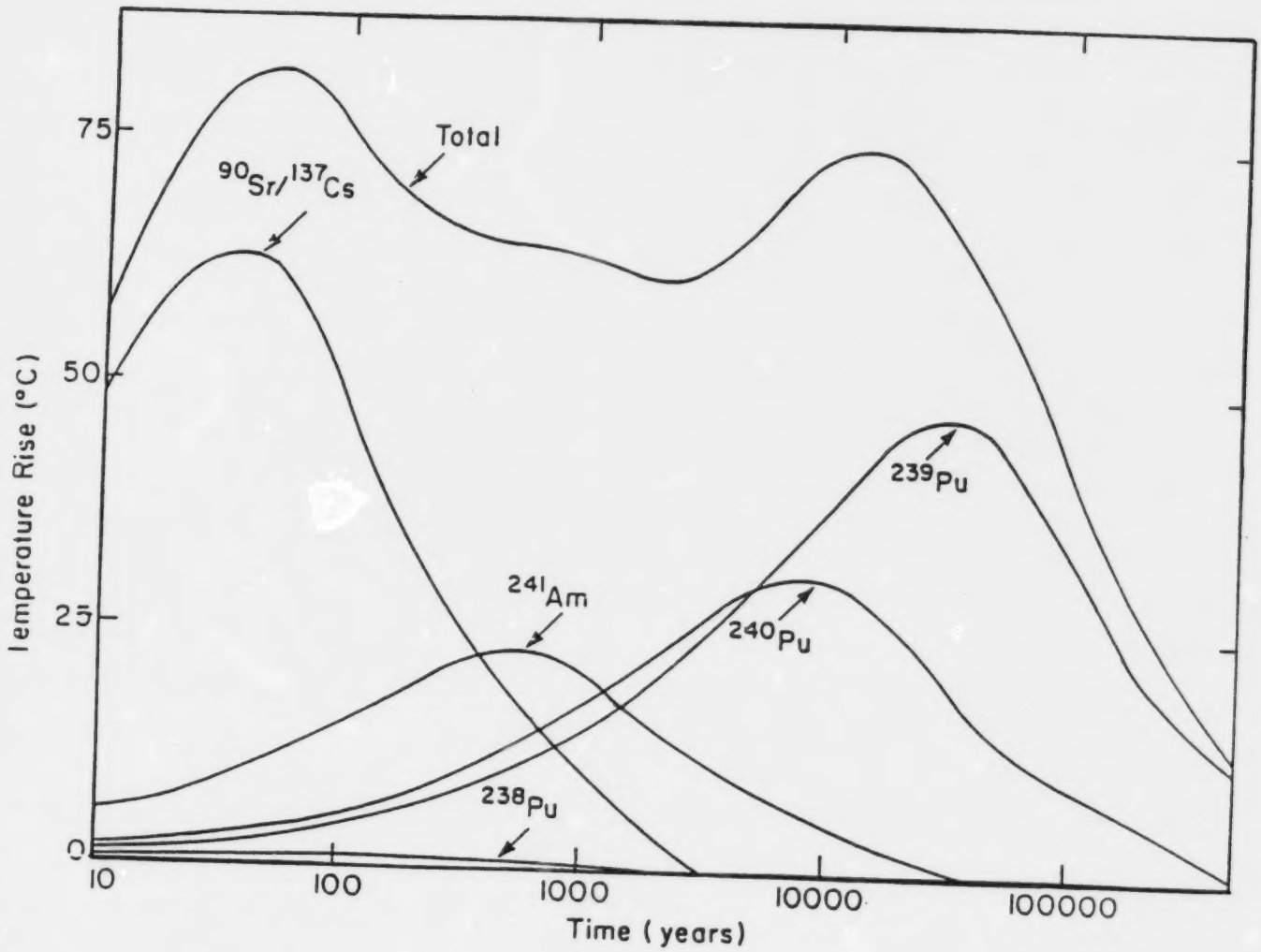

Figure 5.6: Contribution of Each Radionuclide to the Temperature Rise in the Vault as a Function of Time: Candu Fuel (Ref. 9)

6. Nuclear Radiation Environment

For the current concept assessment engineering study of nuclear fuel waste disposal centres (Ref. 1), the estimated inventory of radionuclides in either the used fuel or fuel recycle waste vault at the time of closure is that arising from 191,133 Mg of elemental uranium fed into the reactors. This will lead to 140,256 containers in the UF vault, or 32,976 FRW containers and 316,714 drums of transuranic waste in the FRW vault.

Radiation effects on near field components of the waste repository can arise from two sources: alpha and beta radiation from isotopes in contact with the components, and gamma and neutron radiation emitted from the UF and FRW containers.

Most of the alpha and beta particles emitted by the radioactive isotopes do not penetrate the walls of the UF or FRW containers. However, if a container is breached, the isotopes can be carried in groundwater pathways, irradiating the materials in contact with them.

The radioactive materials in a typical Pickering fuel-bundle are listed in Table 6.1 (Ref. 10 p. 9). The initial inventory of selected radionuclides in the UF and FRW vaults used for the "Second Interim Assessment of the Canadian Concept for Nuclear Fuel Waste Disposal" are given in Tables 6.2 (Ref. 11, p. 25) and 6.3 (Ref. 11, p. 30) respectively. It is noted that the current concept assessment (Ref. 1) study which is the most recent assumes a lower initial inventory than the second interim assessment (Refs. 10 and 11).

The radioactivity decay with time is shown on Figure 6.1 (Ref. 10, p. 10) for a Pickering fuel bundle. This is typical of the decay of the activity in a UF container. When the actinides (Uranium and Plutonium) are removed for the recycling concept the radioactivity decay with time is altered to that shown on Figure 6.2 (Ref. 10, p.14) which is applicable to the FRW container.

Gamma photons and neutrons penetrate the walls of the containers and cause external radiation doses to the surrounding components.

The surface photon flux and dose rate emanating from a UF and a FRW container at time of emplacement, assuming 10 years cooling time, are shown in Table 6.4 (Ref. 1, Table A 5.1a). Similarly the surface neutron flux and dose rate are shown in Table 6.5 (Ref. 1, Table A 5.1b).

As the activity within the containers decays with time, the surface dose rates from photons and neutrons decay as shown on Figure 6.3 (Ref. 10, p.12) for a Pickering fuel bundle in air. The natural radiation background dose equivalent rate of about

Table 6.1: Composition of a Typical Pickering Fuel Bundle (Ref. 10, p. 9)

Constituent	Grams per Kilogram of Initial Uranium	
	Fresh Fuel	Used Fuel*
Naturally Occurring Uranium		
^{238}U	992.9	985.5
^{235}U	7.1	2.3
^{234}U	0.05	0.04
Other Actinides		
^{239}Pu	0.0	2.6
Other Pu isotopes	0.0	1.2
^{236}U	0.0	0.7
Other elements	0.0	0.04
Fission Products		
Stable	0.0	6.5
Active	0.0	1.1
Zircaloy Activation Products	0.0	0.07
Activation Products of Fuel Impurities	0.0	0.0004

*Assuming a burnup of 650 GJ.$(kg(U))^{-1}$ and a cooling time of 0.5 a.

Table 6.2: Initial Inventory of Selected Radionuclides in the Vault for Used Fuel (Ref. 11, p. 25)

Radionuclide	Source	Half-life (a)	Initial Amount*	
			(mol.kg(U)$^{-1}$)	(Bq.kg(U)$^{-1}$)
^{225}Ac	Fuel	2.74×10^{-2}	0.0	0.0
^{227}Ac	Fuel	2.18×10^{1}	0.0	0.0
^{108m}Ag	Fuel	1.30×10^{2}	6.528×10^{-8}	6.640×10^{6}
^{241}Am	Fuel	4.32×10^{2}	7.660×10^{-4}	2.340×10^{10}
^{243}Am	Fuel	7.38×10^{3}	8.449×10^{-6}	1.516×10^{7}
^{210}Bi	Fuel	1.37×10^{-2}	0.0	0.0
^{14}C	Fuel	5.73×10^{3}	1.301×10^{-5}	3.001×10^{7}
^{14}C	Zircaloy	5.73×10^{3}	1.923×10^{-6}	4.437×10^{6}
^{41}Ca	Fuel	1.30×10^{5}	8.804×10^{-7}	8.950×10^{4}
^{135}Cs	Fuel	2.30×10^{6}	2.567×10^{-4}	1.478×10^{6}
^{137}Cs	Fuel	3.02×10^{1}	1.670×10^{-3}	7.337×10^{11}
^{129}I	Fuel	1.59×10^{7}	3.274×10^{-4}	2.725×10^{5}
^{93}Mo	Fuel	3.50×10^{3}	3.659×10^{-9}	1.387×10^{4}
^{94}Mo	Zircaloy	3.50×10^{3}	4.720×10^{-9}	1.779×10^{4}
^{59}Nb	Zircaloy	2.00×10^{4}	3.149×10^{-7}	2.086×10^{5}
^{59}Ni	Fuel	8.00×10^{4}	2.864×10^{-6}	4.740×10^{5}
^{63}Ni	Zircaloy	8.00×10^{4}	6.864×10^{-7}	1.141×10^{5}
^{63}Ni	Fuel	1.00×10^{2}	4.508×10^{-7}	5.970×10^{7}
^{237}Np	Zircaloy	1.00×10^{2}	1.081×10^{-7}	1.428×10^{7}
^{239}Np	Fuel	2.14×10^{6}	1.252×10^{-4}	7.737×10^{5}
^{231}Pa	Fuel	6.43×10^{-3}	0.0	0.0
^{233}Pa	Fuel	3.28×10^{4}	1.488×10^{-10}	6.057×10^{1}
^{205}Pb	Fuel	7.39×10^{-2}	0.0	0.0
^{210}Pb	Zircaloy	1.40×10^{7}	1.185×10^{-9}	1.117×10^{0}
^{107}Pb	Fuel	2.23×10^{1}	0.0	0.0
^{210}Pd	Fuel	6.50×10^{6}	4.993×10^{-4}	1.017×10^{6}
^{239}Po	Fuel	3.79×10^{-1}	0.0	0.0
^{240}Pu	Fuel	2.41×10^{4}	1.154×10^{-2}	6.260×10^{9}
^{242}Pu	Fuel	6.54×10^{5}	4.208×10^{-3}	8.510×10^{9}
^{223}Ra	Fuel	3.76×10^{5}	7.127×10^{-4}	7.271×10^{6}
^{224}Ra	Fuel	3.13×10^{-2}	0.0	0.0
^{225}Ra	Fuel	1.00×10^{-2}	0.0	0.0
^{226}Ra	Fuel	4.05×10^{-2}	0.0	0.0
^{228}Ra	Fuel	1.60×10^{3}	2.879×10^{-13}	2.380×10^{0}
^{222}Rn	Fuel	5.75×10^{0}	1.776×10^{-19}	4.085×10^{-4}
^{79}Se	Fuel	1.05×10^{-2}	0.0	0.0
^{151}Sm	Fuel	6.50×10^{4}	1.509×10^{-5}	3.072×10^{6}
^{121m}Sn	Fuel	9.30×10^{1}	1.579×10^{-5}	2.247×10^{9}
^{121m}Sn	Fuel	5.00×10^{1}	6.302×10^{-9}	1.669×10^{6}
^{126}Sn	Zircaloy	5.00×10^{1}	8.347×10^{-7}	2.211×10^{8}
^{90}Sr	Fuel	1.00×10^{1}	3.666×10^{-5}	4.851×10^{6}
^{157}Tb	Fuel	2.90×10^{1}	1.071×10^{-3}	5.043×10^{11}
^{99}Tc	Fuel	1.50×10^{2}	8.854×10^{-11}	7.770×10^{3}
^{99}Tc	Fuel	2.13×10^{5}	1.970×10^{-3}	1.224×10^{8}
^{227}Th	Zircaloy	2.13×10^{5}	1.182×10^{-8}	7.425×10^{2}
^{228}Th	Fuel	5.13×10^{-2}	0.0	0.0
^{229}Th	Fuel	1.91×10^{0}	0.0	0.0
^{230}Th	Fuel	7.34×10^{3}	9.236×10^{-15}	1.665×10^{-2}
^{231}Th	Fuel	7.70×10^{4}	5.817×10^{-9}	9.994×10^{2}
^{232}Th	Fuel	2.91×10^{-3}	0.0	0.0
^{234}Th	Fuel	1.40×10^{10}	9.909×10^{-10}	9.361×10^{-4}
^{233}U	Fuel	6.60×10^{-2}	0.0	0.0
^{234}U	Fuel	1.59×10^{5}	4.156×10^{-10}	3.480×10^{1}
^{235}U	Fuel	2.44×10^{5}	2.014×10^{-4}	1.091×10^{7}
^{236}U	Fuel	7.04×10^{8}	9.413×10^{-3}	1.769×10^{5}
^{238}U	Fuel	2.34×10^{7}	3.142×10^{-3}	1.775×10^{6}
^{93}Zr	Fuel	4.47×10^{9}	4.140×10^{0}	1.225×10^{7}
^{93}Zr	Fuel	1.50×10^{6}	1.734×10^{-3}	1.530×10^{5}
	Zircaloy	1.50×10^{6}	7.430×10^{-5}	6.550×10^{5}

* Derived from values given by Mehta (1982) for 10-year cooled fuel with a burnup of 650 GJ/kg(U) in a CANDU Pickering reactor.

Table 6.3: Initial Inventory of Selected Radionuclides in the Vault for Fuel Recycle Waste (Ref. 11, p. 30)

Radionuclide	Source	Half-life (a)	Initial Amount	
			(mol.kg(U)$^{-1}$)	(Bq.kg(U)$^{-1}$)
^{225}Ac	Glass	2.74×10^{-2}	0.0	0.0
^{227}Ac	Glass	2.18×10^{1}	0.0	0.0
^{108m}Ag	Glass	1.30×10^{2}	6.528×10^{-8}	6.640×10^{6}
^{241}Am	Glass	4.32×10^{2}	2.904×10^{-4}	8.870×10^{9}
^{243}Am	Glass	7.38×10^{3}	8.449×10^{-6}	1.516×10^{7}
^{210}Bi	Glass	1.37×10^{-2}	0.0	0.0
^{14}C	Barium Carbonate	5.73×10^{3}	1.493×10^{-5}	3.446×10^{7}
^{41}Ca	Glass	1.30×10^{5}	8.804×10^{-7}	8.950×10^{4}
^{135}Cs	Glass	2.30×10^{6}	2.567×10^{-4}	1.478×10^{6}
^{137}Cs	Glass	3.02×10^{1}	1.670×10^{-3}	7.337×10^{11}
^{129}I	Iodine Waste Form	1.59×10^{7}	3.274×10^{-4}	2.725×10^{5}
^{93}Mo	Glass	3.50×10^{3}	3.659×10^{-9}	1.387×10^{4}
^{93}Mo	Zircaloy	3.50×10^{3}	4.720×10^{-9}	1.779×10^{4}
^{94}Nb	Zircaloy	2.00×10^{4}	3.149×10^{-7}	2.086×10^{5}
^{59}Ni	Glass	8.00×10^{4}	2.864×10^{-6}	4.740×10^{5}
^{59}Ni	Zircaloy	8.00×10^{4}	6.864×10^{-7}	1.141×10^{5}
^{63}Ni	Glass	1.00×10^{2}	4.508×10^{-7}	5.970×10^{7}
^{63}Ni	Zircaloy	1.00×10^{2}	1.081×10^{-7}	1.428×10^{7}
^{237}Np	Glass	2.14×10^{6}	1.252×10^{-4}	7.737×10^{5}
^{239}Np	Glass	6.43×10^{-3}	0.0	0.0
^{231}Pa	Glass	3.28×10^{4}	1.488×10^{-10}	6.057×10^{1}
^{233}Pa	Glass	7.39×10^{-2}	0.0	0.0
^{205}Pb	Zircaloy	1.40×10^{7}	1.185×10^{-9}	1.117×10^{0}
^{210}Pb	Glass	2.23×10^{1}	0.0	0.0
^{107}Pd	Glass	6.50×10^{6}	4.993×10^{-4}	1.017×10^{6}
^{210}Po	Glass	3.79×10^{-1}	0.0	0.0
^{239}Pu	Glass	2.41×10^{4}	5.770×10^{-5}	3.130×10^{7}
^{240}Pu	Glass	6.54×10^{3}	2.104×10^{-5}	4.255×10^{7}
^{242}Pu	Glass	3.76×10^{5}	1.064×10^{-6}	3.637×10^{4}
^{223}Ra	Glass	3.13×10^{-2}	0.0	0.0
^{224}Ra	Glass	1.00×10^{-2}	0.0	0.0
^{225}Ra	Glass	4.05×10^{-2}	0.0	0.0
^{226}Ra	Glass	1.60×10^{3}	2.879×10^{-13}	2.380×10^{0}
^{228}Ra	Glass	5.75×10^{0}	1.776×10^{-19}	4.085×10^{-4}
^{222}Rn	Glass	1.05×10^{-2}	0.0	0.0
^{79}Se	Glass	6.50×10^{4}	1.509×10^{-5}	3.072×10^{6}
^{151}Sm	Glass	9.30×10^{1}	1.579×10^{-5}	2.247×10^{9}
^{121m}Sn	Glass	5.00×10^{1}	6.302×10^{-9}	1.669×10^{6}
^{121m}Sn	Zircaloy	5.00×10^{1}	8.347×10^{-7}	2.211×10^{8}
^{126}Sn	Glass	1.00×10^{5}	3.666×10^{-5}	4.851×10^{6}
^{90}Sr	Glass	2.90×10^{1}	1.071×10^{-3}	5.043×10^{11}
^{157}Tb	Glass	1.50×10^{2}	8.854×10^{-11}	7.770×10^{3}
^{99}Tc	Glass	2.13×10^{5}	1.970×10^{-3}	1.224×10^{8}
^{99}Tc	Zircaloy	2.13×10^{5}	1.182×10^{-8}	7.425×10^{2}
^{227}Th	Glass	5.13×10^{-2}	0.0	0.0
^{228}Th	Glass	1.91×10^{0}	0.0	0.0
^{229}Th	Glass	7.34×10^{3}	9.236×10^{-15}	1.665×10^{-2}
^{230}Th	Glass	7.70×10^{4}	5.817×10^{-9}	9.994×10^{2}
^{231}Th	Glass	2.91×10^{-3}	0.0	0.0
^{232}Th	Glass	1.40×10^{10}	9.909×10^{-10}	9.361×10^{-4}
^{234}Th	Glass	6.60×10^{-2}	0.0	0.0
^{233}U	Glass	1.59×10^{5}	6.379×10^{-12}	5.341×10^{-1}
^{234}U	Glass	2.44×10^{5}	1.007×10^{-6}	5.455×10^{4}
^{235}U	Glass	7.04×10^{8}	4.707×10^{-5}	8.845×10^{2}
^{236}U	Glass	2.34×10^{7}	1.571×10^{-5}	8.875×10^{3}
^{238}U	Glass	4.47×10^{9}	2.070×10^{-2}	6.125×10^{4}
^{93}Zr	Glass	1.50×10^{6}	1.734×10^{-3}	1.530×10^{7}
^{93}Zr	Zircaloy	1.50×10^{6}	7.430×10^{-5}	6.550×10^{5}

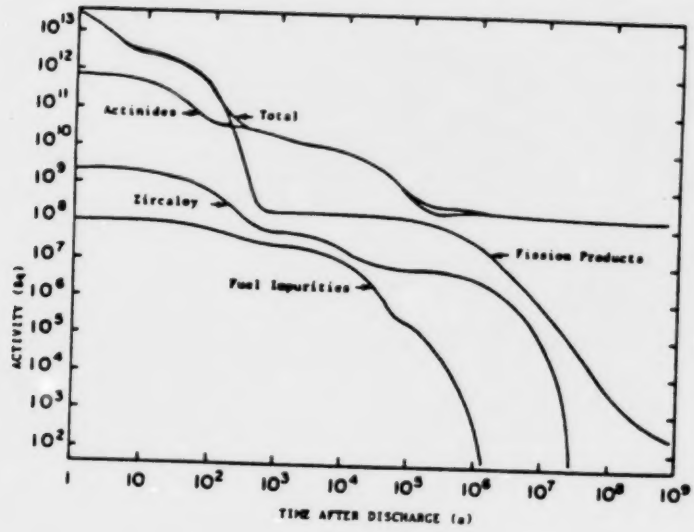

When a fuel bundle is discharged from a reactor, it is intensely radioactive. Two major groups of radionuclides contribute to this radioactivity: the long-lived actinides, which are largely alpha emitters, and the shorter-lived fission products, which are largely beta emitters. Minor contributors are the activation products of Zircaloy (fuel sheath and bundle structural material) and the activation products of the fuel impurities. Radioactivity decreases rapidly during the first few hundred years, when fission products are the major contributors, and decreases more slowly thereafter, when the actinides are the major contributors.

Figure 6.1: Radioactivity of Pickering Used Fuel Per Kilogram of Initial Uranium (Ref. 10, p. 10)

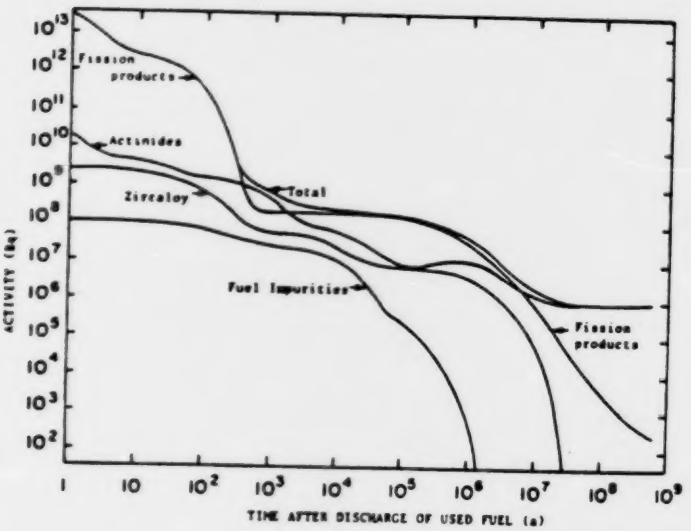

As is the case for used fuel, the activity of fuel recycle waste decreases with time. The four contributors to the total radioactivity are the same as those in used fuel. However, their relative contributions are different (see Figure 4), because there are much lower amounts of actinides (uranium and plutonium) in fuel recycle waste than in used fuel. Therefore, the fission products in fuel recycle waste are the major contributors to radioactivity for the first million years.

Figure 6.2: Radioactivity of Fuel Recycle Waste Per Kilogram of Initial Uranium (Ref. 10, p. 14)

Table 6.4: Container Surface Photon Flux and Dose Rate (Ref. 1, Table A-5.1a)

Energy (MeV)	Used Fuel Container		Fuel Recycle Waste Container	
	Axial ($p/s/cm^2$)	Radial ($p/s/cm^2$)	Axial ($p/s/cm^2$)	Radial ($p/s/cm^2$)
1.40×10^{1}	0.0	0.0	0.0	0.0
5.00×10^{0}	0.0	0.0	0.0	0.0
3.00×10^{0}	4.78×10^{4}	7.41×10^{4}	9.41×10^{1}	2.23×10^{2}
2.00×10^{0}	2.76×10^{5}	6.14×10^{5}	1.14×10^{5}	6.53×10^{5}
1.50×10^{0}	7.41×10^{6}	1.21×10^{7}	4.00×10^{6}	1.91×10^{7}
1.00×10^{0}	5.70×10^{8}	8.12×10^{8}	2.26×10^{9}	4.85×10^{9}
4.00×10^{-1}	2.83×10^{8}	8.01×10^{8}	3.28×10^{9}	7.88×10^{9}
2.00×10^{-1}	2.10×10^{8}	4.14×10^{8}	2.97×10^{9}	5.24×10^{9}
1.00×10^{-1}	4.40×10^{8}	5.34×10^{7}	2.18×10^{5}	1.00×10^{9}
Total Flux	1.51×10^{9}	2.10×10^{9}	3.53×10^{9}	1.90×10^{10}
Total Dose Rate (Sv/hr)	14.7	20.4	69.1	154.

Table 6.5: Container Surface Neutron Flux and Dose Rate (Ref. 1, Table A-5.1b)

Energy (MeV)	Used Fuel Container		Fuel Recycle Waste Container	
	Axial ($n/s/cm^2$)	Radial ($n/s/cm^2$)	Axial ($n/s/cm^2$)	Radial ($n/s/cm^2$)
1.49×10^{1}	3.84×10^{-1}	2.10×10^{-1}	0.0	0.0
6.07×10^{0}	3.30×10^{1}	5.48×10^{1}	3.57×10^{1}	8.57×10^{1}
2.23×10^{0}	7.78×10^{1}	1.13×10^{2}	7.54×10^{1}	1.98×10^{2}
8.21×10^{-1}	9.02×10^{1}	1.47×10^{2}	1.10×10^{2}	2.12×10^{2}
3.02×10^{-1}	1.38×10^{2}	2.10×10^{2}	1.26×10^{2}	2.66×10^{2}
6.74×10^{-2}	3.35×10^{1}	7.93×10^{1}	3.29×10^{1}	1.08×10^{2}
2.48×10^{-2}	3.50×10^{1}	6.64×10^{1}	3.54×10^{1}	9.41×10^{1}
5.53×10^{-3}	1.72×10^{1}	3.58×10^{1}	4.01×10^{1}	7.45×10^{1}
7.49×10^{-4}	3.70×10^{0}	9.66×10^{0}	5.78×10^{0}	1.36×10^{1}
1.01×10^{-4}	3.15×10^{-1}	1.25×10^{0}	1.30×10^{0}	5.68×10^{-1}
2.26×10^{-5}	2.48×10^{-2}	2.03×10^{-1}	0.0	0.0
3.93×10^{-6}	0.0	1.80×10^{-2}	0.0	1.22×10^{-1}
6.83×10^{-7}	0.0	0.0	0.0	0.0
Total Flux	4.30×10^{2}	7.20×10^{2}	4.64×10^{2}	1.05×10^{3}
Total Dose Rate (mSv/hr)	0.21	0.35	0.23	0.51

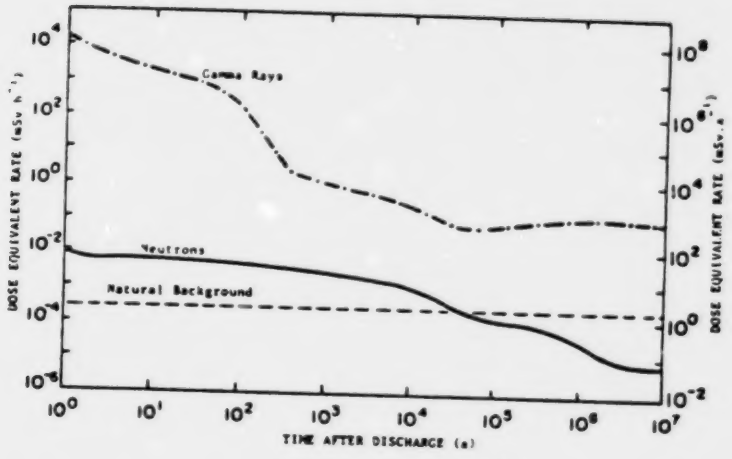

Almost all alpha particles and a large majority of beta particles emitted by used fuel are stopped within the bundle itself. However, gamma radiation and neutrons emerge from fuel bundles and can cause an external radiation dose. As the radioactivity of the bundle decreases, the dose rates also decrease. These rates can be compared with that due to natural background radiation, which is caused by natural sources such as cosmic rays and naturally occurring radionuclides in the earth's crust, in the air, and in the body.

Figure 6.3: External Dose Equivalent Rate from a Pickering Fuel Bundle at a Distance of 36 cm in Air (McKean 1978) (Ref. 10, p. 12)

$1.8 mSv.a^{-1}$ (equivalent to about $2x10^{-4} mSv.h^{-1}$) is shown for comparison.

As the integrated dose at the surface of the UF and FRW containers is needed for radiation effects comparisons and no published information was available, an estimate was made based on the surface photon fluxes given in Table 6.4 and the thermal decay shown on Table 5.3. The resulting integrated doses are shown as a function of time on Figure 6.4. Since the neutron dose rates are approximately two decades lower than the photon dose rates the figure approximates the total doses. Note that these doses arise from a single container of each type. The actual doses will be greater when multiple containers are placed in the vaults and the data are not yet available.

The photon and neutron flux at the surface of the UF and FRW containers are attenuated by the clay buffer and the granite in the repository as shown on Figure 6.5 (Ref. 1, Figure A 5.6) for the UF containers and Figure 6.6 (Ref.1, Figure A 5.8) for the FRW containers. The container surface dose rates are the maximum received by the buffer. They are then attentuated by a factor of 100 by 277 mm of clay for the UF geometry and by a factor of 170 by 312 mm of clay for the FRW geometry to give the maximum dose rates to the granite. Based on Figure 6.5, at approximately 1.5 m from the container centre, the dose rate in the granite from a single container of either type approaches the natural background dose rate (at the surface) noted above. Depending on the amount of naturally occuring radioactivity in the rock surrounding the repository, the natural background dose rate in the storage area may be greater than that at the surface. Beyond the distance at which the rock attenuates the direct radiation to the natural background level, any direct radiation effects will be limited to those occuring naturally. Note that the above data are for a single containber and the dose rates from multiple containers will be required to evaluate the radiation environment.

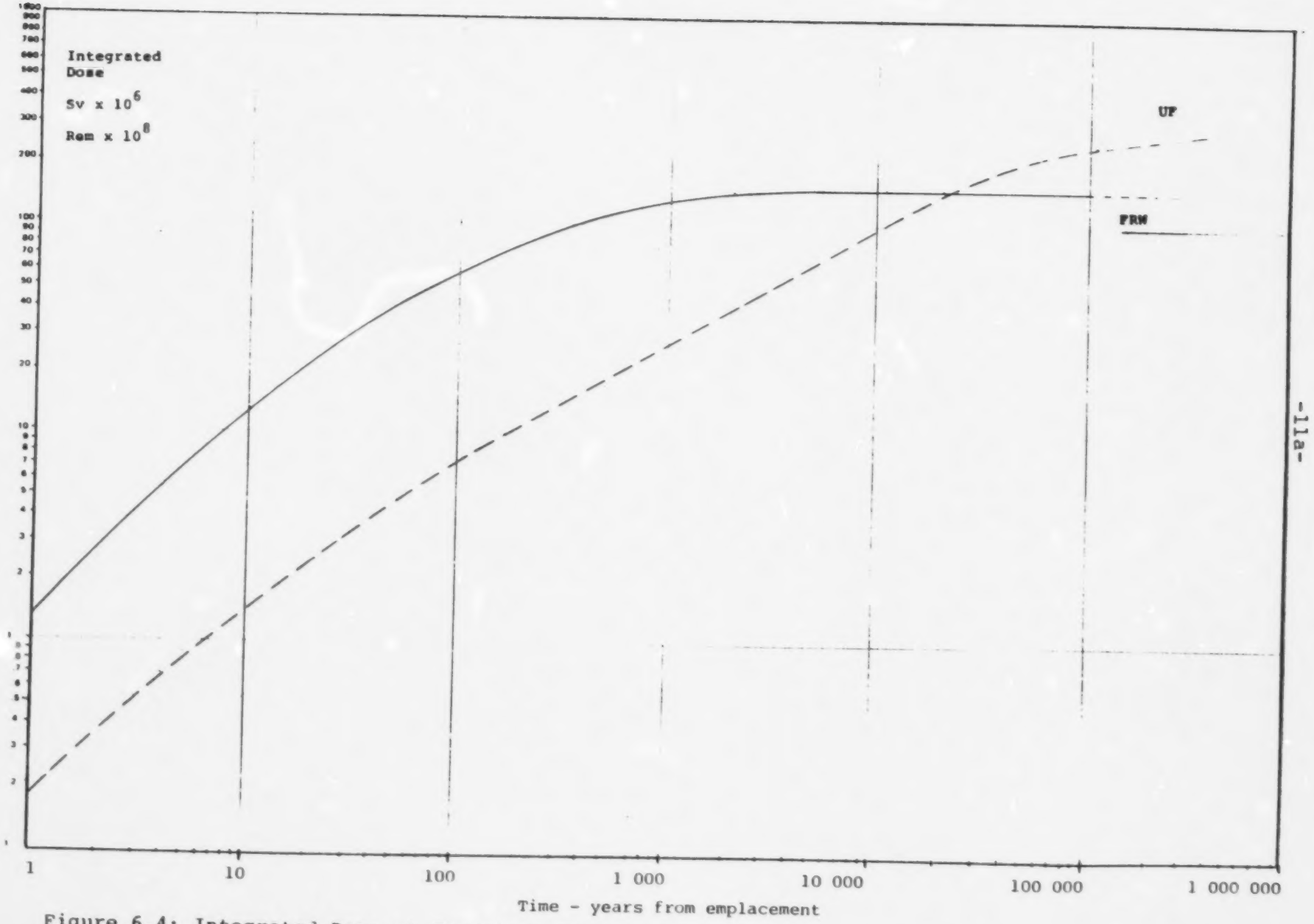

Figure 6.4: Integrated Dose at Container Surface

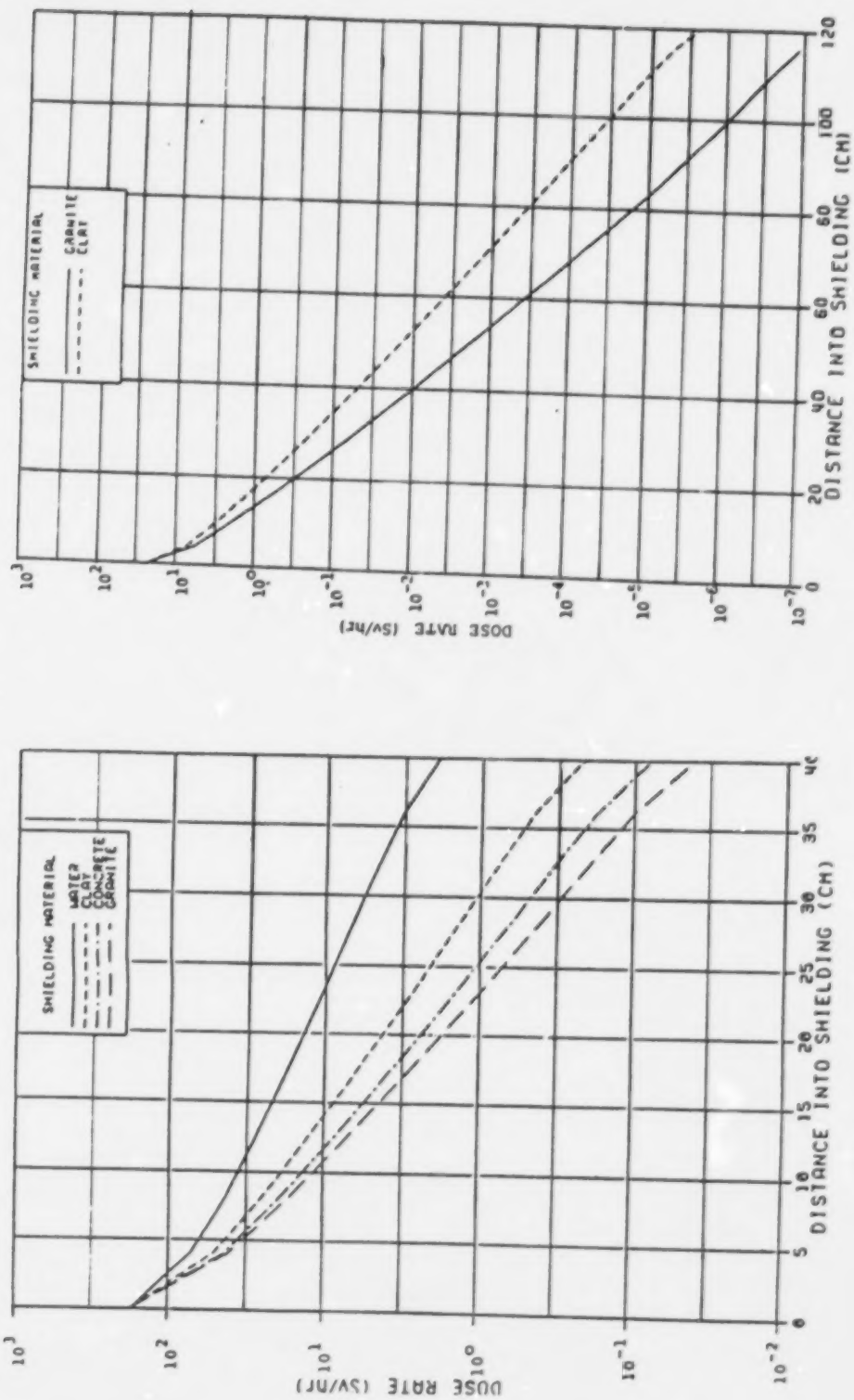

Figure 6.5: Total Attenuation for UF Container
(Ref. 1, Fig. A-5.6)

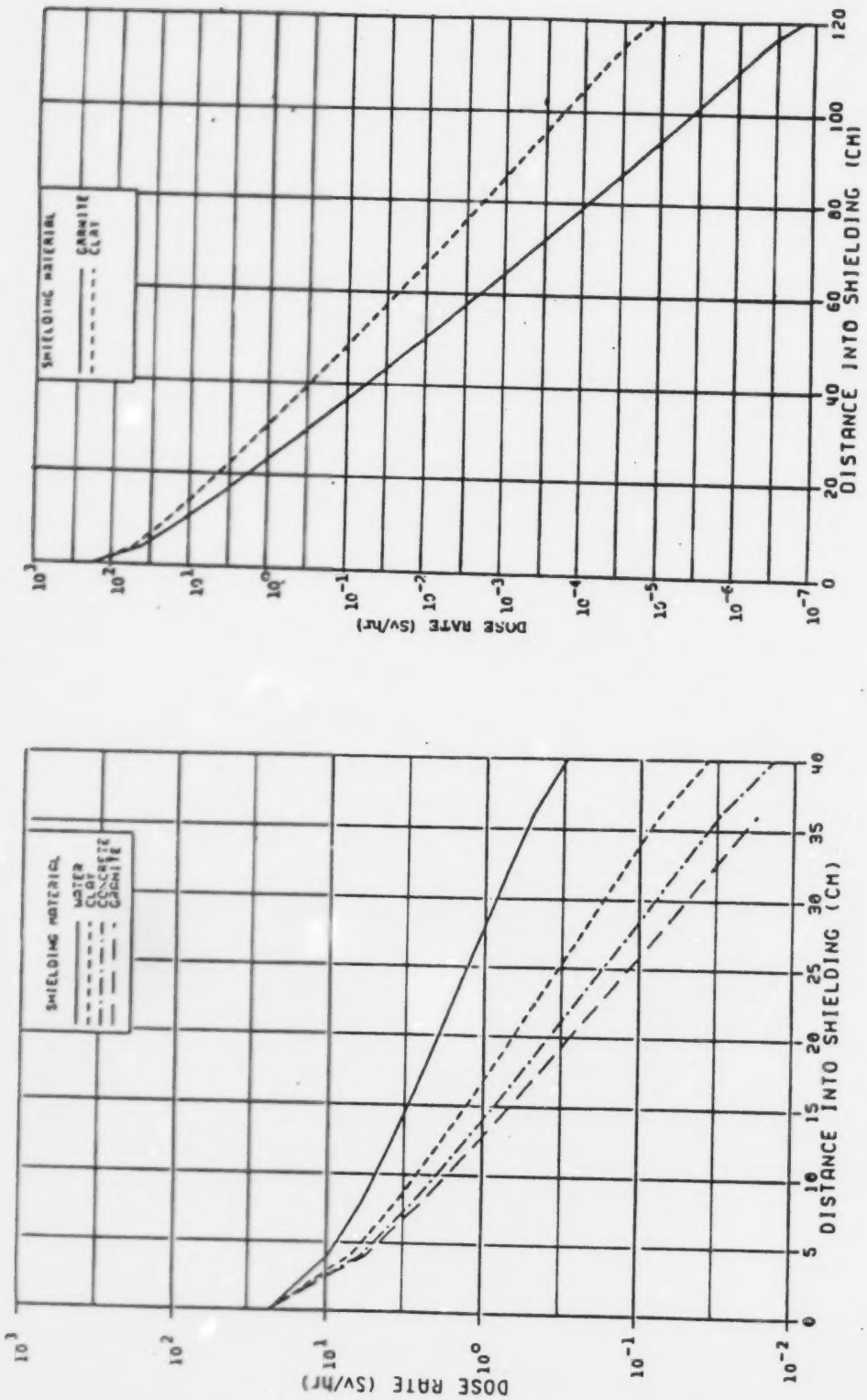

Figure 6.6: Total Attenuation for FRW Container
(Ref. 1, Fig. A-5.8)

7. Properties of Engineered Components

7.1 Waste Containers

Used Fuel (UF) Containers (Ref. 1, p. A-4)

The current prime candidate for primary containment of used fuel is the TEC-II container shown in Figure 7.1 (Ref. 1). This is a cylindrical vessel of Grade 2 Titanium with a 4.76 mm wall and top plate thickness and a 6.35 mm thick bottom. The container is 642 mm in diameter and 2246 mm in height. Inside the vessel is a perforated basket assembly made of carbon steel tubes which hold 72 CANDU used fuel bundles in 4 arrays of 18 bundles. The container derives its strength from a pack fill of soda lime glass beads 0.7 to 1.2 mm in diameter. These beads fill all the interstices around the fuel bundle tubes and are compacted during filling by vibration. Other fill materials, (weldron sand, steel shot and bauxite grains), have been considered but are not actively being pursued or studied. The container top is welded on.

A similar concept has a solid basket assembly which provides structural support. The basket tubes are capped after the fuel bundles are in place. The glass beads then fill only the space between the basket and the container wall, as shown in Figure 7.2 (Ref. 11, p. 43).

A secondary concept is the same container and perforated basket assembly but with a fill of molten lead which flows into all the interstices around the fuel bundle tubes (Ref. 12, p. 3). Other materials, (lead alloy, zinc and aluminum - 7 wt% - silicon alloy) have been considered but are not actively being pursued or studied.

The TEC-II design container with a shell of copper or Inconel 625 and a glass bead pack is being studied but only as a remote back-up (Ref. 11, p. 33).

Fuel Recycle Waste (FRW) Containers (Ref. 1, p. A-4)

Fuel recycle waste will be poured as a molten glass into a thin wall (6.35 mm) stainless steel canister, 500 mm in diameter and 1895 mm high as shown in Figure 7.3a (Ref. 13, p. 81). The canister will hold 288L of glass and the remaining 27.3L will be filled with compacted silica sand. This canister is sealed and placed inside a TEC-IIR thin wall (4.76 mm) titanium container 560 mm in diameter by 2080 mm high as shown in Figure 7.3b (Ref. 12, p. 82). The void betwen the waste container and the canister will be filled with glass beads packed by vibration. The container top is welded on.

USED FUEL CONTAINER BASKET

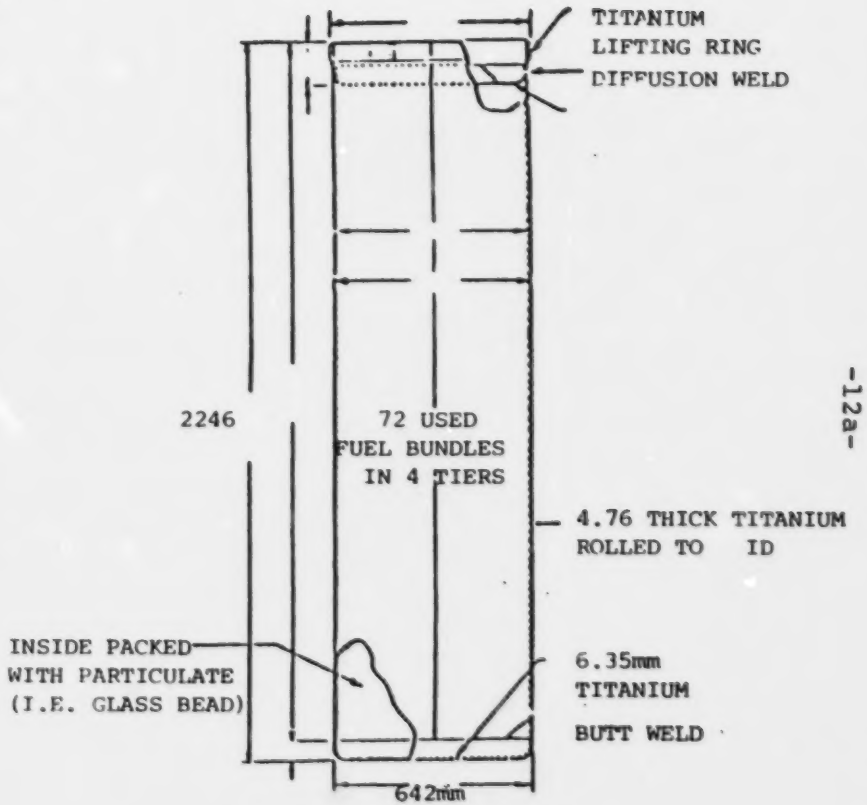

TEC-II USED FUEL CONTAINER

Figure 7.1: Tec-II Used Fuel Basket and Packed-Particulate Container (Ref. 1, Fig. A3-1)

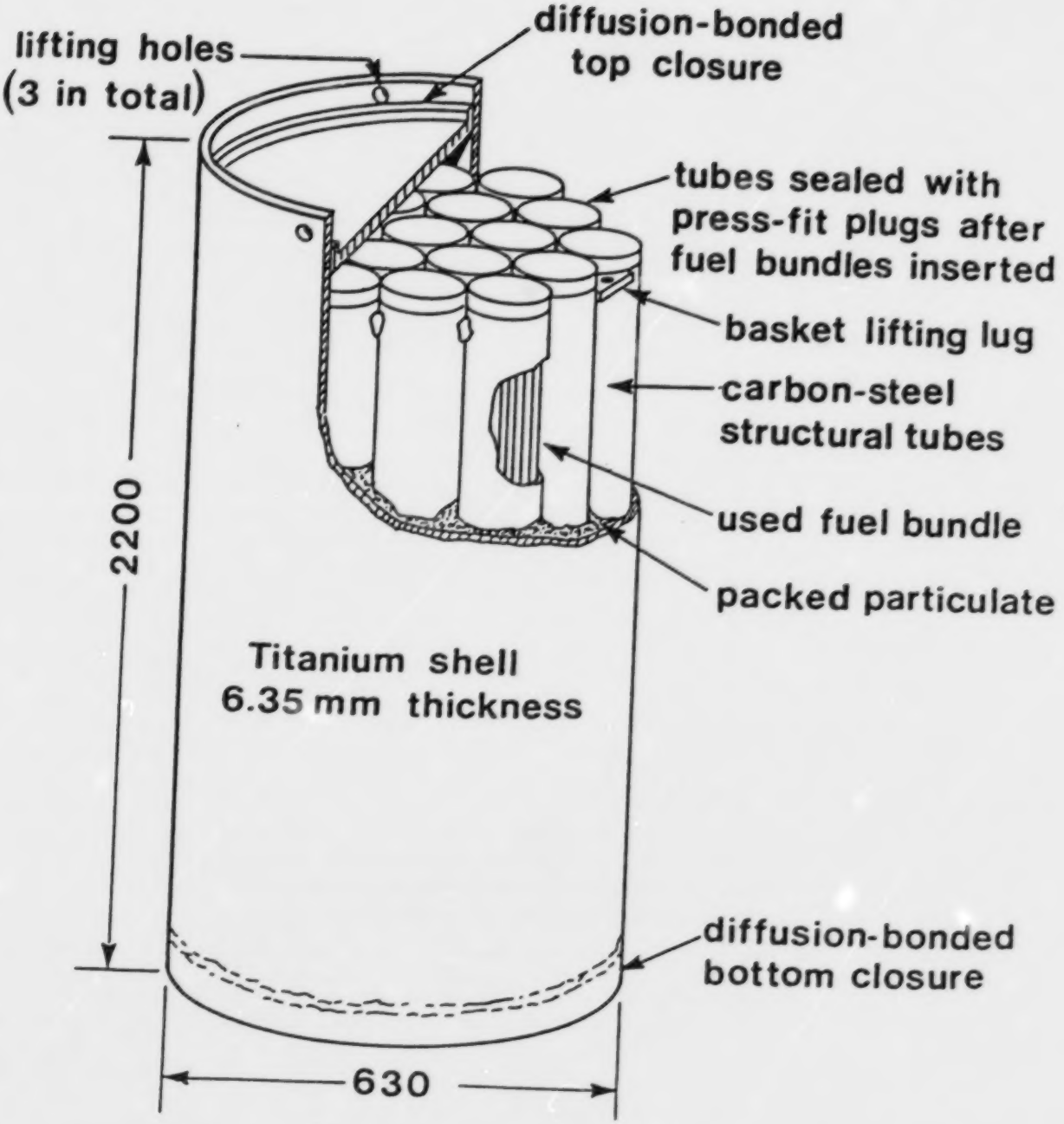

Figure 7.2: Prototype Titanium-Shell Structurally Supported Container for Used Fuel (Ref. 11)

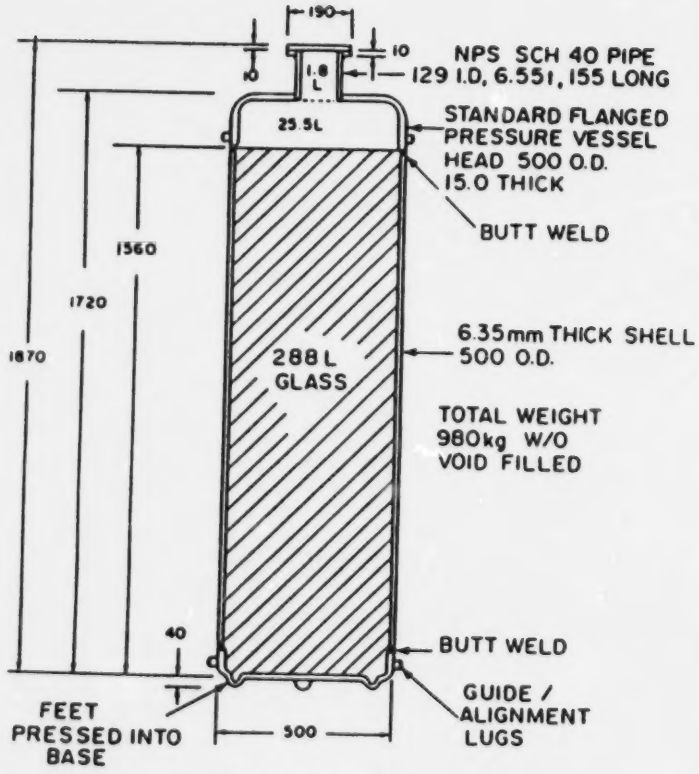

Figure 7.3a

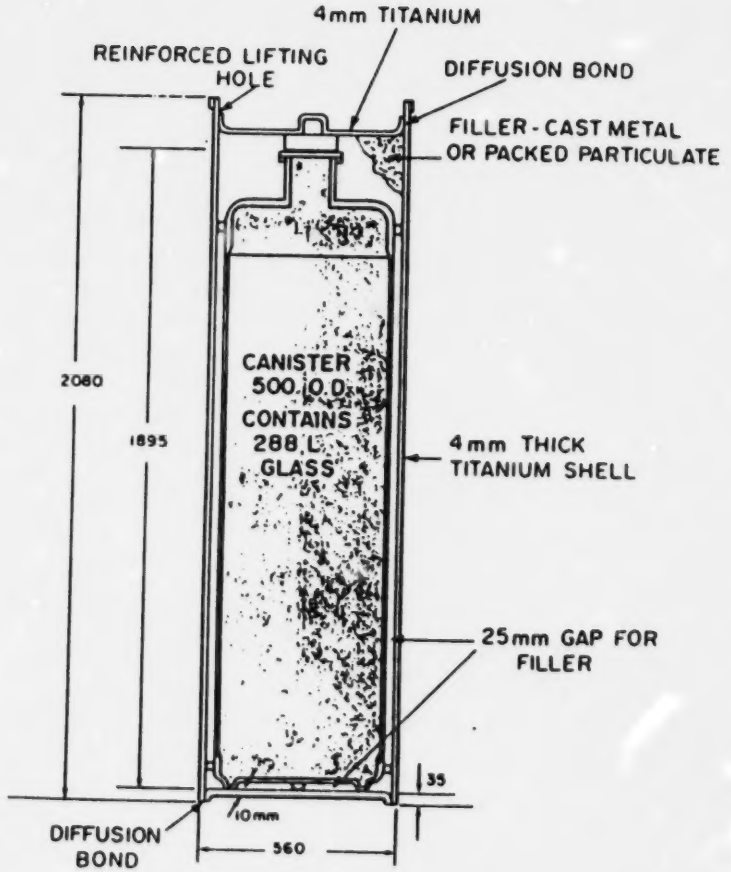

Figure 7.3b

Figure 7.3: TEC-IIR Fuel Recycle Waste Canister and Packed Particulate Container (Ref. 13)

Transuranic Waste (TRU) Containers

The transuranic waste will be packed and sealed in standard 225L carbon steel drums with a net volume of 210L (Ref. 1, p. A-5).

7.2 Buffer and Backfill

Considerable study has been undertaken and much work is still ongoing relating to selection of the most effective materials and methods for buffering adjacent to the emplaced containers and for backfilling above the buffer material to fill the vault rooms and accessways. The major components of the sealing program as currently envisaged are illustrated on Figure 4.4 (Ref. 5). Typical material characteristics of some of the materials being considered for backfill and buffering are contained on Table 7.1 (Ref. 5). Thermal conductivities of some buffer materials are shown on Table 7.2 (Ref. 4).

A considerable number of materials and combinations of materials have been tested for use as potential buffer or backfill materials.

It has been recognized (Ref. 14) that ideal buffer materials should have the following physical and chemical properties:

low permeability to ground water

thermal conductivity equal to or greater than that of the surrounding rocks

long-term thermal stability at the pressure and temperature of the vault

very low solubility in ground water

good sorption properties to retard the movement of radionuclides should the containers be breached

ability to condition incoming ground water to render it benign with respect to container materials

No single constituent buffer geological material provides all these properties. High thermal conductivity requires large particles (sand). Good sorption or ion exchange requires small particles (clay). A mixture of sand and clay shows most promise, and the addition of small amounts of other substances can provide the water conditioning. Impermeability to water is enhanced in those clays and clay-like minerals that swell strongly on hydration, of which bentonite is a prime example.

The list of potential buffer materials contained on Table 7.3, (Ref. 14) although not exhaustive, illustrates the wide range of materials that have been or could be considered for use for vault closure.

Table 7.1: Typical Material Properties of Geological Materials Relevant to Buffer and Backfill Use (Ref. 5)

Material	State	Moisture Content (%)	Dry Density (kg/m^3)	Thermal Conductivity (W/(°C.m))		Information Source
				Moist	Dry	
Quartzite Rock	natural	1.5	2400-2700	9.0	8.0	
Granite Rock	natural	2.0	2600	4.0	3.3	
Limestone	natural	4.0	2400-2600	3.5	2.5	
Sandstone	natural	2.0	2300-2700	4.0	3.0	
Shale	natural	4.5	2000-2300	1.8	1.0	
Crushed Quartz	compacted	6.0	2200	3.0	1.6	AECL TR-103
Crushed Limestone	compacted	6.0	2100	2.2	0.8	
Crushed Shale	compacted	10.0	2100	1.3	0.6	
Silty Clay	compacted	14.0	1800	1.3	0.6	
Ottawa Sand	compacted	5.0	1700	2.0	0.5	
Glacial Till	compacted	12.0	1900	2.3	0.8	
Bentonite Clay	compacted	25.0	2020	0.9	0.8	
Coal Ash	compacted	15.0	1500	1.0	0.3	
Water	non-convective	-	-	0.63	-	
Air	non-convective	-	-	0.025	-	

Table 7.2: Thermal Conductivity of Candidate Buffer/Backfills (a)

Mix Composition*	Moisture Content Range (%)	Dry Density Range (kg/m^3)	Thermal Conductivity in Moist Condition (W/(m.°C))	Thermal Conductivity in Dry Condition (W/(m.°C))
WSAB-15	6-17	1100 - 1770	1.3 - 2.8	0.7 - 1.0
WSAB-25	5-16	1200 - 1760	1.2 - 2.7	0.6 - 0.9
WSAB-50	15-29	1330 - 1400	1.2 - 2.0	0.5 - 0.6
GSBB-10	6-10	1850 - 2000	2.0 - 3.0	0.4 - 0.7
GSBB-25				
GSBB-50				
GSSB-15	4-9	2050 - 2175	3.0 - 4.0	1.5 - 1.7
GSK-15	4-9	2000 - 2200	2.5 - 3.5	1.8 - 2.0
GSK-15	5-12	1725 - 1850	0.8 - 3.5	1.8 - 2.0
CGBB-15	5-19	1750 - 2000	1.3 - 2.6	0.8 - 1.0
CGBB-25	6-12	1620 - 1710	1.0 - 1.5	0.6 - 0.8
CGBB-50	12-17	1500 - 1550	0.8 - 1.0	0.5 - 0.6
CGSB-15	6-10	1890 - 2200	2.4 - 3.4	1.4 - 1.8
CGSB-25	7-12	1600 - 2050	1.4 - 2.4	0.8 - 1.0
CGSB-50	9-15	1850 - 1980	1.8 - 2.4	0.9 - 1.0
CGK-15	6-10	1900 - 2050	2.2 - 3.0	1.7 - 2.0
CGK-25	9-12	1850 - 1980	1.7 - 2.5	0.9 - 1.2
CGK-50	9-15	1770 - 1860	2.1 - 2.2	1.0 - 1.2

*WS = Wedron sand, GS = Graded Silica, CG = Crushed Granite
AB = Avonlea Bentonite, BB = Blackhill (Wyoming) Bentonite, SB = Sealbond, K = Kaolin
The Figures represent the percentage of the second constituent
(a) From Ref. 4, Radhakrishna, H.S. (1982); TR-183

Table 7.3: Some Possible Buffer Materials (Ref. 14)

1. Bentonite clays with crushed rock or silica added to improve mechanical strength and thermal conductivity.

2. Synthetic swelling materials such as mixtures of magnesia and silica gel.

3. Crushed rock materials which will hydrate readily and increase in volume.

4. Inorganic metals, oxides, sulphides, carbonates and phosphates:

   (a) Cu, Cu_2O, Cu_2S, basic Cu carbonates
   (b) Pb, PbO, PbS, $PbCO_3$ systems
   (c) Other metal oxide, sulphide and phosphate systems.

5. Graphite.

6. Zeolite minerals.

7. Anhydrite.

Conceptual design considerations are ongoing to finalize the components of each material, however the currently considered reference materials (Ref. 1) are:

Buffer - Na-Bentonite clay 50% mixed with well graded clean silica sand 50%

Backfill - Lake Agassiz clay mixed with crusher run granite of 19 mm down

The reference buffer material properties as determined by experimental testing in saline and distilled water are as follows (Ref. 15):

Dry Density - 95% Modified AASHO - 1.67 T/m^3

Moisture Content - 17-19% (95% saturated - slightly dry of Proctor Optimum moisture content)

Dry Shrinkage - < 2%

Free Swell - 125 - 175% (in distilled water)
80 - 120% (in saline water)

Swell Pressure - 2.5 MPa (distilled water)
- 800 kPa (saline water)

Atterberg Limits LL 120% (distilled) 60% (saline)
PL 100% (distilled) 40% (saline)

Hydraulic conductivity $\sim 10^{-13}$ m/sec

Diffusion coefficient $\sim 10^{-11}$ m^2/sec

The currently optimized reference specifications for the material are summarized on Table 7.4 (Ref.1).

The reference backfill material has been developed based on testing at McGill University, (Ref. 16) and is comprised of:

20-30% Lake Agassiz (montmorillonite rich) clay mixed with crushed granite to give an envelope of:

95 - 100% passing 19 mm
40 - 60% passing 2 mm
20 - 30% passing 0.006 mm

The detailed grading called for in the current AECL reference specification (Ref. 1) is given on Table 7.5.

Based on laboratory test work, it has been found that the backfill material when mixed with typical granite groundwater of pH 6.5 or distilled water has the following properties (Ref. 16):

Table 7.4: Specification for Reference Buffer Material (Ref. 1)

Name	Raw Materials		Reference
	Silica Sand	Bentonite	Buffer
Liquid limit, %	N.A.*	210	135
Plastic limit, %	N.A.	45	18
Air dry W, %	<0.5	6 to 7	3 to 5
Minimum specific surface, m^2/g	N.A.	590	290
Predominant clay mineral	N.A.	Na-montmorillonite	Na-montmorillonite
Cation Exchange Capacity (CEC), meq/100g (approximate)	N.A.	40	80
particle size distribution			
< 2 mm, %	92-100	100	96-100
< 1.5 mm, %	86-98	100	92-100
< 1 mm, %	76-88	100	88-94
< 0.5 mm, %	52-64	100	76-82
< 0.25 mm, %	24-35	100	50-56
< 0.1 mm, %	0-11	100	50-56
< 0.06 mm, %	0-3	100	46-52
< 2 μm, %	0	70	32-38
Minimum dry density, Mg/m^3	N.A.	N.A.	1.67
Compaction water content, %	N.A.	N.A.	17-19

* N.A. - not applicable

Table 7.5: Specification for Reference Backfill Material (Ref. 1)

	Raw Materials		
	Crushed Granite	Clay	Reference Backfill
Liquid Limit %	N.A.*	112	28
Plastic Limit %	N.A.	31	not plastic
(Air dry w%)			
Particle size distribution			
< 12.7 mm %	-	-	82-100
< 9.5 mm %	-	-	65-77
< 4.76 mm %	-	-	44-56
< 2.38 mm %	-	-	29-41
< 1.19 mm %	-	-	19-31
< 0.297 mm %	-	-	5-19
< 0.149 mm %	-	-	0.9
< 0.074 mm %	-	-	0.7
< 2µm	-	-	0.5
Minimum Dry Denisty Mg/m^3	N.A.	N.A.	2.1
Compaction water content %	N.A.	N.A.	6-8

* N.A. - not applicable

	Mixture	Clay Alone
Atterberg Limits, LL	28 - 35%	112%
PL	20 - 22%	31%
Hydraulic Conductivity	10^{-10} m/sec	10^{-10} m/sec
Free Swell	4.2%	6.0%
Swell Pressure	c. 17 kPa	-
Modified AASHO 95% dry density	2.15 T/m^3	-

To date, full scale trials of placement techniques have not been undertaken, so data are not available on achievable in situ properties of placed buffer and backfill materials. It is, however, currently envisaged that the materials will be pre-prepared on surface and supplied by a containerized system to the underground rooms. Accordingly, a surface preparation plant is envisaged in which the materials will be blended to the required specification gradings and moisture contents. Water will be added at this stage as required for transportability. Such water will most likely be from surface water sources developed specifically for the purpose. The reference clays for both the buffer and backfill will require importing to the site as will the sand required for the buffer mixture. However, it is considered that all the crushed granite for the backfill mixture will be derived from the vault excavation. It is likely that this would be passed through a conventional quarry crushing and screening plant at some location on surface in close proximity to the shaft headframe and the buffer and backfill preparation plant.

Once the materials are delivered underground, additional water may need to be added to aid in achieving the required density and optimum compacted moisture content. Again, this water would probably be derived from surface supplied reservoirs and piped underground.

8. Properties of Rock, Minerals and Groundwater

Because of their long term stability and durability, granitoid plutonic rocks are being considered for disposal of high level radioactive wastes.

8.1 Rock Material

Of the plutonic rocks occurring in the Shield, the vast majority (some 75%) are granites, 15% are gabbros, 10% syenites and the remainder anorthosites and other minor assemblages (Ref. 17).

Although individual plutons may vary considerably in composition one to another, it is considered that the range of material properties from granitic to gabbroic assemblages encompasses the likely spread of rock types found in almost all Shield plutons.

8.1.1 Mode of Origin

Plutonic rocks are generally formed by slow crystallization and solidification at appreciable depth within the earth. In consequence, their chemical composition, mineralogical structure, hardness and strength are all dependent upon their precise mode and temperature of emplacement and subsequent geological history. Many plutons though are relatively uniform in tectonic structure and mineralogical composition even though they vary in size from small plugs to large batholiths.

Batholiths are the largest of the igneous plutons and are emplaced predominantly in mountain belts. They are chiefly granitic in composition without a detectable or inferable floor of older rocks. Stocks are small batholiths of less than approximately 100 square kilometers of outcrop area.

Some plutons contain primary flow banding and zones of substantial interaction with the enclosing country rock, which may be metamorphosed by the emplacement of the pluton. The thickness of this altered zone (aureole) depends greatly on the temperature and the depth of emplacement of the pluton. Plutons emplaced within about six kilometers of the ground surface tend to be of lower temperature and generally will have a smaller aureole than those emplaced at greater depth. Complex interaction effects can occur where several pluton types may occur in a single orogenic belt.

Frequently, batholiths are not emplaced during single plutonic events. Numerous intrusions of magma may take place. Some of these events may be forceful, causing fracturing and faulting within the existing pluton. In such cases, most of the fissures so created become filled and sealed by mobile hydrothermal fluids. Other emplacements may be relatively quiet with magma filling pre-existing cracks and fissures. Some melting of existing rock may occur. Later uplift and

tectonic activity may also create joints and faults unrelated to the original pluton emplacement.

At least two phases of structural evolution have occurred to most of the plutonic bodies exposed across the Canadian Shield. An initial structural fabric of joints and microstructures was imparted to the rock during emplacement; often a second fabric of jointing (and not infrequently faulting) has then been imposed after solidification of the magma.

The Geological Survey of Canada (GSC) on behalf of AECL have been categorizing many of the plutons across the Canadian Shield and in particular, in Ontario. They have recognized three major types of deformation and discontinuity patterns which occur within such bodies, based on emplacement and post emplacement history. These have been labelled as Types I, II and III.

Post-kinematic intrusions

(type-I) - undisturbed plutons (emplaced plutons that are essentially last phase events),

Pre- and Syn-kinematic intrusions
(type-II) - intermediate plutons (bodies that show some signs of post-emplacement or contemporaneous structural dislocation), and

(type-III)- deformed plutons (typically bodies that have undergone significant fracturing and strain).

Preliminary geological characterization of plutons by rock type, percentage outcrop, lineament density and presence of faults has also been undertaken for Ontario by the GSC. The current AECL research area programs are also dovetailed into this approach. Specific representative pluton types are:

the Lac Du Bonnet Batholith, Underground Research Lab (URL) site at Pinawa - a relatively undisturbed (type-I) pluton,

The Eye-Dashwa plutonic body - a much deformed syn-kinematic (type-III) intrusive body, associated with greenstone belt rocks,

the Chalk River site - a complex of metamorphic rocks and plutonic pre- and syn-kinematic (type-III) intrusives, and

the East Bull Lake site - intermediate (type-II) intrusive complex showing some signs of post-emplacement structure.

8.1.2 Composition

The coarse grained igneous rocks that comprise the vast majority of the plutons across the Canadian Shield fall into two groups: the granitoid (granitic) and gabbroid (gabbroic) associations based on mineralogical composition. Figure 8.1 presents the most commonly used classification, which is based on the relative proportions of quartz, feldspars and feldspathoids (Ref. 18, 19).

Granitic rocks or granitoids have essential quartz and feldspar, either as alkali (K-Na) feldspar or coexisting K-feldspar and plagioclase. Biotite is the most common ferromagnesian mineral, though hornblende is found in more Ca-rich granitoids. Minerals common in granitic rocks are given in Table 8.1 (Ref. 20).

Gabbroic rocks form a family of basic rocks, containing less silica (45-52%) than the granitoids. They resemble the granites in texture, but generally are much darker in colour. Quartz may be present in amounts up to 20% in rocks of the gabbroic association, but in gabbro (sensu stricto) quartz is always less than 5%.

Gabbros usually have a large amount of plagioclase (between 30-60%) and very little K-feldspar. The rest of the rock is made up of varying amounts of ferromagnesian silicates - pyroxenes, olivine and amphiboles. Equivalent K-feldspar-bearing rocks are the syenites. Minerals common in gabbroids are given in Table 8.2 (Ref. 20).

In addition to the major mineral variations which characterize the rocks, wide differences also occur in the minor constituents as is indicated by the chemical composition variations shown on Table 8.3 (Ref. 18 and 19). Trace constituents also vary, typical chloride concentrations ranging from 60 ppm in gabbroic rocks to values in excess of over 200 ppm in granite (Ref. 19). Isotope concentrations for strontium and lead which can be considered as radiogenic tracers also vary considerably as shown on Figure 8.2 (Ref. 19).

8.2 Fractures

8.2.1 Fracture Systems

Because of the tectonic history of most of the Canadian Shield, fractures (joints and faults) are commonplace throughout plutonic rock bodies. These fractures are of considerable significance in the context of nuclear fuel waste disposal in that they constitute potential pathways for groundwater flow. Furthermore, such fractures are often lined or filled with minerals which may be quite distinct from those of the host rock. In any system where flow is appreciable (fractures wider than 20 μm), so that mass-transport is by flow rather than

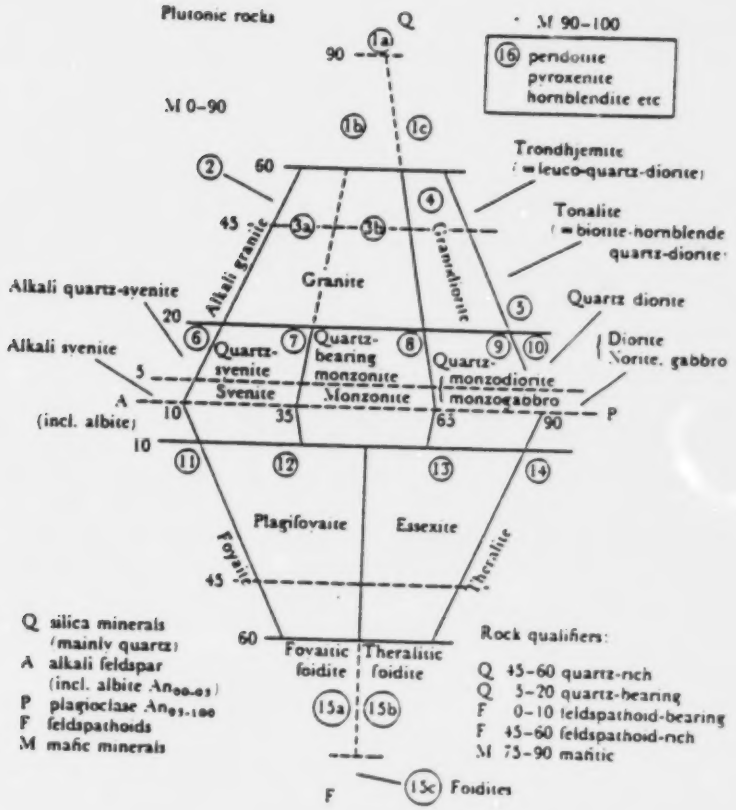

Figure 8.1: Classification of Plutonic Rocks in the Double Triangle Q-A-P-F, According to Their Actual Mineral Composition (Ref. 19)

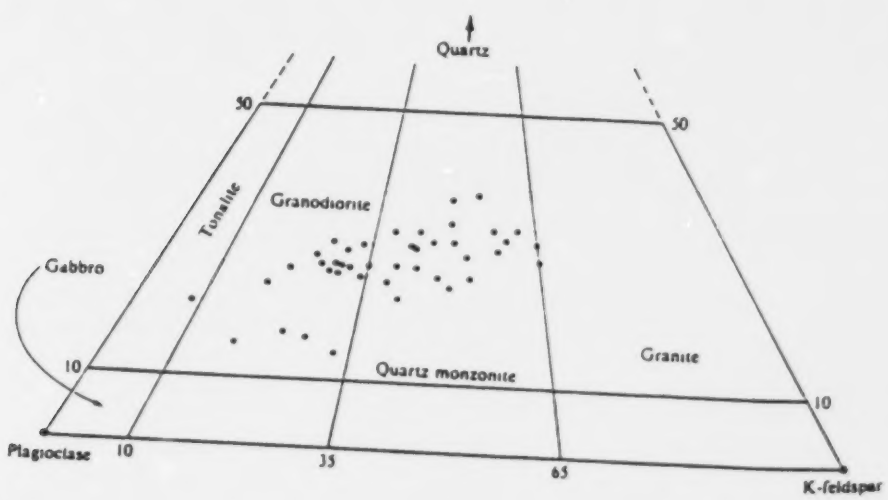

Plot of 40 Average Model Compositions of Granitic Rocks, Sierra Nevada Batholith, Represeting 597 Analyses (Ref. 19)

Table 8.1: Common Minerals in Granitic Rocks (Ref. 20)

Major Minerals (> 10%)	Major Minerals (0-20%)	Accessory Minerals (0-5%)
Quartz	Biotite	Apatite
K-feldspar (orthoclase, microline)	Muscovite	Sphene
Albite	Hornblende	Zircon
Plagioclase (An_{0-60} usually andesine + oligoclase)	Cordierite	Tourmaline
	Chlorite	Magnetite
		Ilmenite
		Rutile
		Pyrite
		Pyrrhotite
		Arsenopyrite
		Monazite
		Allanite
		Fluorite
		Garnet
		Calcite

Table 8.2: Common Minerals in Gabbroic Rocks (Ref. 20)

Major Minerals (5-90%)	Minor Minerals (0-20%)	Accessory Minerals (0-5%)
Plagioclase	Feldspathoids	Sphene
Orthopyroxene	- nepheline	Zircon
Clinopyroxene	- analcine	Monazite
Olivine	Micas	Apatite
Hornblende	- biotite	Calcite
	- phlogopite	Siderite
	Fe-Ti oxides	Sulphides
	- magnetite	- pyrite
	- ilmenite	- pyrhotite
	- ulvospinel	- chalcopyrite
	Sulphides	

Table 8.3: Average Chemical Compositions of Common Plutonic Rocks (Refs. 18 and 19); Tabulated as % of Oxides

	Alkali Granite	Grano-diorite	Quartz Diorite (Tonalite)	Nepheline Syenite	Gabbro
SiO_2	73.86	66.88	66.15	55.38	50.78
TiO_2	0.20	0.57	0.62	0.66	0.77
Al_2O_3	13.75	15.66	15.56	21.30	20.40
Fe_2O_3	0.78	1.33	1.36	2.42	1.75
FeO	1.13	2.59	3.42	2.00	6.20
MnO	0.05	0.07	0.08	0.19	0.09
MgO	0.26	1.57	1.94	0.57	6.49
CaO	0.72	3.56	4.65	1.98	10.24
Na_2O	3.51	3.84	3.90	8.84	2.20
K_2O	5.13	3.07	1.42	5.34	0.45
P_2O_5	0.14	0.21	0.21	0.19	0.05
H_2O	0.47	0.65	0.69	0.96	-

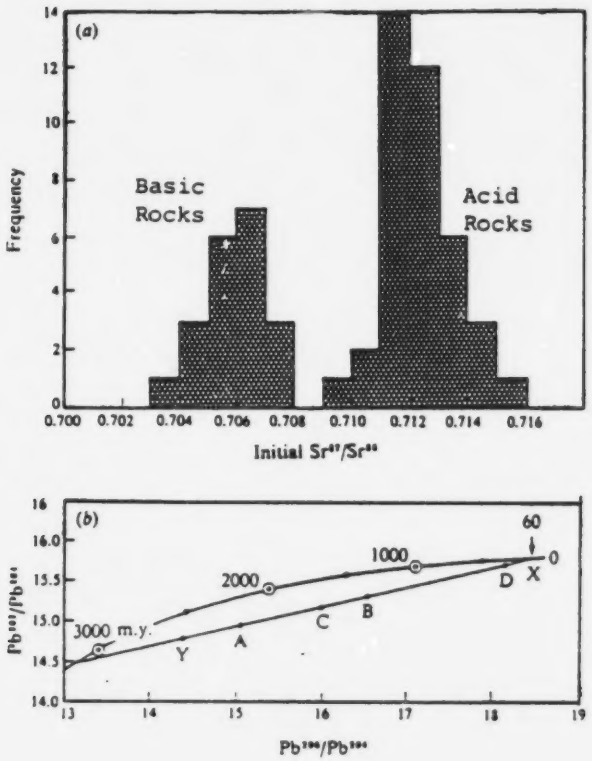

Figure 8.2: Isotopic Data for Strontium and Lead, Hebridean Tertiary Volcanic Province. (a) Strontium Data for Basic Rocks and Granitic Rocks; (b) Lead Data for the Same Suite of Rocks: Granitic Rocks AB: Basic Rocks CD: Average Lead of Basement is Y. Upper Curve is the "Primary Single-Stage Growth Curve" (μ_o = 8.92) for Lead Derived From "Primordial Meteoric Lead", Intersecting AD at X, 60 m.y. (Age of Hebridean Lavas) (Ref. 19)

diffusion, and the stability and sorptive properties of these fracture infill minerals are of great importance.

Most of the PreCambrian plutons existing in the Canadian Shield exhibit two main types of fracturing. The first - hydraulic fracturing - occurred during deuteric activity in the final stages of crystallization, associated with the formation of pegmatites and aplites at temperatures around 600-650°C (Figure 8.3) (Ref. 21). At this stage, when progressive crystallization of the major mineral phases was giving rise to increased viscosity of the cooling magma, complex local stress fields controlled the patterns of fissures that developed to release trapped hydrothermal and magmatic fluids. In consequence, many of the older fracture patterns found in plutonic rocks exhibit structural trends sympathetic to the geometry of the intrusion.

The second type of fracturing commonly seen in plutonic bodies generally post-dates initial emplacement and frequently results in several discrete scales of fracturing and associated mineral complexes, including:

faults and shear zones-frequently containing clay or breccia infill and often exhibiting slickensided surfaces coated with sheet silicate minerals;

dykes - injected through the pluton mass, often on old weakness lines, they frequently exhibit extremely complex marginal infill mineral assemblages;

veins - usually similar in chemical composition to the host rock but often in the form of a distinctly different mineral suite; and

joints and undifferentiated micro and macro fractures - often well developed and open or infilled in the weathered, near-surface zone and adjacent to major faults or shears.

Not all of the fractures present in the rock mass constitute zones or conduits with preferentially increased permeability (as many of the fractures are tight or sealed by the infill materials). Based on deep hydrogeological testing of boreholes at the Underground Research Laboratory (URL) site in Manitoba, most fracture zones identified in the holes that exhibited any measurable hydraulic conductivity were noted to be either stained or infilled with haematite or limonite, whereas elsewhere infillings of calcite and/or chlorite seemed to dominate. At depth, these open fracture zones (Figure 8.4) (Ref. 22) were found to be confined to discrete horizons associated with major fracture systems (Figure 8.5) (Ref. 6).

Micro fracturing in these zones and elsewhere has been found to be extremely complex, although broad scale orientation patterns can be recognized where adequate mapping detail is available.

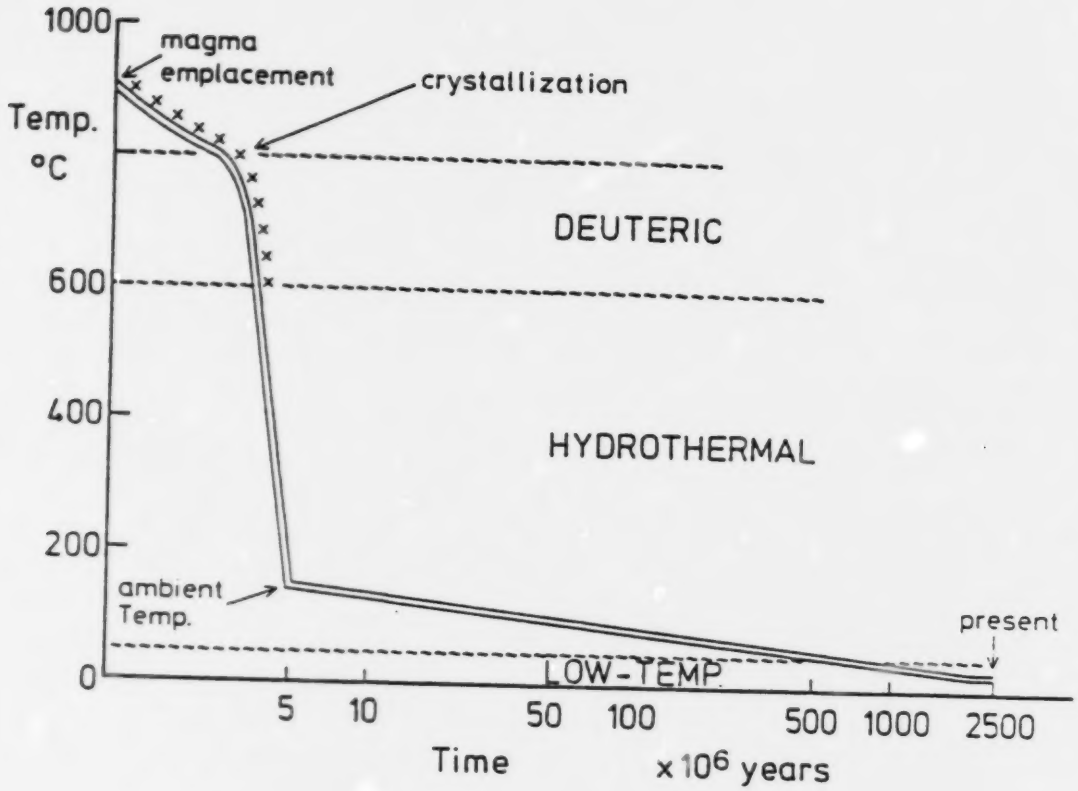

Typical crystallization in fractures:

600 - 650°C	pegmatites/aplites
300 - 500°C	epidote
200 - 450°C	chlorite
<100°C	clays, Fe-oxides, gypsum, carbonate

Figure 8.3: Schematic Diagram Illustrating the Cooling History of the LAC Du Bonnet Granite, and the Three Stages of Post Solidification Alteration. (The Rb/Sr Age for this Granite is About 2500 x 10^6 Years). The Ambient Temperature at a Depth of 5 KM Assumes a Precambrian Geothermal Gradient of 30°C/KM) (Ref. 21)

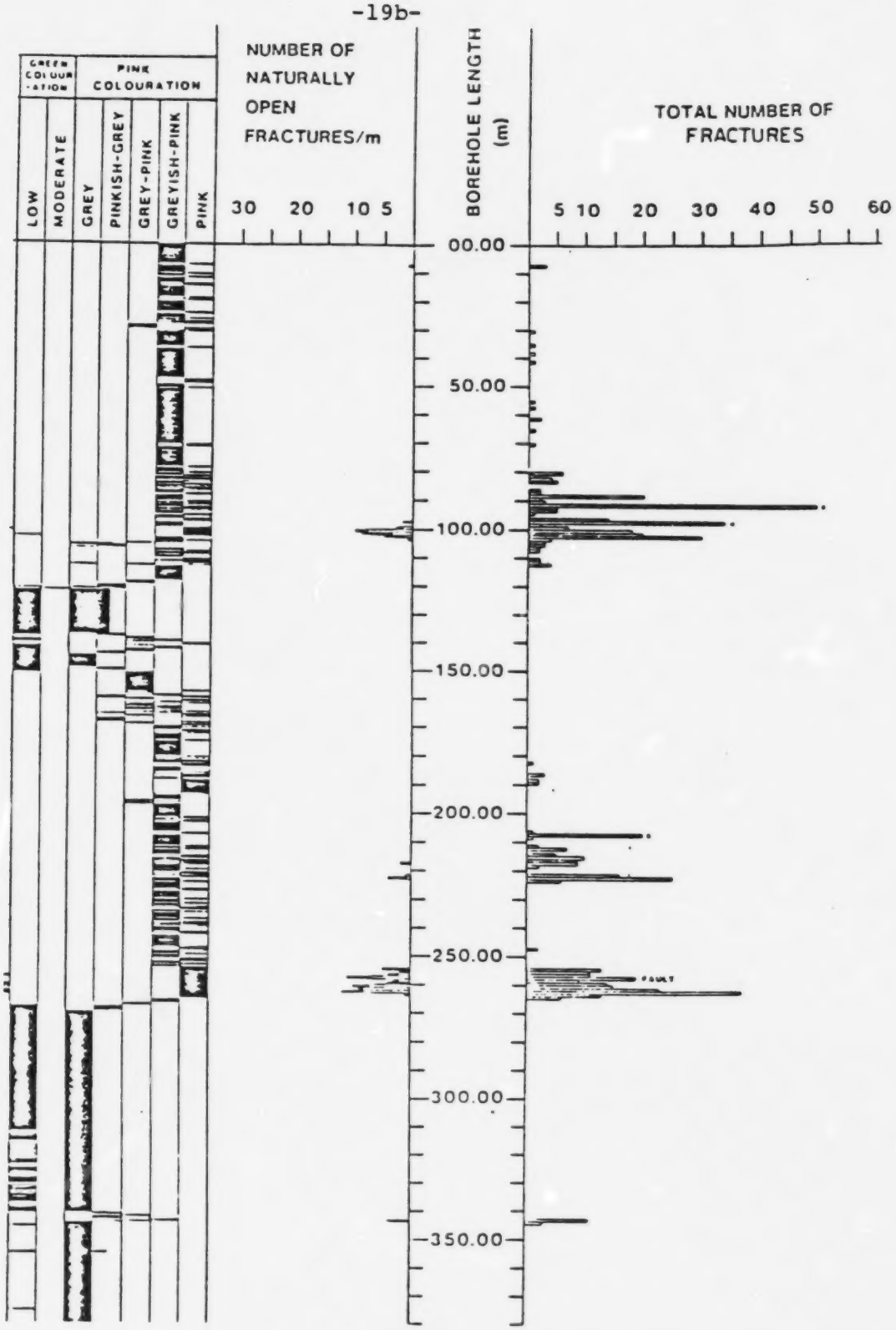

Figure 8.4: Summary Colouration and Fracture Log of Borehole at the Underground Research Laboratory Site, Lac Du Bonnet Batholith, Manitoba (Ref. 22)

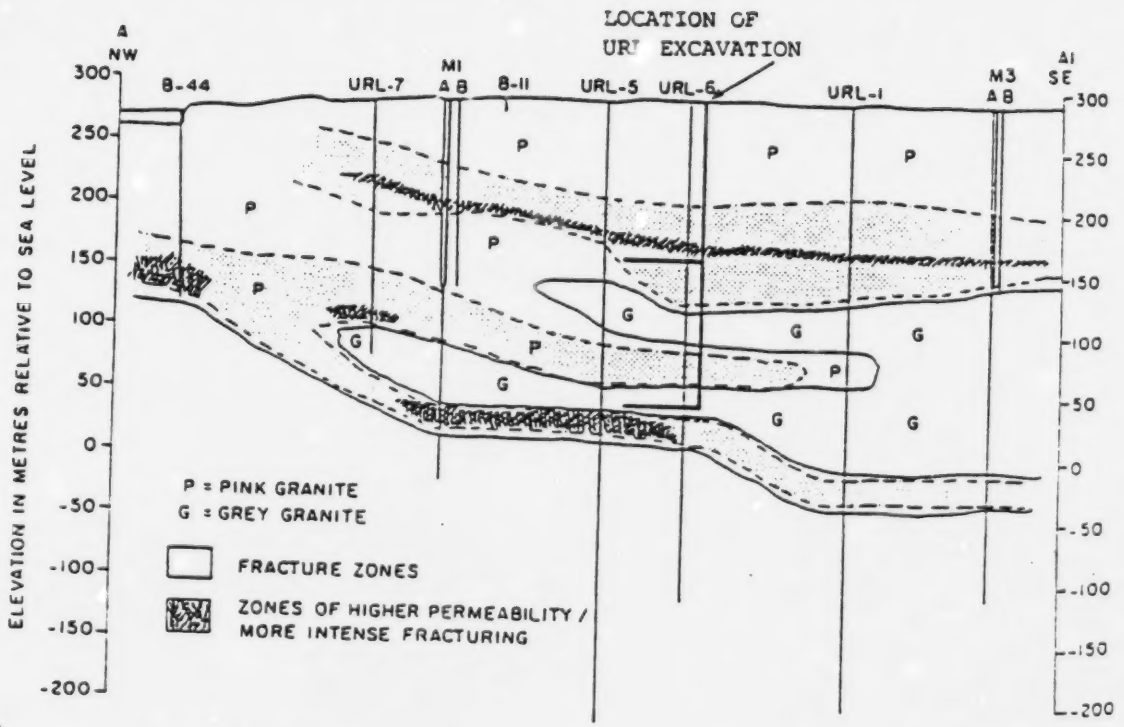

Figure 8.5: Fracture Zones at Depth in the LAC Du Bonnet Batholith (URL Site) (Ref. 6)

Fracture patterns examined with the acoustic televiewer or borehole TV camera vary from simple hairline fractures to complex zones of multiple braided fractures (Figure 8.6) (Ref. 22).

Similar patterns of fracturing and infill material have been identified from the Marysville and Empire Creek Stocks in Montana where mild geothermal conditions still exist within the pluton body (Refs. 74, 35). In such situations, often cross-cutting relationships can be found within the pluton between fractures with different fillings. This is considered to be indicative of several episodes of fracturing during which many fractures were reactivated and filled with new minerals. The major alteration zones (often marked by distinct red/pink coloration changes in the top few hundred metres of some of the plutonic rock masses and adjacent to the major fracture zones) are particularly important in this respect, as fracture properties within them can differ appreciably from elsewhere in the pluton.

8.2.2 Fracture Fillings

Most of the fractures identified within plutonic bodies exhibit one or more of the following filling materials: chlorite, epidote, (including clinozoisite), three varieties of haematite (specular haematite, purple crystalline haematite and the common red-brown haematite), calcite, gypsum, adularia, quartz, fluorite, clay, sphene, sulphides (mainly pyrite), sericite, limonite-goethite, mica, and/or ground-up granitic fracture-wall material. The filling materials in a fracture occur in various proportions and in numerous combinations, but epidote, chlorite and/or haematite appear to be the most common major filling materials (Ref. 3).

It seems that the majority of fractures contain two fillings, but three or four fillings are common. The widest fractures are commonly well-indurated shear fractures that contain large amounts of ground-up wall rock material within a matrix of several mineral fillings.

Some variation of filling type tends to occur with depth. Notably, the content of epidote and gypsum increases, whereas chlorite and to a lesser degree, calcite decrease; haematite is least common at moderate depths. Clay occurs mainly near the rock surface and along selective fractures at depth.

It is evident that in many cases the composition of fracture filling materials varies with the age of the fracture. Higher-temperature minerals such as epidote and chlorite occur in older fractures. Reactivated fractures and new younger fractures are inferred from the presence of lower temperature minerals such as calcite, gypsum and clay, and from cross-cutting relationships (Figure 8.7 Ref. 3).

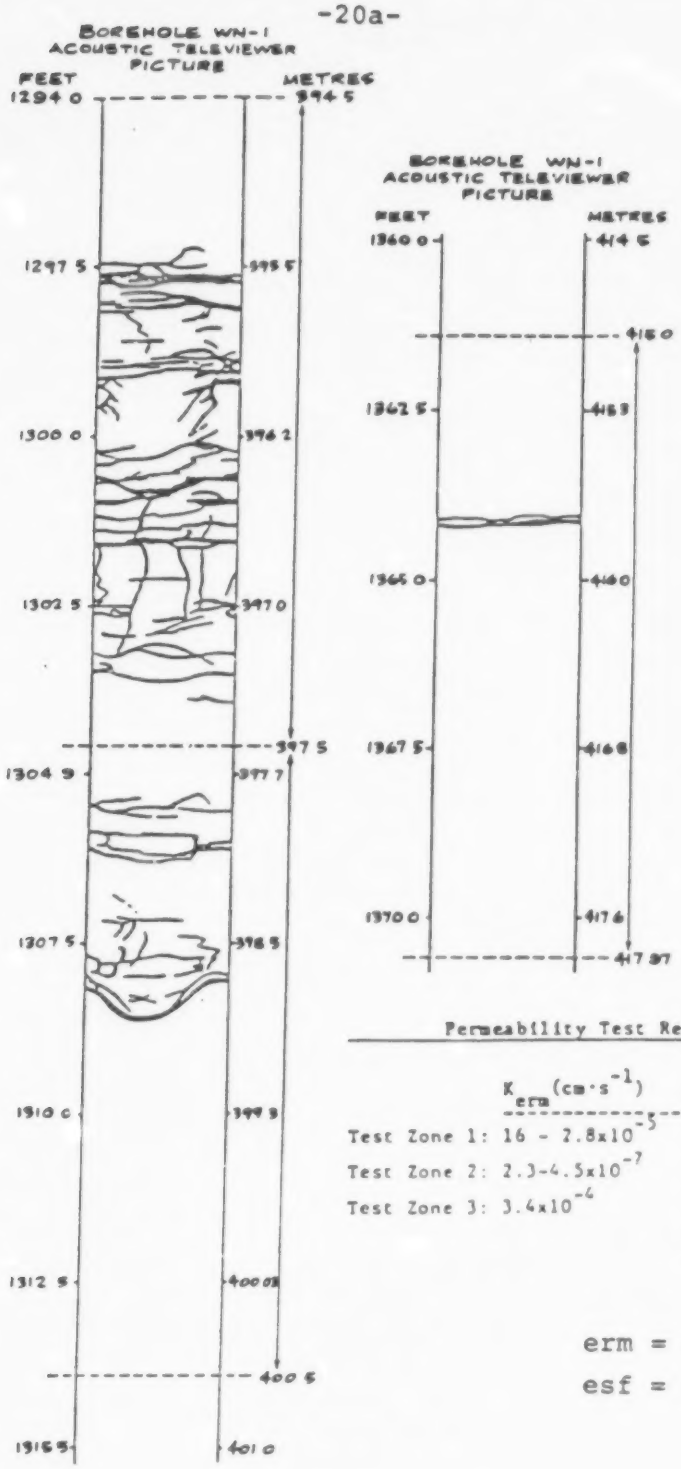

Permeability Test Results

	K_{erm} ($cm \cdot s^{-1}$)	$2b_{esf}$ (um)
Test Zone 1:	$16 - 2.8 \times 10^{-5}$	96-115
Test Zone 2:	$2.3 - 4.5 \times 10^{-7}$	23- 29
Test Zone 3:	3.4×10^{-4}	265

erm = equivalent rock mass

esf = equivalent single fractur

Figure 8.6: Accoustic Televiewer Logs of Borehole WN-1 Showing Typical Complex Fracture Pattern Seam in Borehole Sidewall (Ref. 22)

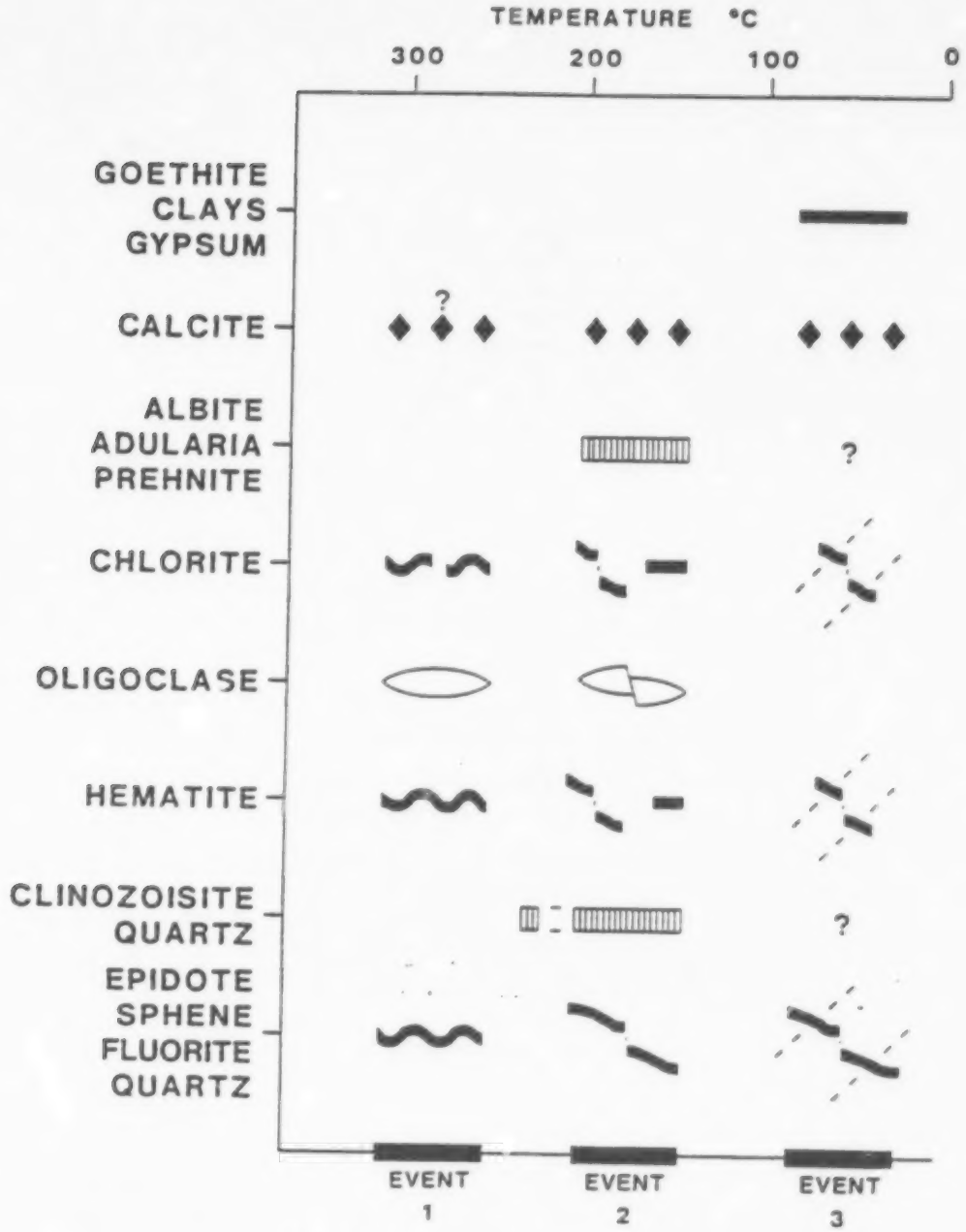

Figure 8.7: Typical History of Fracture Filling Minerals in Plutonic Rocks Showing Decrease in Temperature of Crystallization With Decreasing Age (Ref. 3)

Note: Solid sympbols indicate crystallization; dashes show dislocations of previous fillings

An excellent illustration of fracture-fill systems is provided by the detailed study that has been made of the fractures of the Eye-Dashwa Lakes granite pluton at Atikokan, Ontario (Refs. 23, 24). Four main stages of fracture filling were identified, representing decreasing age and temperature of the circulating fluids. These are:

(1) pegmatite-aplite (650-600°C)
(2) epidote (500-300°C)
(3) chlorite (450-200°C)
(4) low-temperature minerals (< 100°C - clays, Fe-oxides, gypsum and carbonate.

The lower temperature minerals (< 500°C) appear to be derived largely by wall/rock alteration as evidenced by replacement textures. The pegmatite-aplite fractures were found to be well sealed and seldom reactivated, but the other fractures being essentially weaker than the granite frequently exhibited reactivation, as characterized by altered original mineralogy and deposition of new phase fracture infill minerals.

Based on the detailed core logging and televiewer surveys that have been carried out on the cores from some of the AECL research sites, there also appears to be some correlation between fracture filling type and fracture zone width (Table 8.4, Ref. 25) and between filling mineralogy and fracture aperture, Figure 8.8 (Ref.25).

Three salient points emerge from these detailed core assessment studies:

(1) Epidote and chlorite tend to be the main fillings in wider fractures while calcite and haematite tend to be dominant in thin fractures. Because epidote is an early filling and calcite and haematite are later fillings (Ref. 24), the data suggest that fractures that have been reopened or recently formed tend to be narrower.

(2) The majority of fractures that contain mainly epidote or chlorite, or both are wider than 1 mm.

(3) Most fractures are less than 0.2 mm wide.

It should be noted that only about 4% of the populations sampled on Figure 8.8 are interpreted to be open fractures.

8.2.3 Weathering and Hydrothermal Alteration

The abundance of largely unaltered granitic plutons, even from the Precambrian, attests to the relative stability of granite on a global scale at low temperatures and near-surface conditions. However, on the local scale, within granite bodies, there is evidence for mineralogical instability. In tropical or unglaciated areas deep geological weathering and kaolinization can lead to breakdown of the upper 100 or so

Table 8.4: Veins and Heterogeneous Zones From Borehole Core in the Eye-Dashwa Pluton at Atikokan (Ref. 25)

Type	Number	Percent of population	Average true thickness	Veins and Zones >300 mm thick		
				Thickness	Depth	Strike/dip
hornblende-bearing veins	33	8	350 mm	2634 mm	102.422 m	158/45
				3326 mm	114.325 m	252/50
				925 mm	280 145 m	228/37
				578 mm	479 741 m	295/24
				1050 mm	603.899 m	103/46
				872 mm	837 139 m	058/27
				952 mm	884.577 m	048/27
granitic* veins	318	74	45 mm	512 mm	71 967 m	348/44
				585 mm	463 812 m	350/36
				1550 mm	611 646 m	357/24
				602 mm	875 750 m	019/85
				1938 mm	905.207 m	216/64
heterogeneous zones	43	10	200 mm	925 mm	280.145 m	275/56
				1144 mm	410.575 m	**
				589 mm	414.280 m	255/13
				507 mm	413 300 m	171/04
				730 mm	518 025 m	**
				625 mm	551.600 m	**
				1050 mm	648 123 m	325/27
quartz veins	33	8	64 mm			
Total	427	100%				

*Includes all types of aplitic, granitic and pegmatitic veins

**Strike and dip are often difficult to obtain where contacts are irregular and diffuse.

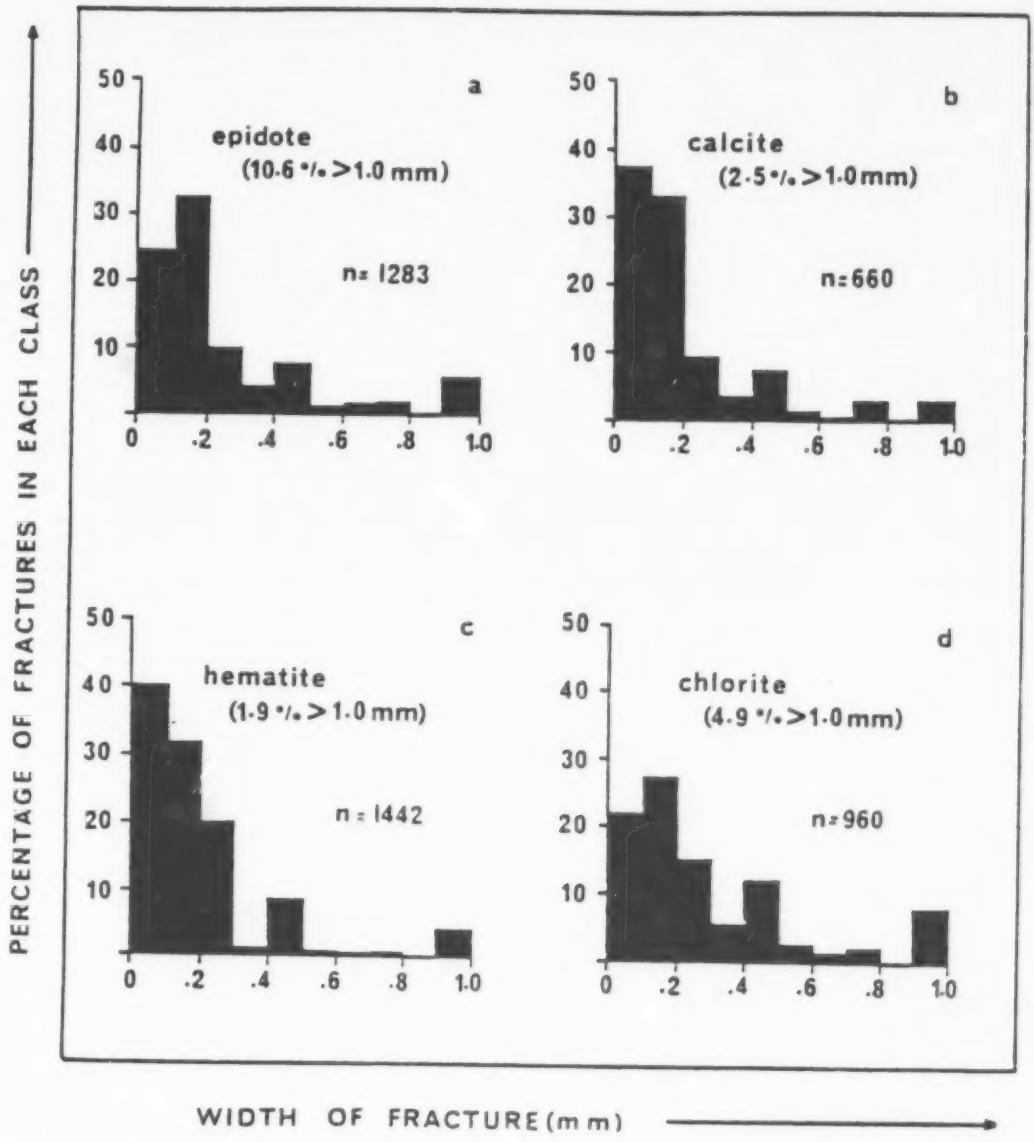

Figure 8.8: Correlation Between Dominant Filling Type and Width of Fractures From Borehole Core Through the Eye-Dashwa Pluton at Atikokan (Ref. 25)

metres. In glaciated areas where this skin has frequently been removed, alteration is usually only evident locally as dissolution/reprecipitation in fractures. Such effects are most pronounced in the near surface zone as a result of weathering, or adjacent to major fracture systems due to low-temperature hydrothermal alteration associated with ore deposits or geothermal effects. In fact, based on recent studies of low temperature geothermal systems (Refs. 35, 74, 100) fracture fillings in such alteration zones can be subsequently modified or disolved by the circulating fluids, giving rise to younger, lower temperature infillings if the correct chemical environment develops in the fracture.

The alteration of granitic rocks in the weathering profile has been studied extensively, and general trends are well documented, Table 8.5 (Ref. 26). Because gabbroic rocks are composed of mafic minerals and plagioclase, they are more susceptible to alteration than granite and thus over geologic time they tend to break down primarily to clay mineral assemblages (Table 8.6, Ref. 26).

This has also been shown by recent experiments carried out on prepared samples of granite and syenite placed in simulated granite groundwater and anorthosite and gabbro samples placed in simulated basalt groundwater maintained at 150°C. The results of these experiments indicate that the more basic rocks show the greatest alteration with the granite least affected. The clay mineralogy although not determined precisely by the experimenters was considered to follow the normal weathering breakdown process while the radionuclide sorption and desorption was found to be least on the granite and most on the syenite possibly as a result of enhanced sorption due to breakdown of the component mineralogy of the more basic rocks to clays and Fe-oxides (Ref. 99).

These data may not be directly translatable to the likely effects at vault depth in a closed system such as will exist on closure and final vault sealing. This is because weathering occurs in an open system where dissolved CO_2 can exert considerable influence on mineral solubility. The differences between shallow CO_2 - rich waters and moderately deep waters with less dissolved carbonate can be made by comparison of ephemeral and perennial springs in the Sierra Nevada (Ref. 27). The shallower, ephemeral, acid spring waters are in equilibrium with kaolinite, while the deeper, perennial, neutral springs are in equilibrium with montmorillonite.

Another naturally occurring alteration phenomenon that is known to affect plutonic rocks is the formation of wall/rock alteration halos around ore deposits. These halos either form directly during the emplacement of the ore or by diagenetic or post-magmatic (i.e. hydration) processes.

Many porphyry copper ore deposits which are emplaced in felsic igneous rocks such as quartz monzonites and granodiorites

Table 2.5: Alteration of Major Minerals in Granitoids During Weathering (Ref. 26)

Major Minerals	Alteration Assemblages		
Quartz	Partial dissolution		
K-feldspar	illite	kaolinite halloysite	gibbsite
Albite	illite montmorillonite	kaolinite halloysite	gibbsite
Plagioclase	illite montmorillonite	kaolinite halloysite	gibbsite
Biotite	chlorite vermiculite smectite	chlorite illite	kaolinite gibbsite
Muscovite	Al-vermiculite smectite illite	illite	kaolinite gibbsite
Hornblende	chlorite sphene hematite epidote	vermiculite smectite chlorite	
Magnetite	hematite		
Ilmenite	hematite	rutile	

Increasing intensity of cation leaching

Table 8.6: Alteration of Major Minerals in Gabbroids During Weathering (Ref. 26)

Major Minerals	Alteration Assemblages		
Plagioclase	smectite illite	illite kaolinite halloysite	gibbsite
Olivine	serpentine	saponite nontronite chlorite (smectites)	hematite maghemite gibbsite goethite
Pyroxenes	chlorite smectite calcite epidote	chlorite kaolinite	hematite gibbsite goethite maghemite
Amphiboles	chlorite smectite epidote	vermiculite smectite chlorite	hematite gibbsite
Fe-Ti oxides (magnetite, ilmenite)	hematite goethite maghemite rutile (leucoxene)		
	——————————→		
	Increasing intensity of cation leaching		

exhibit extensive alteration assemblages, the compositions of which are significantly influenced by the location of the interface developed between the invading magmatic fluids and the natural pluton groundwater. The mineral assemblages that typically occur include both argillitic and sericitic products (Ref. 28).

Natural geothermal systems also provide some insight into the long term effects of hydrothermal alteration. There are several geothermal areas in rock types similar to the host rock proposed for the Canadian nuclear fuel waste disposal vault. One example, the geothermal system at Steamboat Springs, Nevada occurs within granodiorites and rhyolite and andesite flows (Ref. 29). The alteration assemblages, illite, sericite, quartz, Fe-chlorite, K-feldspar, albite and calcite that are found in the relatively hot zones at depth and the chlorite and mixed layer illite-montmorillonite in cooler zones near-surface in close proximity to major areas of fracturing suggest that the alteration products are fissure flow controlled; predominantly as a function of groundwater solution pH and temperature (Ref. 28). Similar observations have been made for the Marysville and Empire Creek stocks in Montana (Refs. 74, 35).

8.3 Rock Mass Conditions

The geomechanical properties of the natural rock mass into which it is proposed to develop the underground vault are significantly affected by fracture characteristics such as spacing, continuity, roughness and by variations in intact rock condition as brought about by in situ stress variations, or by weathering or alteration effects. Because of such variations, several important design parameters, notably rock mass modulus and strength, show distinctly lower values when measured in situ compared to the laboratory. Measurement of insitu properties is therefore an important adjunct to detailed laboratory testing of core samples.

8.3.1 Thermo-mechanical Properties

The normal range of values for the major granite rock properties is given on Table 8.7 (Refs. 30 and 1) for both altered (i.e. in the weathered, pinkish state) and unaltered (i.e. fresh, grey material). Such alteration generally is brought about by degradation of the mafics and feldspathic mineral suites within the parent rock material (Table 8.8, Ref. 20).

Some variation in geomechanical properties for different granitic and gabbroic rock types occurs as a result of differences in petrography and emplacement history. The variation between the properties of typical granitic and gabbroic bodies is given on Table 8.9, Ref. 31; while on Table 8.10 (Ref. 6) some typical values are given for granite

Table 8.7: Properties of Unaltered and Altered Granite Rock (Ref. 30)

Property	Unaltered Rock	Altered Rock	Source or Method
1. Density	2.65 g/cm^3	2.58-2.63 g/cm^3	Immersion method
2. Intrinsic velocity (Compressional)	6.583 km/s	6.503 km/s	Calculated by Wright and Kamineni (1980) method
3. Magnetic susceptibility	20x10^{-3} SI	5x10^{-3} SI	R.L. Coles (1979)
4. Thermal conductivity	3.2 W/(m·K)	3.6 W/(m·K)	M.J. Drury (1981)
5. Mechanical strength	Lower	Higher	Point load test
6. Matrix permeability			Terratek, Salt Lake City, Utah
i. unconfirmed	8.38 uD	0.44 uD	
ii. confirmed	1.59 uD	0.15 uD	
7. Porosity	0.40%	0.09%	Micromeritics, Atlanta, Gorgia
8. Sorption capacity	Lower	Higher	Vandergraaf et al. (1981)

Properties of Reference Granite Host Rock (Ref. 1)

PROPERTY	UNITS	REFERENCE GRANITE ROCK MASS
Thermal conductivity	W/m°C	3.0
Specific Heat	J/kg°C	845
Thermal Diffusivity	10^6m^2/s	1.34
Mass Density	kg/m^3	2650
Young's Modulus	GPa	35
Poisson's Ratio	-	0.25
Coefficient of Thermal Expansion	10^{-6}C^{-1}	8
Blast Fracture Zone (BFZ)	m	0.5
Young's Modulus in Blast Fracture Zone (E_{BFZ})	GPa	0 to 35 (from 0.0 to 0.5m into the rock wall)

Table 8.8: Relative Resistance of Igneous Minerals to Weathering (Ref. 20)

LOW RESISTANCE	MODERATE RESISTANCE	HIGH RESISTANCE
Olivine	Intermediate to Sodic Plagioclase	Quartz
Orthopyroxene	Potassium Feldspar	Zircon
Clinopyroxene	Muscovite Mica	Magnetite
Hornblende		
Calcic Plagioclase		
Biotite Mica		
Feldspathoids		

Table 8.9: Material Properties for Intact Plutonic Rocks (Ref. 31)

Property	Unit	Granites	Gabbros
Young's modulus, E	GPa	55.2	44
Poisson's ratio, ν		0.24	0.2
Density, ρ	$Mg \cdot m^{-3}$	2.670	2.804
Thermal conductivity, k	$W \cdot m^{-1} \cdot K^{-1}$	2.83	2.08
Specific heat, c_p	$J \cdot kg^{-1} \cdot K^{-1}$	880-1100	837
Coefficient of thermal expansion, α_m	K^{-1}	8×10^{-6}	7.2×10^{-6}
Diffusivity/cm^2/s		0.011	-

Table 8.10: Material Properties of Granitic Gneiss at Room Temperature (Ref. 6)

Property	Unit	No. of Determinations	Mean Value	**Coefficient of Variation (Percent)
Thermal Conductivity	W/(m·°C)	8	3.66	7.65
Thermal Diffusivity	10^{-6} m^2/s	8	1.62	7.03
Specific Heat*	J/(kg·°C)	8	845	7.42
Coef. of Linear Thermal Expansion	10^{-6}/°C	8	6.0	8.56
Young's Modulus	GPa	10	60	9.06
Poisson's Ratio	-	10	0.23	9.14
Uniaxial Compressive Strength	MPa	10	194	11.11

* Specific heat not directly determined. Values calculated from conductivity, diffusivity and density, taking density = 2630 kg/m^3

** Coefficient of Variation is defined as $\frac{\text{Standard Deviation}}{\text{Mean Value}}$.

gneisses (see also tabulated data in Appendix B and probability graphs on Figure 8.9) (Ref. 3).

8.3.2 Hydrogeological Characteristics

The influence of fracture continuity, aperture and orientation will affect groundwater flow and hence radionuclide migration more than almost any other factor. Such flow will be controlled by the permeability and porosity, both natural and induced, of the rock mass.

The permeability of the pluton en-masse will comprise flow through the openings between individual grains (interstitial or primary permeability) and flow through fractures or other flaws in the rock (fracture permeability). In igneous rocks, the permeability of the formation is almost exclusively controlled by the fracture permeability. Thus, permeability values based on laboratory core samples generally represent a lower bound value and generally do not reflect fracture permeability. Hydraulic conductivity determinations based on field tests such as full-scale pumping tests are therefore essential for assessing actual in situ values.

An assessment of the variation in rock mass porosities for various fracture widths is presented on Figure 8.10 (Ref. 3). Some data on representative hydraulic conductivities are presented on Table 8.11 and approximate probability relationships for rock material porosity and permeability for Lac du Bonnet and Chalk River rocks are presented on Figure 8.11 (Ref. 3).

The process of radionuclide migration away from the vault will not only be influenced by the physical and chemical characteristics of the fractures and host rock mass through which the groundwater is flowing, but will also be controlled to a large extent by the degree of sorption/desorption processes that occur during the transit time that the groundwater is resident in the fracture system.

Sorption is defined as any process that removes trace ions from solution onto the rock or mineral surface (i.e. ion exchange, substitution, precipitation, etc.). From experimental work, it has been demonstrated (Ref. 32, 99) that, in general, mafic constituents display a greater sorptive capacity than felsic minerals. In addition to data on sorption coefficients obtained on whole rock itself, (Tables 8.12 (Ref. 30) and 8.13 (Ref. 33)) data are also available on a selected suite of individual minerals (Table 8.14) (Ref. 32).

8.4 Groundwater

Groundwater is variable in composition owing to its tendency to dissolve small amounts of every material it comes in contact with, including air constituents (carbon dioxide and other acidic gases, salts, ammonia), products of vegetation, soil

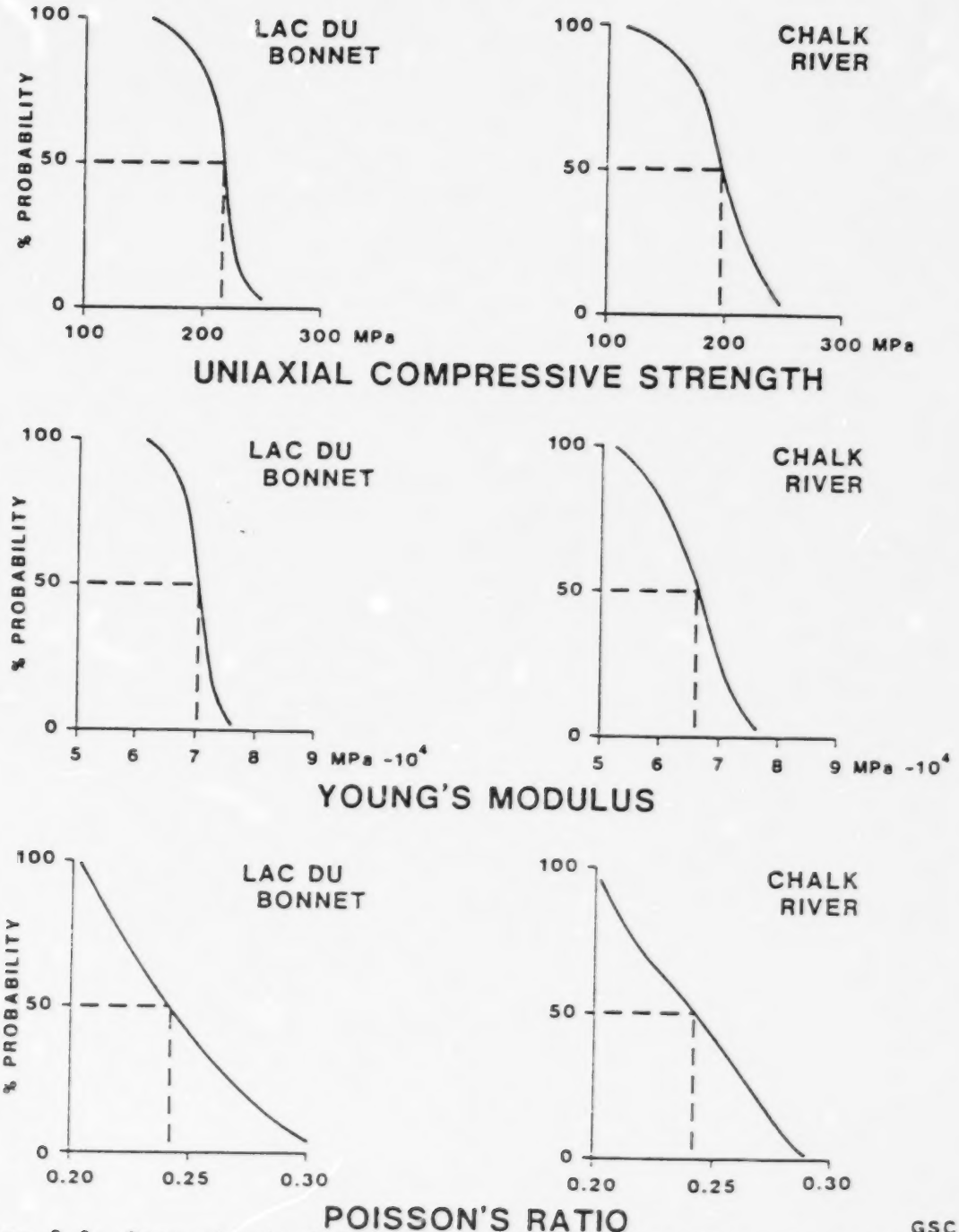

Figure 8.9: Geomechanical Properties for Typical Plutonic Rocks (Ref. 3)

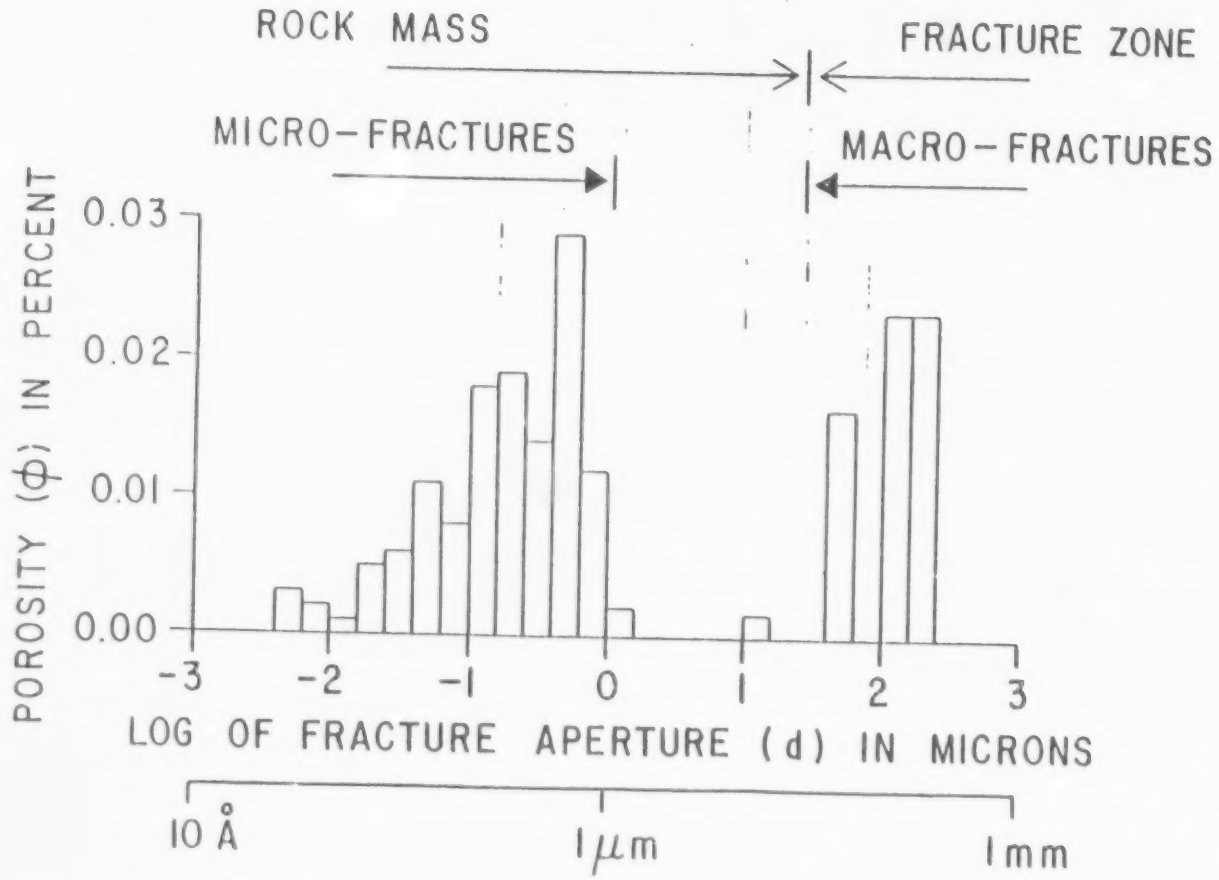

Figure 8.10: Fracture Distribution for Lac Du Bonnet Granites Determined From Samples From Borehole WN-1 and WN-2. The Porosity Values for the Microfractures are Averages of Mercury Porosimeter Measurements for 14 Granite Samples, and the Porosity Values for the Macro-Fractures are Derived from Field Information (Ref. 3)

Table 8.11: Summary of Hydrogeological Measurements in the URL Boreholes (Ref. 6)

Borehole	Depth[1] Interval	Kerm[2] (m/s)	$2b_{caf}$[3] (mm)	Comments
URL-1	73.9 - 91.0	1.5×10^{-7}	36	
URL-1	108.6 - 119.6	4.5×10^{-6}	84	
URL-1	177.2 - 184.3	5.0×10^{-11}	2	
URL-1	310.5 - 347.7	-	-	
URL-1	324.5 - 331.5	5.7×10^{-7}	42	Temporary Piezometer
URL-1	337.9 - 678.2	1.7×10^{-12}	2	
URL-2	45.0 - 55.2	5.0×10^{-6}	98	
URL-2	60.0 - 70.2	1.5×10^{-6}	66	
URL-2	86.0 - 96.2	5.2×10^{-7}	47	
URL-2	105.0 - 115.2	2.0×10^{-6}	72	
URL-2	120.0 - 130.2	2.0×10^{-6}	72	
URL-2	130.0 - 140.2	6.0×10^{-7}	48	
URL-2	140.0 - 150.2	8.0×10^{-7}	53	
URL-2	148.0 - 158.2	2.0×10^{-7}	34	
URL-2	160.0 - 170.2	4.0×10^{-9}	9	
URL-2	100.0 - 180.0	4.5×10^{-7}	87	Temporary Piezometer
URL-2	180.0 -1099.8	4.0×10^{-11}	9	
URL-2	350.0 -1099.8	2.0×10^{-11}	7	
URL-2	700.0 -1099.8	1.0×10^{-11}	4	
URL-3	50.0 - 60.4	7.0×10^{-6}	511	
URL-3	60.0 - 70.4	1.2×10^{-5}	132	
URL-3	76.0 - 86.4	4.2×10^{-7}	63	
URL-3	86.0 - 96.4	3.5×10^{-8}	19	
URL-3	115.0 - 125.4	1.0×10^{-4}	267	
URL-3	125.0 - 135.4	3.2×10^{-6}	86	
URL-3	145.0 - 155.4	3.6×10^{-6}	410	
URL-3	160.0 - 189.4	2.2×10^{-10}	10	
URL-5	79.4 - 94.1	2.6×10^{-8}	19	
URL-5	94.1 - 109.9	9.0×10^{-5}	290	
URL-5	204.1 - 219.9	1.7×10^{-6}	67	
URL-5	219.8 - 234.5	2.0×10^{-8}	8	
URL-5	251.8 - 266.5	2.1×10^{-5}	179	
URL-5	250.2 - 269.4	1.6×10^{-5}	178	
URL-5	334.4 - 349.5	5.0×10^{-9}	11	Temporary Piezometer
URL-5	340.9 - 500.5	4.6×10^{-12}	2	
URL-6	30.0 - 50.1	6.0×10^{-8}	28	
URL-6	90.0 - 102.1	2.2×10^{-7}	47	
URL-6	101.0 - 127.1	1.2×10^{-7}	35	
URL-6	127.0 - 147.1	5.5×10^{-10}	6	
URL-6	147.0 - 167.1	4.0×10^{-7}	53	
URL-6	185.0 - 205.1	2.1×10^{-8}	9	
URL-6	200.0 - 220.1	2.4×10^{-8}	10	
URL-6	230.0 - 250.1	5.0×10^{-8}	17	
URL-6	253.0 - 273.1	2.8×10^{-7}	45	
URL-6	280.0 - 300.1	9.7×10^{-9}	14	
URL-6	250.0 - 280.0	-	-	Temporary Piezometer
URL-7	34.7 - 54.9	1.3×10^{-7}	36	
URL-7	55.0 - 75.1	1.0×10^{-5}	155	
URL-7	70.0 - 90.1	1.5×10^{-5}	177	
URL-7	93.0 - 113.1	4.0×10^{-6}	114	
URL-7	125.0 - 145.1	1.5×10^{-7}	38	
URL-7	145.0 - 165.1	1.1×10^{-6}	74	
URL-7	175.0 - 195.1	5.5×10^{-7}	51	
URL-7	190.0 - 200.0	-	-	Temporary Piezometer

[1] Depth interval is measured distance from first casing joint in metres

[2] Kerm is Permeability, assuming porous media equivalent model

[3] $2b_{caf}$ is Fracture Aperture, assuming single fracture responsible for fluid flow

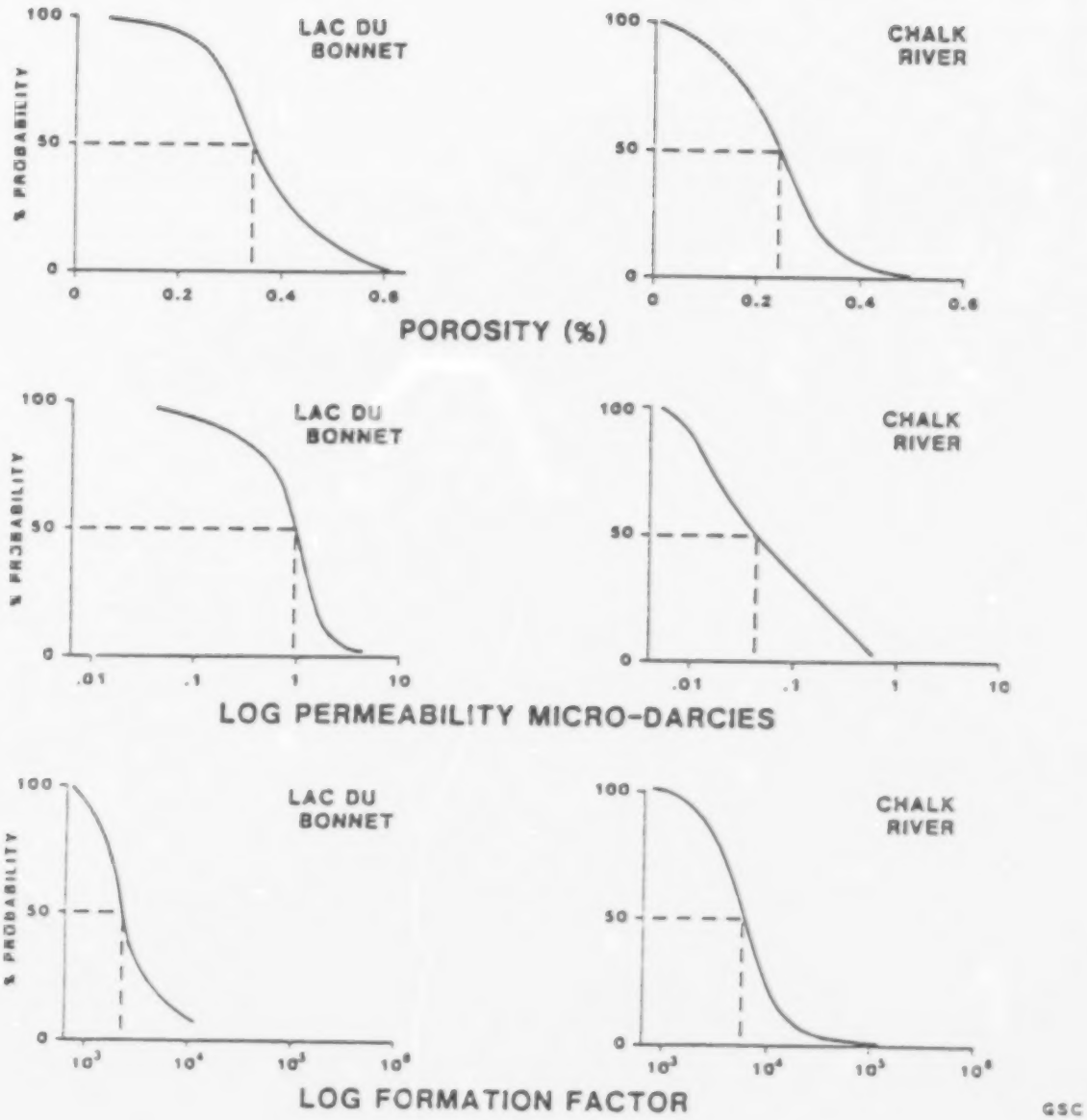

Figure 8.11: Hydrogeological Characteristics for Typical Plutonic Rocks (Ref. 3)

Table 8.12: Sorption Coefficients for ^{238}U on Four Representative Rock Types (Ref.30)

Rock type	K_a 20 days (cm)	K_a 34 days (cm)
Anorthosite	6.6 ± 1.7	7.1 ± 2.3
Gabbro	5.5 ± 5.2	7.2 ± 5.3
Granite	0	0
Hornblende Syenite	0.15 ± 0.12	0.041 ± 0.037

Table 8.13: Sorption of Strontium on Representative Plutonic Rock as a Function of Groundwater Composition (Ref.33)

K_a (cm) for Sr (28-day sorption)

Rock Type / Groundwater	Anorthosite	Gabbro	Granite	Syenite
Granite	-	-	0.35	3.6
Basalt	0.33	0.35	-	-
WM-1* 6 000 ppm CL' (dilute brine)	0.06	0.05	0.03	0.11
SCSSS* 30 000 CL' (concentrated brine)	0.05	0.10	0.05	0.07

* relative error probably ~ 100% due to poor sorption - poor counting statistics.

Table 8.14: Sorption Coefficients for Selected Minerals (Ref. 32)

(7 day results)

Mineral	K_a (cm)			
	^{90}Sr	^{137}Cs	^{147}Pm	^{241}Am
Albite "A"	0.11	0.23	0.76	3.1
Albite "B"	0.05	0.11	1.0	26.0
Apatite "A"	0.04	0.05	470.0	7.3
Apatite "B"	0.02	0.02	600.0	> 1800.0
Biotite "P"	0.02	1.9	10.0	5.2
Biotite "45"	0.00	15.0	37.0	> 1500.0
Biotite "90"	0.03	33.0	58.0	> 2400.0
Epidote	0.11	5.2	510.0	41.0
Hornblende "A"	0.05	2.8	83.0	16.0
Hornblende "B"	0.10	3.4	87.0	> 1800.0
Labradorite	0.11	0.27	2.7	4.5
Microcline 1A	0.04	0.27	2.9	> 1500.0
Microcline 2A	0.02	0.13	5.1	6.3
Microcline 1B	0.08	0.18	1.2	2.7
Microcline 2B	0.03	0.03	-	25.0
Olivine	0.02	0.04	180.0	> 1700.0
Pyroxene	0.10	0.14	280.0	13.0
Titanite	0.06	0.91	0.85	> 2100.0

Biotite

P - Parallel to (100) Clevage Plane
45 - 45° to (100) Cleavage Plane
90 - 90° to (100) Cleavage Plane

Albite, Apatite and Microcline

(A) Parallel to (100) Cleavage Plane
(B) 90° to (100) Cleavage Plane

Hornblende

(A) Parallel to (110) Cleavage Plane
(B) 90° to (110) Cleavage Plane

minerals, and rock components, especially carbonate minerals (Ref. 34). Further interactions by ion exchange can replace, e.g., calcium by sodium or potassium; a near-surface water high in calcium bicarbonate can become nearly free of calcium on passing through a bed of arkosic sandstone. Temperature changes can cause changes in solubility, leading to further dissolution of rock around microscopic cracks, or on the other hand to exsolution that may lead to filling of existing cracks and cementation of grains, with reduction in porosity.

Laboratory experiments and computer simulation (Ref. 33) have demonstrated the possibility of these effects. Field studies have shown that penetration of plutonic rock formations by surface water does take place (Ref. 36), for the discrepancy between precipitation and runoff is too great to be accounted for by evapotranspiration. Johnston (Ref. 34) has shown, by review of literature on groundwater analysis as a function of depth, that regularities in change of composition can be recognized. Specifically, near-surface water often contains chiefly calcium and bicarbonate ions resulting from attack of limestone by normal rainwater. When it penetrates to moderate depths (+ 100m) the calcium is largely replaced by sodium, and some chloride is present. At greater depths (> 400m) the bicarbonate is absent, and salt concentrations increase, the typical list of ions including chloride, sodium, calcium and sulphate. Johnston emphasizes that the presence of saline water at various depths is not at all uncommon.

From the numerous analyses which have been carried out on groundwaters from granitic terrains it has been determined that they have relatively high Na^+, SiO_2 and F^-, but low Ca^{2+}, Mg^{2+} and pH. Gabbroic groundwaters, by comparison have high Ca/Na and Mg/Ca ratios, high SiO_2 and low F^-. If pH and Eh are low, it has been found that Fe and Mn contents are also quite high (Table 8.15 - Ref. 38). These trends are also shown by other suites of analyses (Table 8.16 - Ref. 34).

Much work has been concentrated on defining the chemical composition and age of the brines found within many PreCambrian crystalline rock terrains and considerable debate still continues regarding their mode of origin (Ref. 39). Summary analysis results for typical brines as determined from this research are presented on Table 8.17 (Ref. 39) and the ionic composition for typical granitic brine is shown on Table 8.18 (Ref. 34).

The trends established from literature searches (Ref. 34) of depth variable groundwater composition as discussed previously have also been documented for the bedrock at the URL site in the Lac du Bonnet batholith in Manitoba, Table 8.19 (refs. 34 and 40). These results indicate that the water in the upper 50 m of bedrock is of the Ca/HCO_3 type. The water below 400 m is saline. Carbon-14 dating of these waters was uncertain but showed that the age of the groundwater increased with depth, from less than 500 years at 37 m depth, 2500 years at 98 m, to

Table 8.15: Groundwater Compositions From Granitic and Gabbro Terrains (Selected Analyses[1]) (Ref. 38)

Rock Type and Location	(Mississippian) Granite West Warwick RI	(Carboniferous) Granite McCormick Co. SC	(Paleozoic) Granite Ellicott City MD	Gabbro Harrisburg NC	Gabbro Laurel MD
Depth* (ft)	140	252	28	79	35
SiO_2	20	35	39	56	21
Al	0.0	0.1	0.9	-	0.3
Fe	0.19	0.18	1.6	0.06	1.2
Mn	0.0	0.13	0.0	0.0	0.16
Cu	0.0	0.0	-	-	-
Zn	0.07	0.09	-	-	-
Ca^{2+}	6.5	13	27	32	16
Mg^{2+}	2.6	4.3	6.2	16	10
Na^{+}	5.9	8.4	9.5	25	15
K^{+}	0.8	3.5	1.4	1.1	1.5
HCO_3^-	38	72	93	203	20
CO_3^{2-}	0	0	0	0	0
SO_4^{2-}	0.9	6.9	3.2	10	59
Cl^-	5.0	3.8	5.2	13	25
F^-	0.3	0.2	0.0	0.2	0.1
NO_3^-	1.5	0.4	7.5	2.7	2.2
PO_4^{3-}	0	0.1	-	-	0
Specific conductivity (at 25°C)	76	150	258	388	259
pH	7.6	7.0	6.6	6.8	5.6
Temp (°C)	11.1	18.1	6.0	16.7	
Ra (pCi/L)+	0.4	0.2	-	-	
U (pCi/L)+	1.4	0.4	-	-	

1 Results in mg/L except where noted
* 1 ft = 0.3048 m
+ 1pCi = 37 GBq

Table 8.16: Mean Chemical Composition[1] of Waters Collected on Granitic Massifs and Basic Rocks (after Tardy, 1971) (Ref. 34)

Location	No.		pH	HCO_3^-	Cl^-	SO_4^{2-}	SiO_2	Na^+	K^+	Ca^{2+}	Mg^{2+}
granitic massifs											
Norway	28	M	5.4	4.9	5.0	4.6	3.0	2.6	0.4	1.7	0.6
		σ	0.6	3.6	4.0	1.6	1.6	1.7	0.2	1.6	0.3
Vosges	51	M	6.1	15.9	3.4	10.9	11.5	3.3	1.2	5.8	2.4
		σ	0.5	13.0	1.9	8.5	6.2	2.0	0.8	4.7	2.4
Brittany	7	M	6.5	13.4	16.2	3.9	15.0	13.3	1.3	4.4	2.6
		σ	0.5	6.2	6.0	2.0	7.2	6.1	0.4	3.0	1.1
Central Massif	10	M	7.7	12.2	2.6	3.7	15.1	4.2	1.2	4.6	1.3
		σ	0.5	6.0	1.5	2.0	10.2	2.8	0.9	3.2	0.9
Alrance Spring F	77	M	5.9	6.9	<3	1.15	5.9	2.3	0.6	1.0	0.4
		σ	0.3	1.3	-	0.45	1.6	0.3	0.3	0.3	0.1
Alrance Spring A	47	M	6.0	8.1	<3	1.1	11.5	2.6	0.6	0.7	0.3
		σ	0.4	2.4	-	0.5	1.2	0.2	0.2	0.1	0.05
Corsica	25	M	6.7	40.3	22.0	8.6	13.2	16.5	1.4	8.1	4.0
		σ	0.4	36.0	15.3	6.2	7.4	12.1	0.9	7.1	4.0
Sahara	8	M	6.9	30.4	4.0	20	9	30	1.8	40	-
		σ	0.5	5.0	2.0	4	3	2	0.3	10	-
Senegal	7	M	7.1	43.9	4.2	0.8	46.2	8.4	2.2	8.3	3.7
		σ	0.9	24	2.5	0.7	31.2	5.4	1.1	5.3	2.5
Chad	2	M	7.9	54.4	<3	1.4	85	15.7	3.4	8.0	2.5
		σ	-	-	-	-	-	-	-	-	-
Ivory Coast (Korhogo, dry season)	54	M	5.5	6.1	<3	0.4	10.8	0.8	1.0	1.0	0.10
		σ	-	-	-	-	-	-	-	-	-
Ivory Coast (Korhogo, wet season)	59	M	5.5	6.1	<3	0.5	8.0	0.2	0.6	<1	<0.1
		σ	-	-	-	-	-	-	-	-	-
Malagasy (High Plateaus)	2	M	5.7	6.1	1	0.7	10.6	0.95	0.62	0.40	0.12
		σ	-	-	-	-	-	-	-	-	-
basic rocks											
Norway	9	M	5.5	5.0	3.5	4.8	3.4	3.5	0.5	1.7	0.9
		σ	0.8	3.2	2.9	2.1	1.1	2.4	0.3	1.0	0.4
Vosges	14	M	6.1	19.3	2.2	5.8	9.2	2.3	0.6	4.5	1.5
		σ	0.6	11.1	0.9	3.0	3.1	1.2	0.3	3.1	0.9
Central Massif	10	M	8.2	57.0	12.6	7.4	30.5	13.1	7.1	23.8	9.4
		σ	0.6	30.0	7.4	5.1	6.3	7.5	3.2	12.1	5.3
Corsica	7	M	7.1	16.5	33	13.7	21.4	20.5	1.58	16.0	13.7
		σ	0.5	16.0	21	7.9	4.3	14.8	1.1	9.4	5.3
Sahara	5	M	6.8	30.0	10.6	16.1	14.5	6.9	4.4	31.6	3.9
		σ	0.4	6.0	6.0	5.0	5.1	4.3	0.7	14.3	1.6
Senegal	32	M	7.0	198	4.1	1.6	55	24	2.5	24	23
		σ	1.0	176	2.7	1.8	22	24	1.6	19	22
Ivory Coast	2	M	7.3	597	3.0	0.40	120	37	1.5	52	50
		σ	-	-	-	-	-	-	-	-	-
Malagasy (Eastern Coast)	5	M	6.1	18	5.5	2.4	16.2	4.3	0.4	2.8	1.4
		σ	0.2	5	1.1	0.9	3.7	0.8	0.2	0.7	0.3

1. Values in mg/L

Table 8.17: Representative Brine Chemistries From Sites on the Canadian Shield (Ref. 39)

Location	Sudbury, Ontario	Thompson, Manitoba	Yellowknife, N.W.T.
Depth (m)	1500	1500	1500
pH	6.80	5.00	5.55
Temperature (^{o}C)	22.0	18.0	22.5
Density	1.185	1.086	1.174
Element ($mg.L^{-1}$)			
Ca	63 800.00	28 600.00	57 300.00
Na	18 500.00	10 100.00	32 600.00
Mg	23.50	2 490.00	920.00
K	371.00	59.90	495.00
Sr	1 440.00	457.00	1 640.00
Cl	166 200.00	74 600.00	142 000.00
Br	1 200.00	896.00	1 520.00
SO_4	265.00	6.00	< 1.00
HCO_3	43.00	19.00	2.00
Ba	27.20	15.10	46.50
Li	0.77	0.12	1.67
I	13.80	1.33	0.20
F	7.00	5.88	26.90
Si	9.60	6.90	8.00
B	3.60	1.88	9.19
Al	1.81	1.18	17.50
Fe	1.96	1.22	18.60
Mn	0.72	3.77	21.80
Cr	0.43	0.83	0.50
Co	22.00	1.12	5.80
Ni	3.28	1.13	12.70
Cu	0.33	0.23	0.81
Zn	0.53	0.24	0.59
Pb	3.10	2.03	2.42
Cd	0.94	0.26	1.02
Ag	0.25	1.33	3.99
Total dissolved solids	252 000.00	117 000.00	237 000.00

Table 8.18: Concentration of Various Ions in Brine (Ref. 34)

Ions	Concentration (mg/L)
Mg^{+2}	200
SO_4^{-2}	790
Cl^-	34, 310
Na^+	5047
Sr^{+2}	20
SiO_3^{-2}	50
HCO_3^-	10
NO_3^-	50
K^+	50
Ca^{+2}	15,000

Table 8.19: Summary of Groundwater Chemistry[1] Whiteshell Nuclear Research Establishment, Pinawa (Ref. 34)

	WN-3-37m		WN-3-90m		WN-1-133m		WN-1-445m		WN-1-457m		WN-4-915m	
	surface	downhole[2]	surface	downhole	surface	downhole	surface	downhole	surface	downhole	surface	downhole
Ca	116	111	47.0	25.4	64.2	16.9	64.6	76.1	1090		1270	
Mg	45.4	45.4	21.1	11.1	22.4	5.8	22.5	22.4	51.9		15.1	
Na	33.9	33.9	123	160	9.8	95.0	8.5	9.3	992		1950	
K	4.3	4.4	4.5	3.3	2.9	1.2	3.0	3.0	9.0		11.9	
Sr	1.3	1.3	1.0	0.5	0.3	0.3	0.2	0.3	8.7		16.4	
B	0.18	0.18	0.60	0.77	0.10	0.74						
Ba	0.20	0.18	0.21	0.37	<0.07	<0.07	<0.04	<0.04	4.3		6.2	
Li	<0.02	<0.02	<0.9	<0.9	<0.04	<0.04	<0.04	<0.04	0.15		0.18	
HCO_3	707		375	328	460	296	420	330	175		18	
SO_4		131	97.6	82.3	7.5	4.9	1.0	1.3	500		676	
Cl		8.2	75.6	119	<0.4	23.3	5.6	6.2	2780		5410	
F		0.9		4.1		3.8	0.6	0.7	1.1		1.9	
Br				<0.39		<0.39		<0.39	<2.5			
I			<0.12	<0.12		<0.12			<0.12		0.24	
NO_3		<0.19	<0.40			<0.40	<0.17	<0.17	<0.9		<0.9	
NO_2			<0.19			<0.19		<0.22			<0.6	
NH_4			0.32			0.22		0.44	1.25		<0.20	
Si	7.0	7.9	4.6	3.3	9.2	8.5	6.6	7.6	4.8		2.4	
Al	<0.20	<0.20	0.34	0.27	0.20	0.20	<0.14	<0.14	5.6		7.0	
Fe	0.60	<0.20	0.09	0.30	<0.11	0.39	0.23	0.15	5.3		0.30	
Mn	0.11	0.10	0.08	0.04	0.13	<0.03	0.10	0.09	0.7		0.08	
Cu	<0.04	<0.04	<0.06	<0.06	<0.04	<0.04	<0.02	<0.02	<0.06		<0.06	
Pb	<0.06	<0.06	<0.04	<0.04	<0.04	<0.04	<0.06	<0.06	0.2		0.34	
Ni	<0.10	<0.10	<0.10	<0.10	<0.02	0.05	<0.03	<0.03	0.43		0.57	
Zn	0.03	0.05	0.69	<0.10	<0.04	<0.04	<0.03	<0.03	1.0		<0.10	
Co	<0.18	<0.18	<0.02	<0.02	<0.07	<0.07	<0.06	<0.06	0.12		0.26	
Cd	<0.02	0.06	<0.06	<0.06	<0.05	<0.05	<0.05	<0.05	<0.06		0.09	
Cs	<0.04	<0.04	<0.05	<0.05	<0.03	<0.03	<0.02	<0.02	<0.05		0.06	
U	0.20	0.20	0.34	0.34	0.030	0.080					0.002	
pH(field)	7.3		7.8	8.0	7.8		7.6					
pH(lab)				7.9	8.4			7.7			8.6	
Eh(mV)	+140		+110		+400		+180					
cond(mS/m)			91.7		39.0	43.8		48			1480	

1. Results in µg/mL except where noted.
2. Analyses shown are for the last surface water sample collected during pumping and the sample retrieved downhole at the end of the pumping period.

much greater ages at 400 m, perhaps approaching 20,000 years (Ref. 40).

Studies of groundwaters elsewhere in the Canadian Shield have shown that such saline brines are also very common at depths greater than 650 m (Ref. 39). Above this level, waters are typically Na-Ca-HCO_3-SO_4 dominated with low total dissolved solids. The brines by contrast have up to 280 $g.L^{-1}$ total dissolved solids, and are Ca-Na-Cl dominated. They form a chemically and isotopically unique grouping, but overprinting of the local host rock type is evident.

In an attempt to categorize groundwater types for undertaking tests on the selected reference backfill and buffer materials, and to aid in determining physical and chemical interaction effects for groundwater flow through fractured plutonic rock, several synthetic groundwater compositions have been developed. These duplicate most of the salient properties of real groundwaters found within the plutons that have been sampled. Table 8.20 (Ref. 32) lists the chemical constituents of these synthetic solutions.

It should be appreciated that of these synthetic groundwaters, the granitic groundwater composition is based on a number of granite groundwater compositions reported in the literature; the WN-1 saline solution is based on an early analysis of groundwater from the WN-1 borehole at Pinawa (Analytical Science Branch, 1979); and the SCSSS solution is based on average high salinity groundwater from the Canadian Shield.

Furthermore the history of the groundwater should also be considered, as this is as important as the composition of the rocks in the immediate vicinity. Isherwood et al. (Ref. 37) make clear the dangers of simulating groundwater by attempting to equilibrate water with rocks in the laboratory. They report large differences between the composition of real granite groundwater and laboratory equilibrated "granite water". Some care may therefore be needed in interpreting laboratory tests with synthetic waters to the in situ environment.

Table 8.20: Ionic Composition of Synthetic Groundwaters (Ref. 32)

Ion	Concentrations ($mg \cdot L^{-1}$) in Groundwaters		
	Granite Groundwater	WN-1 Saline Solution	Standard Canadian Shield Saline Solution
Na	8.73 ± 0.09	1800 ± 13	5180 ± 120
K	3.53 ± 0.51	17.3 ± 0.5	58.2 ± 5
Mg	3.85 ± 0.03	57.5 ± 0.3	189 ± 2
Ca	12.0 ± 0.7	1840 ± 43	15100 ± 430
Sr	-	26.3 ± 0.6	30.0 ± 0.6
Fe	-	0.17 ± 0.06	-
Si	-	-	19.4 ± 0.8
Cl	5.37 ± 0.10	5650 ± 100	32100 ± 1000
SO_4	11.0	938 ± 20	866 ± 20
NO_3	< 0.2	21 ± 2	36 ± 2
F	0.22 ± 0.03	0.2 ± 0.1	1.7 ± 0.3
PO_4	-	-	-
HCO_3	98 ± 2	58 ± 2	43 ± 2
pH	8.0	7.0	7.6

9. Construction Perturbations

During the excavation and development phase of vault construction, considerable perturbations will be introduced into the natural groundwater system by the construction sequence. In addition, major adjustments in the local stress field will occur around the vault in response to excavation; and extensive fracture development may occur locally to the excavations. Mostly such fracturing will develop as a result of blast induced stress effects however some may develop in response to the modified in situ stress field.

Following completion of excavation and commencement of borehole emplacement of wastes, buffer and backfill placement will commence. Even though the buffer material will be placed relatively moist, it is considered that it will dry out immediately adjacent to the canisters due to radiogenic heat effects. In consequence, shrinkage cracks may develop. Although less likely to be significantly affected by such shrinkage affects, cracks may also develop through the backfill material.

Considerable effort is therefore being expended towards ensuring that the buffer material will re-seal once it rewets. Such rewetting will occur when natural rock mass groundwater conditions re-establish themselves after some unknown time-dependent radiogenic heating delay.

Initially, because of the on-surface preparation process and underground placement methods, the backfill and buffer material will be virtually saturated with natural surface-type water. With time, and resaturation of the desaturated, depressurized zone of the rock mass surrounding the vault, natural groundwater flow will resume. Initially, the desaturated zone will reflood with groundwater which may contain remnants of the construction drillwater introduced into the rock mass during excavation drilling and blasting. Such waters can contain considerable quantities of nitrates remaining from degradation of the explosives used during excavation.

With time, and primarily because of radiogenic heating effects, it is anticipated that groundwater flow patterns will change. Rather than flow occurring towards the vault as in the initial stages after vault sealing, flow patterns may well become controlled by the thermal gradients set up between the vault location and other, natural groundwater controls in the region around the vault. The original, natural influence of lakes and other major surface controls or of the natural density gradients governing the flow paths of the deep saline groundwaters may thus be considerably altered by the presence of the hot water environment created by the vault, especially if an upwelling thermal plume develops within the more permeable blast-fractured zone adjacent to the shaft.

The establishment of this radiogenically controlled thermal field around the vault will influence not only the movement of the groundwater but also its chemistry. Rock/groundwater interaction affects will also occur, predominantly in the immediate vicinity of the vault but also along preferred flow paths through the rock mass.

Such processes may also be infuenced by changes to the rock mass and engineered barrier materials brought about by direct thermal and radiochemical affects.

10. Effects of Radiation on Solid Materials

10.1 Waste Containers

The likely effects of radiation on the waste containers include direct effects on the metal, and the acceleration of chemical and electrochemical corrosion of the containers.

10.1.1 Direct Effects

Radiation effects on metals have generally been studied for application in nuclear reactors where the predominant effects are caused by neutrons. Physical properties such as yield strength, tensile strength and hardness are increased while ductility and elongation are decreased at neutron fluences above 10^{17} fast (>1 Mev) neutrons/cm^2 (Ref. 41, p. 439). At the maximum surface neutron flux of 300 n/cm^2.s (Ref. 1, Figure A-5.2, FRW container), this dose will be applied to the container material in 10^7 a, neglecting decay of the neutron source with time. Since the assumed mean container failure times due to corrosion are 16,900 a (Ref. 11, p. 41) for the UF container and 18,100 a (Ref. 11, p. 50) for the FRW container, the effect of neutron irradiation does not appear to be significant in general. Specific data on the effects of gamma and neutron irradiation on titanium were not found.

10.1.2 Chemical and Electrochemical Corrosion

In normal deep groundwater, which is expected to be anoxic, most metals of construction are expected to be corroded very slowly. This includes copper, the apparent Swedish choice, which is low on the electrochemical series, but also metals higher in the series such as zirconium and titanium, which are thermodynamically unstable towards corrosion in such an environment, but which are normally protected by a layer of dense, adhering oxide. If the expected lifetime of titanium containers in the order of 17,000 years noted above (Ref. 11) is based on uniform corrosion, this estimate is probably optimistic, as the assumption of uniform corrosion is not likely to be valid for the whole period.

The rate of corrosion can be accelerated by non-uniformity in the physical state of the metal surface. This may arise from (a) stress due to non-uniform mechanical forces (b) the presence of seams or welds or (c) non-uniform composition or packing of the buffer material around the container. In any of these conditions, an electro-chemical cell can be set up in which the stressed region becomes the anode, where corrosion is accelerated, and the unstressed regions are cathodic, and protected. The result may be local pit corrosion, and the container may be locally pierced, the contents being exposed to groundwater much earlier than would otherwise be expected. The rate of this local corrosion will not necessarily be very rapid. Its rate depends on the concentrations of ions in general, and notably chloride ions in particular, and will be

close to a minimum in the nearly neutral pH of the groundwater expected at depth. It is suggested in the Second Interim Assessment that the model will be improved by obtaining data from field and laboratory experiments (Ref. 11, p. 130).

Some clays may contain small particles of iron in the metallic state. Such a particle, if it came into intimate contact with a titanium surface would make an electrochemical cell in which the iron would be the cathode and neighbouring areas of the titanium would be subject to accelerated corrosion. Characterization of clays for use in buffer mixtures should include analysis for metallic iron.

As described below, gamma radiation can induce a reaction in which water decomposes to hydrogen and hydrogen peroxide (chiefly). The hydrogen can diffuse away relatively quickly, leaving an oxidizing halo around the waste containers. The hydrogen peroxide decomposes further to water and oxygen. In the resulting oxygenated groundwater, uniform corrosion of titanium is still slow, though perhaps not quite so slow. The electrolytic processes described above would also be operative. The net effect would be to enhance the rate of local corrosion, perhaps by as much as an order of magnitude. As noted below, this oxygenated condition is sustained only during the period of relatively high radiation dose rate, perhaps 50 years (Ref. 42, p. 14) . The use of corrosion rates estimated for anoxic conditions is probably nearly correct for the calculation of container lifetimes.

The relative importance of container lifetimes has been a subject of disagreement. At the OECD Paris meeting (Ref. 42, p. 16) it was noted that workers in the United States and West Germany considered solubility and leachability much more important than container lifetimes. Wuschke et al. (ref. 11), noting that certain soluble radionuclides, including Cs, are at least in part present in intergranular spaces in the used fuel, assumed that they would escape promptly from a breached container. Their estimates of groundwater transit times (>70,000 a) agree in order of magnitude with those calculated by Chapman (Ref. 43, 44) (55,000 to 500,000 a) for Cs^+ in granite from available estimates of the highly variable ion-exchange capacity and permeability of granite (Refs. 37, 45). These workers disagree, however, on the consequences of these estimates, Chapman et al. calling for a more durable container, while the Canadians (Wuschke et al) suggest that neither the container nor the buffer provide important delays, except in a few simulations of the FRW vault (Ref. 11, p. 22), where groundwater transit times of less than 10,000 a were calculated.

10.2 Radiation Effects on Waste Form

10.2.1 Direct Effects

The physical and chemical properties of materials may change when they are subjected to very high doses of ionizing radiation. Thus it is conceivable that the radiation emitted by high level radioactive waste could have a negative impact on the waste form (glass, ceramic, etc.), the container for the waste, the buffer materials and the plutonic rock itself.

The principal effects of alpha and beta decay include ionization, heating, transmutation of elements and atomic displacement due primarily to alpha-recoil nuclei and to a lesser extent to alpha-particle elastic collisions. Atomic displacements are considered to be the most detrimental towards the solid-state integrity of the waste form, as they could lead to swelling or compaction of vitreous materials or metamictization* of crystalline ceramic phases, with the risk of development of porosity. Petit et al. (Ref. 46) observed that implantation of ca. 200 keV Pb ions, simulating alpha recoils, greatly increased the dissolution rate of certain uranium-bearing minerals, suggesting that autoradiolysis of the waste form might greatly increase leachability. This effect was not observable below a critical fluence of about 5×10^{12} ions cm^{-2}.

Tait (Ref. 47) cites experiments carried out by various workers that enable the comparison of the rates of leaching of amorphous specimens subjected to gamma and alpha irradiation. Only the alpha-irradiated specimens (which had been doped with actinides) exhibited a change in leach rate, suggesting that atomic displacement effects caused by alpha-recoil dominate over ionization effects in the solid. The observed changes in leach rate are, however, less than a factor of 4.

10.2.2 Indirect Effects

All the materials being considered for containers are potentially subject to corrosion, but in the anoxic deep groundwater, corrosion of copper (being considered in Sweden), stainless steel, zircalloy, titanium and lead (being considered as a void-filling material) are all very slow, not necessarily for lack of thermodynamic tendency, but often for kinetic reasons or owing to the formation of a protective oxide layer. As long as the container is intact, it will be subject to this slow corrosion. A breached container provides a new possibility, which is the formation of an electrochemical cell, in which two (or more) metallic or metal-like conductors, in contact with each other, are also in contact with the

[*Metamictization is defined as the transformation of a mineral to a different state, usually amorphous, as a result of exposure to a high radiation dose]

groundwater. In such a situation, one metal is subject to more rapid corrosion while the other, by being made the cathode of the cell, is protected until the more actively corroding metal is exhausted.

Zirconium, in the form of zircalloy, is one of the more active metals, but is normally protected by an oxide layer. It would be subject to corrosion, however, if it were exposed to groundwater while in contact with copper, stainless steel or lead. Once it is gone, and the UO_2 exposed, the UO_2 becomes cathodically protected. Its oxidation to UO_2^{2+} would be prevented by any of the metals above-noted (Ref. 48). This will tend to delay the effects of water radiolysis, discussed below. The time of this delay is difficult to predict, as the rate of the accelerated corrosion of the breached container is dependent upon accidental variables, the chief of which is the electrical resistance of the circuit, which will depend in turn on accidents of local thickness of corrosion deposits, etc. It is likely to extend the time during which radionuclides, other than those already in voids between fuel pellets, remain immobile by a significant fraction of the lifetime of the container.

The same authors also conclude that, even after the oxidation of UO_2 begins, it will be chiefly redeposited as solid UO_3 hydrates. The consequence of this will be the release of Cs, Sr, I, Tc and a few other more soluble elements, while Th and Pu are to a high degree retained. It is not clear whether they considered the effects of bicarbonate, which if present would enhance the solubility and mobility of the actinides. As noted elsewhere, it is expected that in Canadian practice it will be possible to choose a place where the bicarbonate concentration is low.

The assumption of anoxia is likely to be a poor one, even if the groundwater is anoxic, in the immediate vicinity of the stored wastes. The reason is that the effect of radiation on water, in the absence of chemically active substances such as the metal compounds discussed below, is to break it down into hydrogen and oxygen. Since diffusion rates are inversely proportional to the square root of molecular mass, other things being equal, the hydrogen is expected to diffuse away four times as quickly as the oxygen. This will create a highly reducing halo around an oxidizing core. Actinides and many fission products may be oxidized therefore, and put into mobile, anionic form. They may then be transported to the reducing halo and redeposited. While it is unlikely that they will get far, it is all the more important that a mixture of reducing agents in the buffer and backfill be considered. Direct radiation effects on silicate minerals can also release oxygen and create a locally oxic environment. This is expected to be limited to the waste form, however, as only alpha-irradiation seems to be able to produce this oxygen release.

10.3 Mineral Components

The effects of radiation on minerals and rocks may be direct, or indirect, acting through the heating effect of absorbed radiation, or through radiolytic alterations in groundwater geochemistry. Table 10.1 lists some possible effects, and summarizes what is known about them. It is apparent that this knowledge is incomplete. This chapter treats the direct radiation effects. Primarily thermal and aqueous radiochemical effects are discussed in Chapters 12 and 13.

Comparatively little information exists on the influence of radiation on mineral properties. This applies to both the allowable stored radiation energy (energy associated with lattice damage through displacement of atoms, which is released when the material is annealed) and the radiochemical effects (which can result in the decomposition of some crystalline solids).

Certain silicates (e.g. zircon, ref.100) and quartz (ref. 49) can store energy in this way, to the point of metamictization. In quartz, it was reported that temperatures close to 800°C were required for annealing. The radiation regimes and the time scales of these experiments were quite unlike those expected in the present concept.

10.3.1 Buffer

The radiation dose which would be received by the buffer material would be much less than that received by the waste form in the container. As noted in the discussion by Tait (Ref. 50), alpha particles are the only radiation which would cause significant changes in the physical properties. The range of alpha particles is, however, exceedingly small. For example, the 5.2 MeV alpha particles of 239 - plutonium have a range of only 3.8 cm in air and about 0.1 cm in stainless steel.

At the time of burial, assumed to be 10 years after removal from the reactor, the maximum container surface dose rate will be approximately 154 Svh^{-1} (see table 6.4) and will be almost entirely in the form of gamma radiation, with a small component of neutrons (0.51 Svh^{-1}, see table 6.5). With the decadic attenuation distance of 130 mm for UF (from fig. 6.5) and 120 mm for FRW (from fig. 6.6) (cf. 150 mm in salt (Ref. 51) or 133 mm in Climax granite (Ref. 52, p. 17) the dose rate will be below 0.25 Svh^{-1} for UF and 0.9 Svh^{-1} for FRW at the outside of the 277 mm and 312 mm buffer layers respectively. At these dose rates it is not expected that any radiation damage to the clay or sand components will accumulate, as annealing processes are expected similar to those observed in granite (Ref. 53, pp. 8, 9; Ref. 42, pp. 13, 14).

A few minerals are particularly sensitive to radiation damage, but even in the absence of annealing, the doses required to

Table 10.1: INFLUENCE OF TEMPERATURE & RADIATION DOSE ON ROCK MASS PROPERTIES

Property	Effect of Increasing Temperature	Effect of Exposure to high dosage
Density	?often assumed independent	?decreases (e.g. Mica)
Strength	decreases - could be marked	?decreases - degradation?
Modulus	decreases - more plastic	?increases - more brittle
Thermal Conductivity	decreases - less transparent	?
Thermal Diffusivity	decreases marginally	?
Coeff. of Thermal Expansion	increases up to 100%	?
Sorption Coeff.	?	?probably most marked in MAFICS
Porosity	?decreases	?
Matrix Permeability	?	?
Poissons's Ratio	decreases, up to 50%	?
Fracture Hydraulic Conductivity	possibly decreases ?	?possibly decreases

NB - In general, although some changes occur because 'high' temperatures and 'high' radiation levels exist locally to the vault, none of the above effects appear very significant for the actual anticipated radio-thermal field.

cause appreciable physical changes in these sensitive minerals are high. Figures as large as 10^{10} Gy have been reported for mica, and 5×10^6 Gy for certain salts and limestone. Annealing occurs, with the chief consequence that high dose rates are also required, in excess of 10^3 Gy h^{-1} for limestone (Ref. 53). Chemical effects of radiation on buffer material are chiefly expected to consist of changes in the effective ion-exchange capacity, and therefore the radionuclide retarding ability, of the clay or zeolite components. Since neither alpha nor beta radiation is expected to be important outside the container, studies have been mainly of the effects of gamma radiolysis. The effects of gamma radiation on the ion-exchange capacity and leachability of kaolin (Ref. 54), of a natural zeolite and a pollucite (Ref. 55) were found to be slight, and apparently chiefly secondary consequences of decreased pH, owing to the formation of HNO_3 and other acid species. One study was reported (Ref. 56) of kaolin and attapulgite with adsorbed ^{253}Es, in which it was found that the alpha activity did not cause release of the adsorbed radionuclide.

10.3.2 Backfill and Host Rock

Radiation-induced chemical effects on the more remote components, backfill and host rock, are expected to be even less significant. Doses radially away from the emplaced UF and FRW waste canisters can be computed based on the data presented on Figures 6.5 and 6.6. For one UF canister, the doses are illustrated on Figure 10.1 for 30 years and 100 years after emplacement respectively.

The curves suggest that doses will be of the order of 10^5 Gy at the buffer/rock interface and 10 Gy some 50 cm into the rock. These values are approximately four orders of magnitude less than those anticipated for the U.S. salt program (Figure 10.2, Ref. 51).

Because the volume of rock around the waste vault that will be influenced directly by significant radiation doses (Figure 10.1) will be comparatively small, principally limited to the immediate area around the emplacement boreholes, little significant effect is likely to be felt by the general rock mass, though minor damage may occur in the immediate vicinity of the vault to fracture fillings of less stable mineralogical composition.

Comparatively little information exists on the affect of such radiation on the geomechanical properties of rock. Alterations in material character which may affect rock strength are changes in levels of stored radiation energy associated with lattice damage by displacement of atoms released when the material is annealed, and/or radiochemical effects that can lead to decomposition of some crystalline solids. Based on experiments carried out on limestones and on salts at high doses (5×10^6Gy) at 70°C, considerable variation was found in

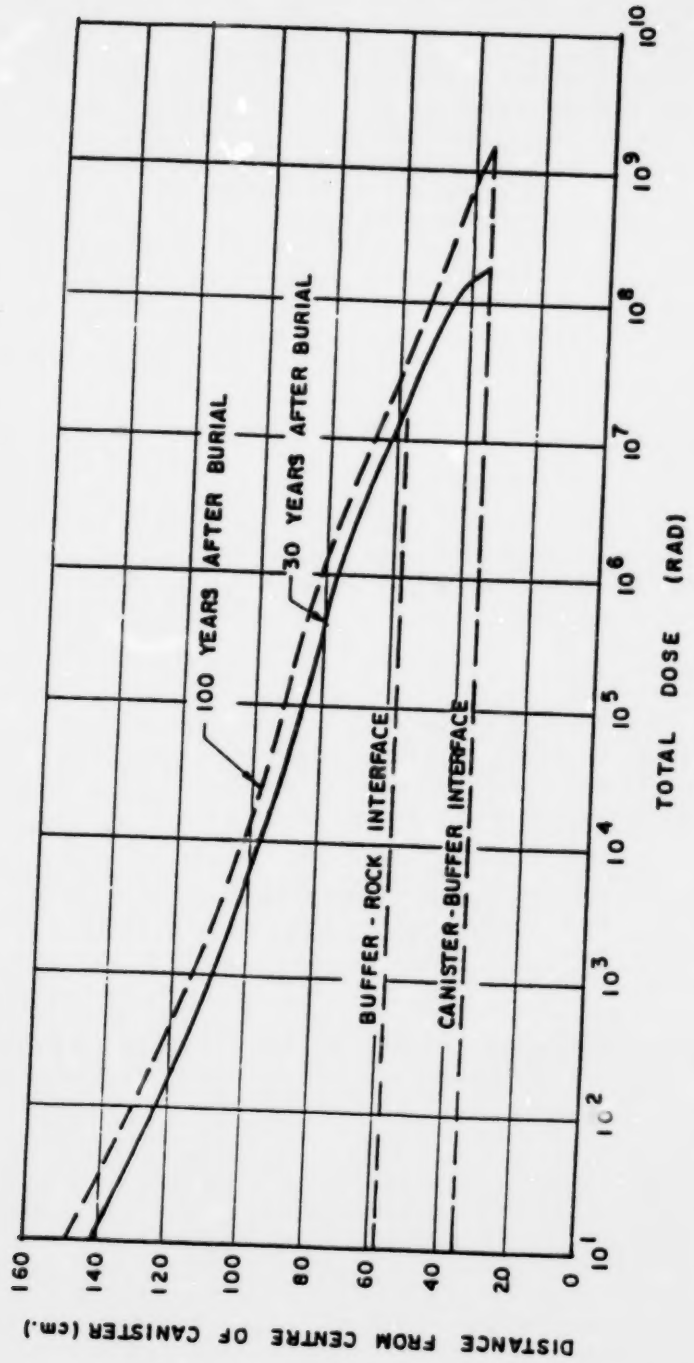

Figure 10.1: Variation in Accumulated Dose With Distance From Canister Centreline (Based on Data on Figure 6.5 For Clay and Granite for UF Vault)

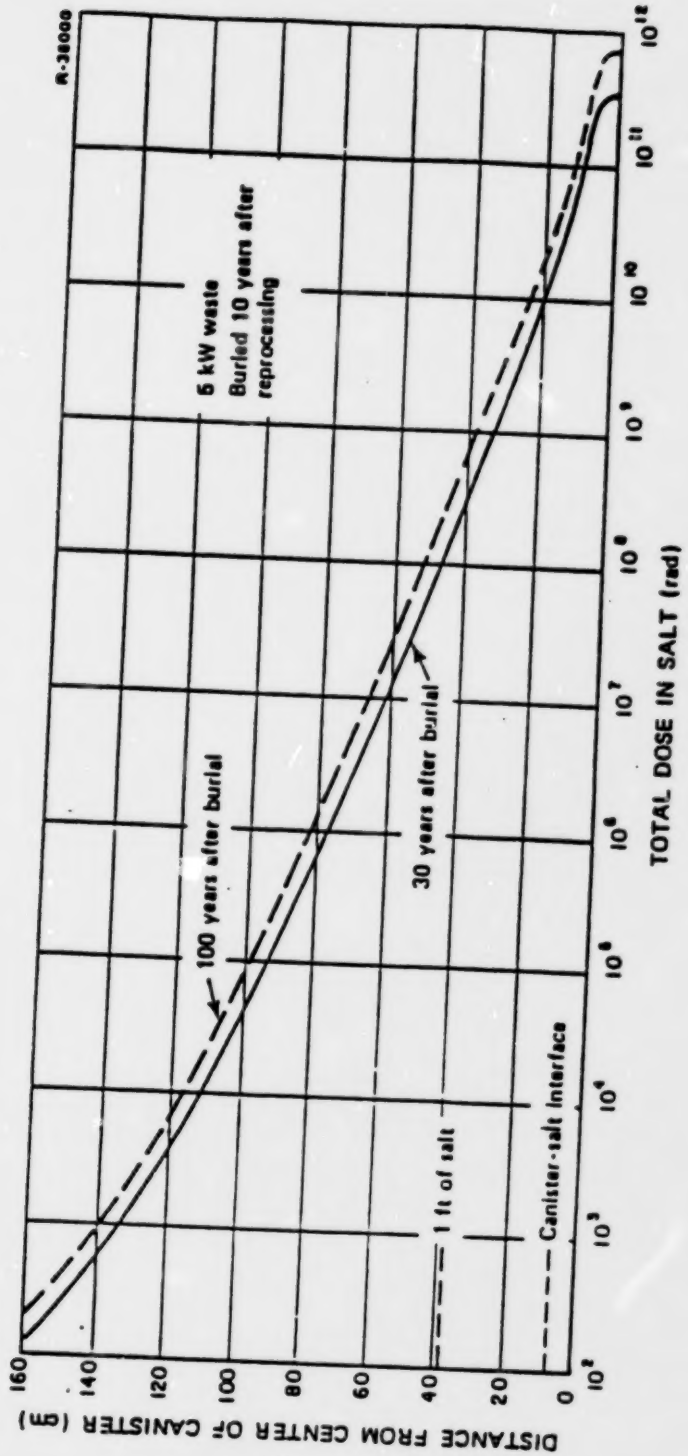

Figure 10.2: Variation in Accumulated Dose With Distance From the Canister Centreline (Ref. 51)

the effect that radiation energy exerts on the materials (Refs. 51, 49).

It was found that, in general, the effects of high radiation doses seems to be manifested in making the materials more brittle with a measurable decrease in compressive strength for certain rocks and a definite increase in moduli for some of the salts. The effects appear to be governed by the crystallinity and microstructure of the material. The maximum alterations occur in salt properties and in some of the more coarsely crystalline limestones. No specific data on plutonic rocks were identified, however based on the trends established from the limestone testing, it is suggested that damage effects will be least for the most fine grained and dense low porosity plutonic rocks such as the diorites, and somewhat more for the coarser rock types - the granites and gabbros.

Nevertheless, even for salts subjected to high radiation doses, the changes are much smaller than those associated with increases in temperature. Furthermore, based on the effects of radiation on the salts there appears to be a threshold level beyond which marked influence occurs but below which little influence is felt.

Accordingly, as it has already been concluded that relatively high radiation dosage effects on the behaviour of even salt are insignificant (Ref. 51), it is considered that the influence of likely radiation doses for the Canadian Concept on the geomechanical properties of the granitic and gabbroic crystalline rocks considered for potential host environments will be inconsequential. Some local influence might however be felt by carbonate fracture filling materials or by clay infillings in close proximity to the waste emplacement vault.

11. Radiation and the Groundwater

11.1 Transport of Radionuclides by Groundwater

As noted above (Sec. 8.4), in general the movement of groundwater at depths below 100m is slow, and the time during which the water remains in contact with various successive parts of the rock mass as it migrates is clearly long enough for local chemical equilibrium to be established. Ion exchange reactions can be expected to lead to retardation of the passage of any foreign ion through the rock. That is to say, if water is percolating through at a certain linear rate, any such ion in solution that can be exchanged with an ion present in the host rock will form a front, ahead of which it is absent, and behind which its concentration increases, eventually reaching a steady value. This front will advance at a slower rate than the water flow. The retardation ratio is commonly expressed by the retardation factor K which represents the ratio of the rate of advance of the solvent to that of a solute species. K values for positive ions in materials of high ion exchange capacity, such as natural or artificial zeolites, tend to decrease with increasing ionic charge. A similar effect is expected in low-capacity materials such as granite. This may in part explain the observations of increased sodium concentration with depth. Thus one would expect that K for transport of radionuclides by moving water would be in the order ^{85}Kr (neutral) < $^{137}Cs^{+}$ < $^{90}Sr^{2+}$. Negative ions are subject to a similar law, but the exchangeability of negative ions in natural minerals is in general much lower, except for a few minerals which contain notable amounts of exchangeable chloride or fluoride. Negative ions such as iodide, molybdate and uranate might be expected to be relatively mobile, while species of the same elements in different oxidation states may be essentially fixed.

At depth, since groundwater is expected to be essentially anoxic, except for a relatively short time before and after the closing of the containment site, oxidation states of the chief actinides should be Th (IV), U(IV or V), Np (IV), Pu(III) and Am(III) (Ref. 42). In these states the mobility is strongly enhanced by the presence of carbonate, owing to the formation of anionic carbonate complexes. It is therefore important that the groundwater be as free from carbonate as possible. This is also expected to be true at depth, as noted above. Fission products in the lanthanide group have somewhat similar chemistry to the actinides, though less complicated. The other fission products are such a heterogeneous collection that it is not possible to generalize. Some details and some problems are set out in the OECD study cited (Ref. 42). They point out that iodine is the most problematic element, owing to the fact that it is anionic or neutral in most of its oxidation states: I^{-}, I_2, IO_3^{-}. As noted above, negative ions are poorly retained by most minerals.

In the "Review of the DOE Waste Package Program" (Ref. 57) a number of useful tables from various sources are printed, which summarize some important chemical facts concerning the radionuclides likely to be leached from breached containers. Three of these tables are reproduced (in slightly modified form) here as Tables 11.1, 11.2 and 11.3. Table 11.3 lists the radionuclides, noting their half lives, whether inactive forms of the element or other elements of similar chemistry (grouped as "analogs") are expected to be present naturally, and the solid, liquid, gaseous or ionic forms in which the radionuclides would be expected to be found, in upper crustal or surface environments. With minor reservations (we note that Sn^{2+} would soon be oxidized at the surface to various Sn(IV) species) we commend this table to the reader as a useful summary of relevant radionuclide chemistry.

Tables 11.2 and 11.3 carry the chemistry a step further, and consider the formation of complex species by the interaction of the cationic forms of the key radionuclides with anionic ligands likely to be present, and with humic and fulvic acids. These last two are common constituents of groundwater that has been in contact with decaying vegetation, and are expected in much of the groundwater of the Canadian Shield, especially near the surface. Whether they would succeed in percolating to the great depth envisioned in the present concept is questionable.

Of all the radionuclides listed, the ones that cause the most concern from the point of view of mobility in groundwater are those that are most likely to be present in anionic form. Of these, ^{129}I, ^{99}Tc, ^{79}Se and ^{93}Se are particularly worrisome. The reason is that most natural minerals are cation exchangers. Clays and zeolites have relatively large capacity; the minerals commonly present in crystalline rocks are also chiefly cation exchangers, but with much lower capacities owing to their non-porous structures. Iodine and selenium exist almost entirely in anionic form, as I^-, IO_3^-, HSe^-, SeO_3^{2-} and SeO_4^{2-}; technetium is most stable as the oxyanion TcO_4^- (pertechnetate) when uncomplexed. The simple cation Tc^{4+} probably does not exist in aqueous medium, being in the form of hydroxy, sulfato, carbonato, etc., complexes $Tc(OH)_6^{2-}$, $Tc(SO_4)_3^{2-}$ etc., which are anionic. With selenium and technetium, neutral species $Se_{(s)}$ and $Tc(OH)_{4(s)}$ (the subscript s means present as a solid phase) can be formed. Tc^{4+} can be accomodated in the crystal lattices of certain minerals, but only under extreme hydrothermal conditions unlikely to be encountered. The consequence is that retardation of these three elements by ion exchange is not really any help. Molybdenum, if present as MoO_4^{2-}, would behave similarly, but both theory and experiment (Ref. 42, p. 127, Ref. 58) show that groundwater at depth is sufficiently reducing to keep molybdenum in the form Mo^{2+}. Lee and Bondietti (Ref. 59) showed that ^{99}Tc, initially present as TcO_4^-, was immobilized partly by collection in the iron minerals maghemite and goethite and partly by precipitation as Tc_2S_7, by contact with iron sulfide likely to be present in the host rock in small quantities. They recommend addition of

Table 11.1: Important Radionuclide Properties (Adapted From ONWI-321, 1982 (Ref. 57)

Nuclide	$t_{1/2}$ (y)	Analog	Possible Forms, Upper Crustal and Surface Environment
^{3}H	12.3	H	$H_2(g)$, H_2O, H^+, OH^-
^{14}C	5×10^3	C	CO_3^{2-}/HCO_3^-, CO_2, CH_4
^{36}Cl	3.1×10^5	Cl	$HCl(g)$, Cl^-
^{63}Ni	100	Ni(Co)	Ni^{2+}, $NiOH^-$, $NiCl_2^o$, $Ni(OH)_2$, $NiS(s)$, $NiCO_3(s)$
^{90}Sr	29	Sr(Ca)	SR^{2+}, $SrCO_3(s)$
^{93}Zr	1.5×10^6	Zr	$Zr(OH)_5^-$, $ZrSiO_4(s)$
^{94}Nb	2×10^4	Nb	$Nb(OH)_5(s)$
^{107}Pd	7×10^6	Pd(pt)	Pd^{2+} $PdCl_4^{2-}$, $Pd(OH)_2$
^{129}I*	2×10^7	I(Cl,Br)	I^-, IO_3^-
^{135}Cs	3×10^6	Cs(Rb)	Cs^+
^{137}Cs	30	--	--
^{154}Eu	8.2	Eu(REE)	$EuSO_4^+$, $Eu(OH)^+$, $Eu(OH)_3(s)$
^{210}Pb*	22	Pb	Pb^{2+}, $PbCl^+$..., $Pb(OH)^+$, $PbS(s)$
^{226}Ra	1.6×10^3	Ra(Ca,Sr,Ba)	Ra^{2+}
^{227}Ac	22	REE	Ac^{2+} (hydrolysis products), $Ac(OH)_3(s)$
^{230}Th	8×10^4	Th	Th^{4+}, $Th(OH)_3^-$, $Th(HCO_3)^{3+}$, $ThO_2(s)$
^{232}Th	1.4×10^{10}	--	--
^{231}Pa	3×10^4	Pa	$Pa(OH)_5$
^{241}Am	432	Nd	$Am(OH)^{3+}$, $Am(SO_4)^{2+}$, $AmO_3(s)$
^{234}Am	7×10^3	--	--
^{79}Se*	6.5×10^4	Se(s)	Se^{2-}, SeO_3^{2-}, SeO_4^{2-}, HSe^-, $Se(s)$
^{93}Mo*	3.5×10^3	Mo	MoO_4^{2-}, $MoS_2(s)$, Mo^{4+}
^{99}Tc*	2×10^5	Se	TcO_4^-, Tc^{4+}, $Tc(OH)_4^o$, $TcO_2(s)$
^{126}Sn	1×10^5	Sn	Sn^{2+}, $SnCl^+$, $Sn(OH)^+$, $SnS(s)$
^{151}Sm	90	Sm(Nd)	--
^{147}Sm	1.3×10^{11}	--	--
^{106}Ru*	1.0	Se(?)	RuO_4^{2-}, $RuO_2(s)$, $RuS_2(s)$
^{235}U*	7×10^8	U	UO_2^{2+}, U_4^+ complexes, $UO_{2+x}(s)$ $NaUO_4(s)$
^{238}U*	4.5×10^9	--	UO_2^{2+} complexes
^{233}U*	--	--	--
^{234}U*	--	--	--
^{237}Np*	2×10^6	$Np^{5+}(U^{6+})$	$Np^{4+}(?)$, $NpP_2(HCO_3)^o$, $NpO_2(s)$, NpO^{2+}
^{238}Pu*	--	$Pu^{4+}(Th^{4+})$	Pu^3, PuO^{2+}, $PuO_2(s)$
^{239}Pu*	2×10^4	$Pu^{6+}(U^{6+})$	--
^{240}Pu*	--	--	--
^{243}Cm	28	Nd	Cm^{3+} (hydrolysis complexes), $Cm(OH)_3(s)$

o = Common ionic substitutions in minerals
* = Redox-sensitive elements; multivalent solution chemistry or easily precipitated depending on whether in oxidizing or reducing environment
s = solid phase
E = gas
REE = Rare earth elements

Table 11.2: Potential Aqueous Species of Key Radionuclides in Natural Groundwaters (Adapted From ONWI-321, 1982) (Ref. 57)

Ion	Species
Simple Anions:	HCO_3^-, CO_3^{2-}
	I^-, IO_3^-
	HSe^-, SeO_3^{2-}, SeO_4^{2-}
	TcO_4^-, MoO_4^{2-}, RuO_4^{2-}
Simple Cations:	Cs^+
	Ni^{2+}, Sr^{2+}, Ra^{2+}, Sn^{2+}, Pb^{2+}, Mo^{2+}, Pd^{2+}, Pu^{4+}, Th^{4+}
	Zr^{4+}, Pa^{4+}, U^{4+}, Np^{4+}, UO_2^{2+}, PuO_2^{2+}, NpO_2^+
Complex Ions:	
Ligand	Simple Cation Forms Mononuclear and/or Polynuclear Species with Ligand to the Left
OH^-	Ni^{2+}, Sr^{2+}, Sn^{2+}, Am^{3+}, Eu^{3+} Zr^{4+}, Th^{4+}, Tc^{4+},
	U^{4+}, Pu^{4+}, Pa^{5+}, UO_2^{2+}
Cl^-	Ni^{2+}, Sn^{2+}, Pd^{2+}, Pt^{2+}, U^{4+}, Pu^{4+}, UO_2^{2+},
	PuO_2^{2+}, Sn^{4+}
HCO_3^-/CO_3^{2-}	UO_2^{2+}, PuO_2^{2+}, Th^{4+}, NpO_2^+, Ni^{2+}, Tc^{4+}(?)
SO_4^{2-}	Eu^{3+}, U^{4+}, Pu^{4+}, Am^{3+}, Tc^{4+}(?), UO_2^{2+}, PuO_2^{2+}
F^-	U^{4+}, Pu^{4+}, UO_2^{2+}, PuO_2^{2+}, NpO_2^+
$H_2PO_4^-/HPO_4^{2-}$	UO_2^{2+}, PuO_2^{2+}, NpO_2^+, U^{4+}, Pu^{4+}, Th^{4+}
Humic and Fulvic Acids	U^{4+}, UO_2^{2+}, Pu^{4+}, PuO_2^{2+}, Ni^{2+}, Pb^{2+}, Th^{4+}

Table 11.3: Predominant Solution Species of Radioelements* (EPA-526/6-78-007a, 1981) (Ref. 57)

Elements	Predominant Solution Species of Elements		
	Little Affected by Oxidation-Reduction	In An Oxidizing Environment	In A Reducing Environment
Am	Am^{3+}, $AmSO_4^+$, $Am(OH)^{2+}$		
Sb		$HSbO_2$, $Sb(OH)_3$, SbOF, $Sb(OH)_4^-$	SbO^+
Ce	Ce^{3+}, $CeSo_4^+$		
Cs	Cs^+		
Co	Co^{2+}, $Co(OH)_2^+$		
Cm	Cm^{3+}, $CmOH^{2+}$, $Cm(OH)_2^+$		
Eu	Eu^{3+}, $EuSO_4^+$, $Eu_2P_2O_7^{2+}$		
I		I^-, IO_3^-	I^-
Np		NpO_2^+, $NpO_2HPO_4^-$, NpO_2HCO_3	$NpOH^{3+}$, Np^{4+}
Pu		PuO_2^{2+}, $PuO_2(CO_3)(OH)_2^{2-}$ PuO_2^+	$PuOH^{2+}$, Pu^{3+}
Pm	Pm^{3+}		
Ra	Ra^{2+}		
Ru		$Ru(OH)_2^{2+}$ RuO_4^-, RuO_4^{2-},	RuO_4^-
Sr	Sr^{2+}		
Tc		TcO_4^-	TcO_2
Th	ThF^{3+}. $Th(OH)_3^+$		
^3H	H^+, ^3H-O-H		
U		UO_2^{2+}, $UO_2F_4^-$, $UO_2(OH_2)$, $UO_2(CO_3)_3^{4-}$	UO_2^{2+}, UOH^{3+}, UO_2 $UO_2(CO_3)_3^{4-}$
Zr	$Zr(OH)_4$, $Zr(OH)_5^-$, ZrF^{3+}		

*In a pH 4 to 9, pO_2 0.68 to 80, pCO_2 1.52 to 5.32, $pCl^- = pNO_3^- = pSO_4^{2-} = 3.0$, pF^- 4.5 and $pH_2PO_4^-$ 5.0 environment without organic ligands. (Symbol $pX = -\log_{10} C_x$; C_x is concentration of x in mol L^{-1}).

ferrous and/or sulfide bearing minerals to buffer and backfill materials.

There remains the problem of iodine. All the common forms of this element are likely to be mobile. Even the elementary form I_2 is volatile and water soluble. This problem was addressed in the O.E.C.D. Paris meeting (Ref. 42, pp. 15-16 *et infra*). Preventing the escape of ^{129}I was seen first as a problem of the isolation of the waste form from water, i.e. by the use of very durable containers and non-leachable waste forms. The addition of silver compounds to the buffer was considered, with the purpose of immobilizing iodide as $AgI_{(s)}$. As a counsel of despair, it was suggested that preprocessing of the waste to remove iodine would allow the iodine to be disposed of in the ocean, where isotope dilution would render it safe.

There is one observation, however, that suggests that the mobility of iodine may be much lower than is feared. McKinley *et al.* (Ref. 60) have reported measurements of concentrations of a number of elements in bottom sediments in Loch Lomond. A marine incursion took place at at some time before 40,000 years ago, with the result that a layer of marine sediment lies undisturbed between earlier and later freshwater sediments. Profiles of concentration through these layers show that iodine has not moved measurably in more than 10,000 years, comparably with Al, Fe, Co and As, and in contrast with Cs and the lanthanides. A somewhat similar observation was made by Walton and Cowan (Ref. 61, 62) at Oklo, discussed further below.

As concerns the other radionuclides, the Paris conference (Ref. 42, pp. 14-15) noted that the effects of nuclide concentration, ionic strength and temperature on the sorption of the actinides on solid surfaces are slight, but that pH and Eh (oxidation/reduction potential) are important. They are most strongly sorbed at intermediate pH values (likely to be encountered at depth) and reducing Eh levels (also likely to be encountered). The solubilities of all (except perhaps Pu in oxic conditions) are greatly enhanced by the presence of carbonate, owing to the formation of anionic carbonate complexes. These are not readily sorbed by common minerals, so it is important that the groundwater be low in carbonate, or bicarbonate. Johnston (Ref. 34) has shown that this is likely to be true at depth. As was reported in Paris (Ref. 42, pp. 127-129), subject to short-term perturbations of the order of 50 years after emplacement and sealing, most Canadian sites will have perineutral or mildly basic pH (ca. 6.5 - 8 or occasionally 10) mildly reducing conditions (Eh from +0.1 to -0.4 V), and moderate ionic strength (0.01 to 0.2 mol L^{-1})*. Reference is made (Ref. 42, p. 16) to experimental difficulty in ensuring that reducing conditions are in fact maintained. Breck (Ref. 63) has discussed this problem and shown that meaningful measurements of Eh of natural waters have been rare in the past, but that with proper technique it can be done.

[*Cf. seawater 0.69 mol L^{-1}]

Among the fission products, a number are chemically classified as rare earth elements (REE) or lanthanides. The most important ones are ^{154}Eu and ^{151}Sm, but others of the family have very similar chemistry, being present almost exclusively as tripositive ions. They form complexes with OH^-, SO_4^{2-} and $P_2O_7^{4-}$ ions,but chiefly in ligand / metal ion ratios that result in cationic species that are sorbable by minerals. Certain other elements behave similarly (^{227}Ac and the Am isotopes, for example). See Tables 11.1 and 11.3).

Hamstra (Ref. 42, p. 15) comments on lack of data concerning several matters. He reports that contributors to the conference questioned the validity of sorption coefficients in the literature, especially for the actinides, for their chemistry is too complicated for their sorption behaviour at a mineral surface to be described by a single constant. A similar lack of data was noted concerning the surface chemistry of I, Tc, Sr, Zr and Sm, especially in low concentrations, as functions of pH, temperature, carbonate concentration and ionic strength. The chief problem is the slowness of surface and solid state processes. Because of this, the time scaling of different phenomena relating to these and other elements creates a severe problem in translating accelerated laboratory test procedures into results that will be meaningful. Field studies of natural analogues are seen as vital (Ref. 42, p.17); even in laboratory studies there are still some surprises in store. For instance, in a study of the rate of diffusion of radionuclides in compacted bentonite, Torstenfelt et al. (Ref. 64) found that Am moved much more slowly than expected, being essentially fixed, while Sr and Cs moved unexpectedly quickly. Beall and co-workers (Ref. 65) reported an unexpectedly high affinity of attapulgite, a clay that was not at the time a serious candidate for buffer material, for lanthanides and actinides.

11.2 Breached Container Scenario

The most adverse event with respect to nuclear fuel disposal that can occur would be breaching of the canister and the titanium shell of a waste container. The direct effect of this breaching would be to allow contact of the contaminated waste with the circulating pore fluids in the buffer and backfill and hence ultimately with the natural groundwater in the pluton. Experiments have been performed to determine the likely concentration of dissolved radionuclides that would develop in granitic groundwaters that come into direct contact with the waste. Figure 11.1 illustrates the early results from one of these experiments (Ref. 6). Ongoing unpublished work indicates that equilibration of concentrations is reached even for ^{137}Cs within relatively short time scales (K. Nuttal (AECL) Pers. Comm).

For the ideal conceptual arrangement of the vault separated some distance from major fracture zones (Figure 11.2) (Ref. 30), radionuclide migration in the groundwater radically away

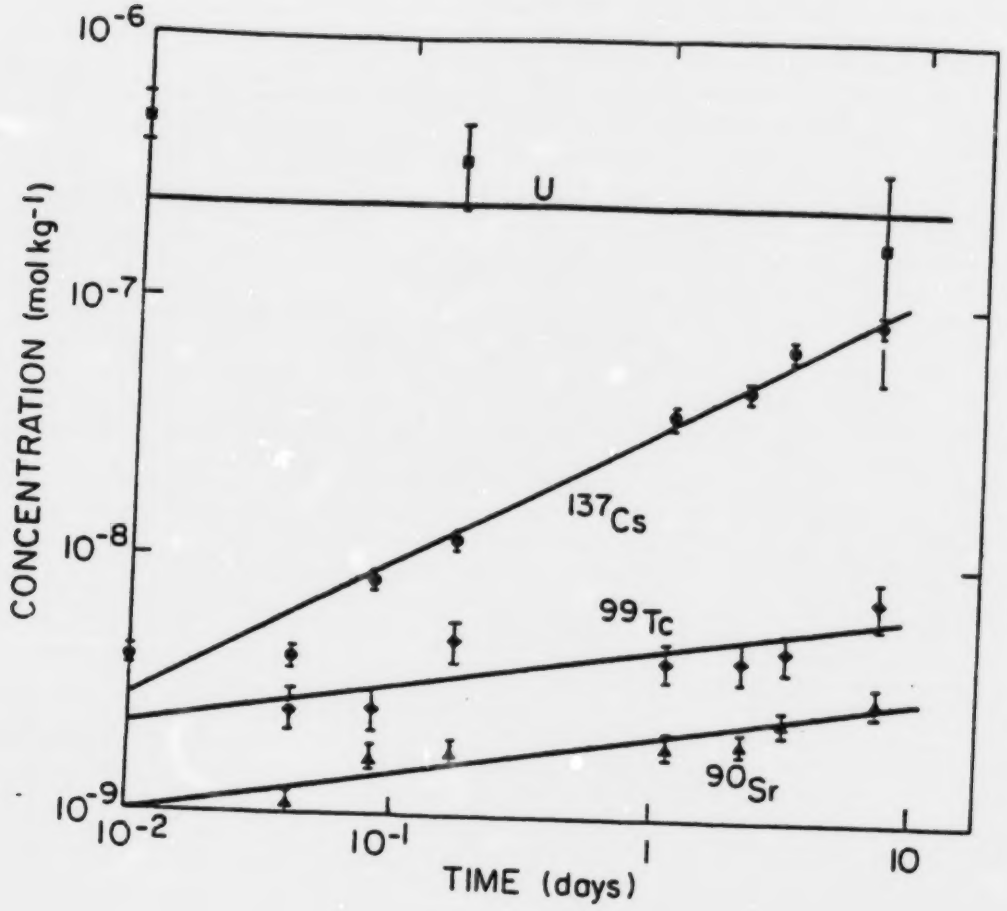

Figure 11.1: Radionuclide Concentrations in Granite Groundwater in Contact With Irradiated Fuel at 150°C (Ref. 6)

Note: Additional work has been completed which indicates that concentrations stabilize with time (AECL, in press)

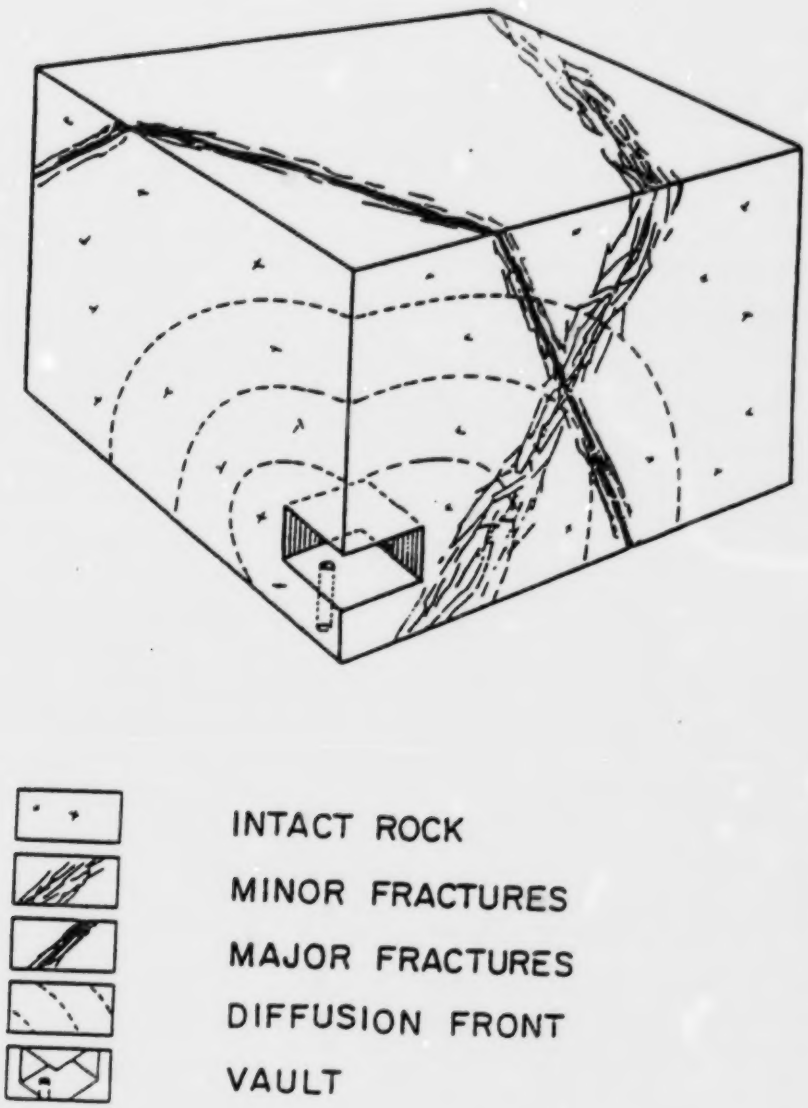

Figure 11.2: Concept of a Vault Isolated From Major Fracture Zones Showing Principal Radionuclide Transport Path Mechanisms (Ref. 30)

from the blast-fractured annulus around the vault may initially be controlled by diffusion through the network of fine fractures that characterize the pluton at vault depth. Breakthrough times for diffusion through typical granites to reach a major fracture front some 100 m from the vault (Ref. 30) range from 3 x 10^6 years for ^{99}Tc to 5 x 10^{10} years for ^{226}Ra. It should be noted that these transit times assume that diffusion will dominate in fractures of less than 0.3 μm and even up to 20 μm due to wall mineralogy diffusion effects (Figure 11.3) (Ref. 30). The analysis also tacitly assume that no preferential flow conduits exist or develop between the blast fractured annulus and any natural fracture zone.

All the reviewed data suggest that where fractures exceed a critical width of about 20 μm, flow rates under a given hydraulic gradient will be too great to allow diffusion to materially affect dissolved radionuclide concentrations. For flow in such fractures it is conceivable that dissolved radionuclides emanating from a vault at 1000 m depth will reach the surface within a time span of about 10^5 years (Figure 11.4) (Ref. 30).

11.3 Radiation Chemical Effects

The indirect radiation chemical effects via the radiolysis of water are important. The effect of gamma radiation on water is chiefly to eject electrons. Slow electrons may be briefly trapped in potential wells of their own creation, by polarization and orientation of surrounding water molecules, creating the species symbolized as $e^-(aq)$. (A similar species can exist long enough in liquid ammonia for leisurely study). The aqueous electron is a very strong reducing agent, and reacts quickly with water, or even more so with hydrated protons H_3O^+, yielding hydrogen atoms. H atoms can react further with water, abstracting a second H atom and leaving behind the hydroxyl radical HO·, which is also chemically very active. Radical recombination reactions between H· and HO· or between two H· atoms or two HO· radicals reform water or yield H_2 or H_2O_2 (hydrogen peroxide). In the absence of other substances, the H_2O_2 in time either decomposes to form O_2 and water, or is reduced by e^- (aq), H· or H_2 back to water. O_2 is also eventually reduced back to water, and the chemically stored energy finally released as heat. These reactions, with some others, are summarized in Table 11.4.

Christensen (Ref. 66), by computer simulation, showed that external radiolysis of water at reasonable rates quickly established a steady state, with concentrations of H_2, O_2 and H_2O_2 low (micromoles per litre) and those of the radicals and atoms even lower (picomoles per litre). The gas concentrations were far below the solubility limits. An experimental study by Erikson and Lind (Ref. 67) of radiolysis of water in a bed of bentonite clay, focusing on H_2 production, showed that at no dose rate reasonable for buffer material was the solubility of H_2 in water exceeded.

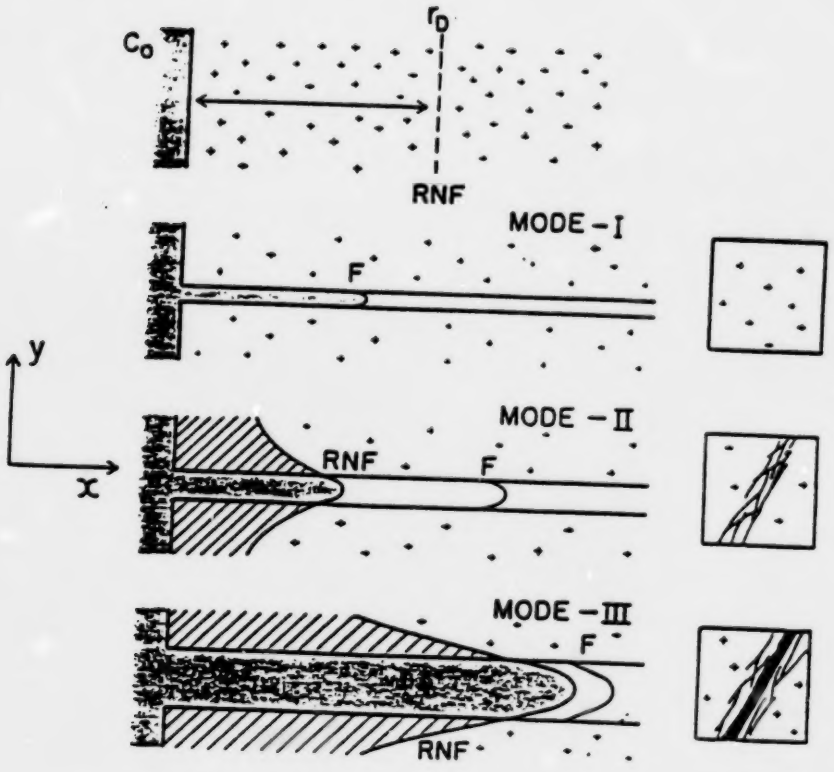

C_o : CONCENTRATION OF RADIONUCLIDE SOURCE

F : FLOW FRONT

RNF : RADIONUCLIDE FLOW FRONT

RADIONUCLIDES

DIFFUSED RADIONUCLIDES

ROCK MATRIX

Figure 11.3: The Concept of Radionuclide Transport Modes ("R_D" is the Diffusion Radius. Mode-1 is the Case Where the Flow Fracture-Aperture is Very Small, so that the Flow Rate in it Falls Behind the Diffusion Rate. Mode-II Depicts the Case Where the Flow Fracture-Aperture is Large Enough to Allow the Flow Rate to Exceed the Diffusion Rate But, at the Same Time, is Small Enough to Allow a Considerable Amount of Retardation to Take Place. This Creates a Situation Where the Actual Radionuclide Flow Rate Falls Behind the Diffusion Rate. Mode-III Represents the Case Where the Flow Fracture-Aperture is Very Large, and the Flow Rate is too Extensive to Allow any Significant Amount of Retardation to take Place. Thus, the Actual Radionuclide Flow Rate Exceeds the Diffusion Rate) (Ref. 30)

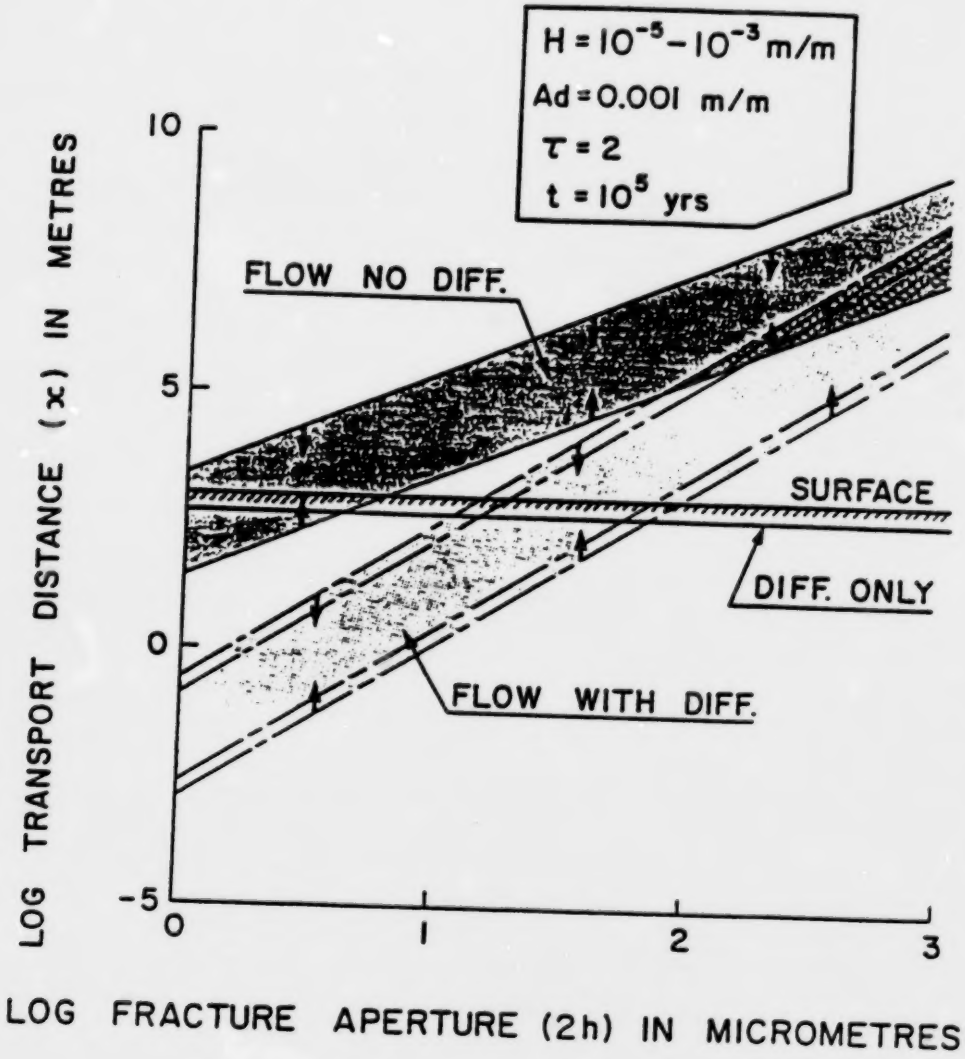

Figure 11.4 : Flow Distances Versus Fracture Aperture During a Time of 10^5 Years, for Cases With and Without Retardation Due to Matrix Diffusion. (Analytical Solutions Developed by G. Grisak and J.F. Pickens are Used to Calculate Retardation Effects. The Upper and Lower Lines of the Two Flow Distance Bands Represent the Cases for Hydraulic Gradients (H) of 10^{-3} and 10^{-5}, Respectively) (Ref. 30)

Table 11.4: Some Reactions in the Radiolysis of Water

1. $H_2O + e^-$ = $H_2O^{\cdot +} + e^-(aq) + e^-$

2. $H_2O^{\cdot +} H_2O$ = $H_3O^+ + HO\cdot$

3. $e^-(aq) + H_2O$ = $H\cdot + HO^-$

4. $e^-(aq) + H_3O^+$ = $H\cdot + H_2O$

5. $3H_2O$ = $H_3O^+ + OH^-$

6. $H\cdot + H_2O$ = $H_2 + HO\cdot$

7. $2H\cdot$ = H_2

8. $H\cdot + HO\cdot$ = H_2O

9. $2HO\cdot$ = H_2O_2

10. $2H_2O_2$ (several steps) = $H_2O + O_2$

11. $H\cdot + O_2$ = $HO_2\cdot$

12. $H\cdot + HO_2\cdot$ = H_2O_2

etc.

In the presence of oxidizable substances (reducing agents) the picture changes considerably. Christensen and Bjergbakke (Ref. 68) found in a further computer study that production of H_2 by radiolysis of water should be enhanced by as much as five orders of magnitude by the presence of Fe^{2+} ions. (On the other hand, the authors of the report, "Final Storage of Spent Nuclear Fuel" (Ref. 48, p. 13:15), state that Fe diminishes the production of H_2 by catalysing the reverse reaction $H_2 + H_2O_2$ to $2H_2O$). This ion is an efficient scavenger of HO· radicals, by the reactions:

$$Fe^{2+} + HO\cdot = FeOH^{2+}$$

$$FeOH^{2+} = Fe^{3+} + OH^-.$$

Other reducing agents have similar effects. The result is that the hydrogen atoms are left to form H_2 molecules, which, being relatively unreactive and very low in mass are free to diffuse away. This increases the oxidation potential in the near field and gives rise to the so called 'redox front' - Figure 11.5. At greater distances the reducing conditions of the natural groundwater will prevail, but should the container be breached, many radionuclides will become oxidized, their solubility will increase, and they may become mobilized. Most will not get far though, as they will be re-reduced when they leave the oxidized region. This was shown clearly by Neretnieks and Åslund (Ref. 69), who found that when U, Np and Tc species diffused past a redox front of this nature, they were precipitated. This reprecipitation was not observed, however, with Pu, Th or Am. In another experimental study, Eriksen (Ref. 70) showed that H_2 production in compacted bentonite containing small amounts of Fe^{2+} was indeed enhanced, but noted that H_2 production fell off sharply at low dose rates. This seems to support an earlier conclusion (Ref. 42, p. 14) that after about 50 years, in the absence of air, radiolysis of ground water will no longer have a large effect on the leach rate.

The addition of granite chips to the backfill material will provide a readily available source of divalent iron in addition to that available from iron compounds in the clay buffer around the encapsulated waste. Such iron species will tend to influence the rate of radiolytic redox reaction in solution (Ref. 68). Reduction of the hydrogen peroxide and other products escaping in the groundwater system will tend to occur until all divalent iron has been oxidized (Ref. 69).

If it is assumed that all produced hydrogen peroxide or an equivalent quantity of other oxidizing species penetrate out to the clay buffer and ultimately to the rock, then when all iron in the clay has been consumed, the hydrogen peroxide will diffuse into the rock and react with the available iron. It will be carried away with the flowing water in the fractures and diffuse into the fracture walls and into the microfissures

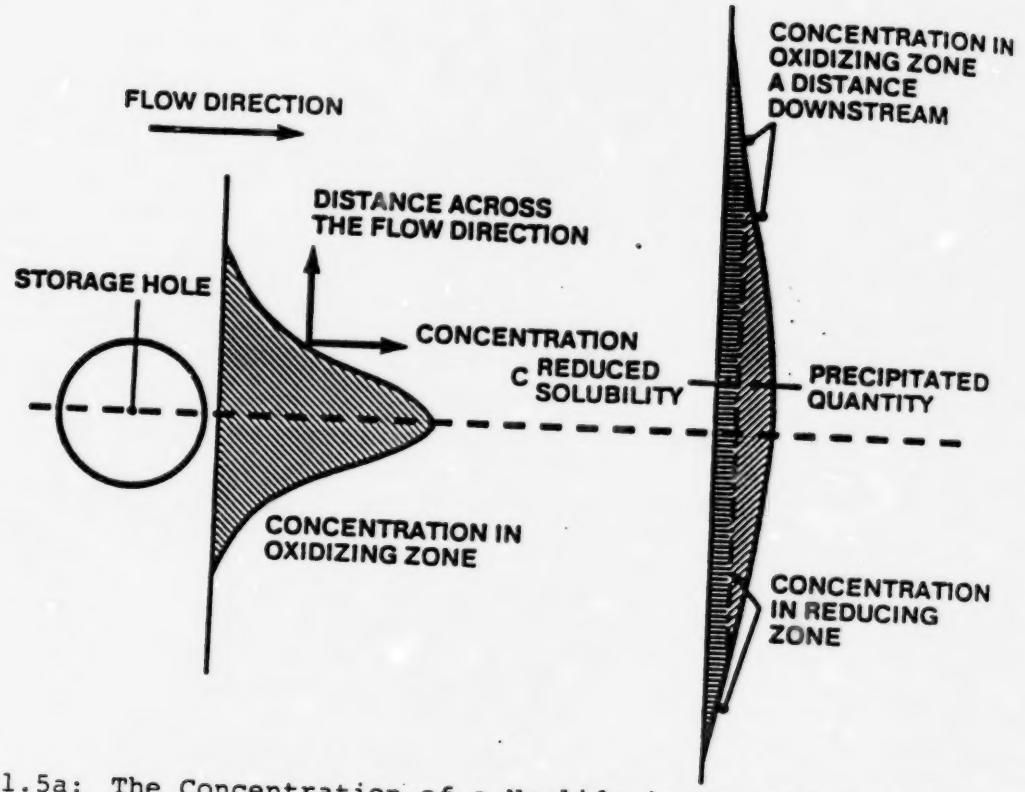

Figure 11.5a: The Concentration of a Nuclide in the Water in a Fracture Plane. A Radionuclide with High Solubility with Oxidizing Conditions Precipitates at the Redox Front. The Water Downstream of the Redox Front has a Low Concentration C_{sol}^{red}, but the Front has Broadened and a Larger Water Flow Transports the Nuclide (Ref. 48)

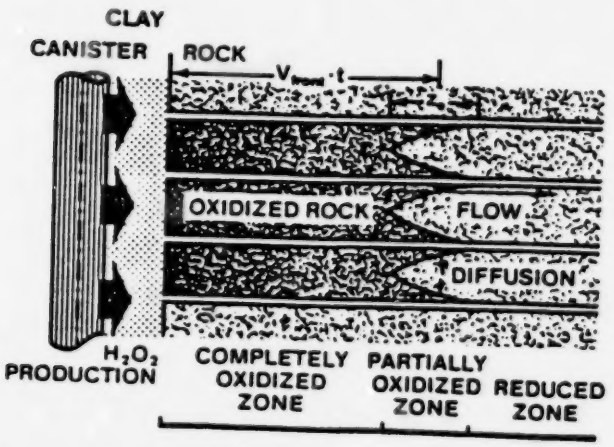

Figure 11.5b: Propagation of the Radiolysis Front Downstream of a Canister. The Hydrogen Peroxide and Other Oxidizing Substances Move with the Water in the Fractures, but also Diffuse from the Fractures into the Rock, Where the Bivalent Iron is Oxidized to Trivalent Iron (Ref. 48)

in the rock where it will oxidize a rock volume determined by the available bivalent iron.

If the greatest possible radiolysis is assumed to take place and all hydrogen peroxide is assumed to be utilized in oxidizing the iron present in the rock, then the propagation of such a front downstream of any individual container can reach a maximum of some 50 metres in one million years in relatively iron-poor rock (0.2% Fe(II)). In practice though, because the redox front propagates in all directions and iron compounds are common on the margins of the more major fractures, it is likely that the front will only move a few metres away from each emplacement borehole.

This transverse outwards propagation of the redox front in the fractures can ultimately give rise to interaction with other fronts from adjacent containers. Ultimately then, most of the groundwater adjacent to the vault will become saturated with nuclides to the maximum concentration sustainable under reducing conditions.

12. Thermal Effects

Canister and vault design constraints limit the temperature rise at the container surface sufficiently that maximum average vault temperature will be maintained below 100°C. However, temperatures close to this level will be maintained for a considerable time, and possibly over 10,000 years (Figure 5.1).

12.1 Effect on Groundwater

The effect of marked temperature gradients set up by the thermal field on mass transport of minerals in solution by groundwater flow is still under investigation by most programs. Some work (Ref. 17) shows that some minerals can be transported from the hot zone in the vault and precipitated in the cooler bulk rock. Laboratory experiments of passing hot fluids through fractured granite samples suggest that measurable decreases can occur in hydraulic conductivity characteristics (Ref. 71). This was attributed to dissolution of silica at high temperatures and its reprecipitation at low temperatures along grain boundaries and microfractures. Other experimental data on the low temperature reactions between granodiorite and water (Figure 12.1, Ref. 72) showed essentially constant solute concentration after 5 days.

Such experimental studies of interaction between groundwater and whole rock samples can, in theory, also provide estimates of reaction rates. However, as alteration proceeds so slowly at temperatures < 150°C it may take years to achieve equilibrium at the temperatures of interest, and even longer to produce identifiable alteration products. Furthermore, alteration products observed in the laboratory are often amorphous, but in natural systems crystalline phases dominate. The behaviour of amorphous and crystalline phases of similar composition, with respect to sorption and dissolution, is sufficiently different that experimental data could have limited applicability to natural systems.

12.2 Effect on Groundwater Movement

One problem that has been considered only recently (Refs. 73, 74) because of its difficulty is the effect of the elevated temperature of the storage vault and its neighbourhood on the circulation patterns of the groundwater. The problem is difficult because the mathematical theory of water motion in a network of fractures is ill-developed, and while coupled thermal and mass flows have been treated successfully in porous media, the treatment of the rock mass as a porous medium is fruitful only on a large scale.

Beddoes and Tammemagi (Ref. 73) have undertaken a review of current theoretical approaches to this problem, and comment that available techniques require solution of many intractable unknowns. They suggest that advances will come through more refined numerical modelling approaches but recommend, in the

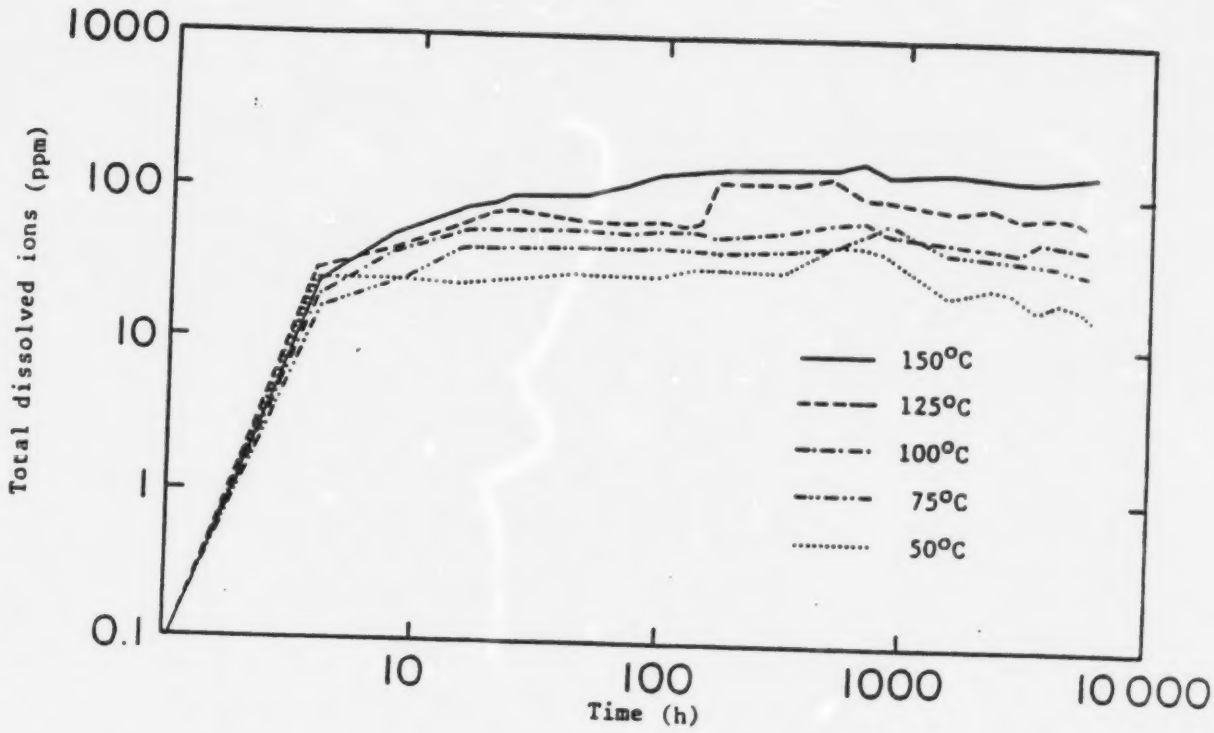

Figure 12.1: Effect of Temperature on Total Dissolved Ions From Groundwater/Granodiorite Reaction (Ref. 33)

interim, that natural analogues be sought to gain insight into the problem.

They do, however, undertake some assessment of the application of the available methods on a scale equivalent to the rock surround to a deep disposal vault and suggest that thermal effects may well be important. They find that convection cells can form downstream from the repository, and could have the effect of accelerating transport of radionuclides to the surface. With other choices of conditions, however, retarding effects appear possible.

No assessment or consideration though is given to the possibility of thermally induced groundwater upwelling in the immediate vicinity of the vault through the zone of preferentially increased permeability created by the excavation process. This will require detailed attention as it is akin to the fracture systems seen in many geothermal areas.

Tammemagi, Grisak and Parrish (Ref. 74) have made a start in examining natural geothermal analogues by preparing a case history of a mild geothermal area, the Empire Creek Stock, near Marysville, Montana, and comparing it with other geothermal areas. There is ample evidence of changes in the stock as a result of movement of warm water. They draw no conclusions, but recommend further experimental, field and mathematical study.

12.3 Effect on Engineered Barrier Materials

The portion of the barrier that might be most subject to thermal effects is the buffer. It is in contact with the container, and the active ingredients of buffers being considered, various clays, especially bentonite, are known to undergo changes on heating. All clays are to a certain extent hydrated, and can lose this hydration on heating. At the same time they lose their ability to retard the diffusion of radionuclides in cationic form by ion exchange, and their impermeability to water. Bentonite begins to undergo recrystallization as the temperature reaches 100°C (Ref. 14). Pusch and Bergstrom (Ref. 75) have noted, however, that bentonites have self-healing properties of swelling and rehydration. After an episode of minor damage through a temperature excursion, the desirable properties of the clay would be restored. Kaolinite similarly, though at higher temperatures, undergoes recrystallization to form mullite. Curiously, radiation doses above 1600 Gy retard and inhibit this change (Ref. 76). Westsik et al. (Ref. 77) concluded that bentonite or sand-bentonite mixtures can indeed function as effective radionuclide retarders when used as buffers.

Based on experimental and analytical work on the buffer materials it has been established (Ref. 78) that under the influence of the thermal effects of the vault prior to resaturation by natural groundwater, such considerable drying

will have occurred that the material will likely fissure. It is considered that some improvement might be achieved with various mix proportions of the buffer material, however considerable uncertainty exists relating to the effects that might occur when the buffer material resaturates on the return of the groundwater (some 10 to 20 years after vault sealing). Although it is likely that resealing of the fissures will occur, complications due to hot water circulation effects may prevent complete resealing of fractures.

12.4 Effect on Rock Mass

The thermal field that is developed around the UF and FRW vaults may lead to relatively high temperatures occurring in the rock mass adjacent to the vault sidewalls. Such temperature effects are expected to be most severe immediately adjacent to the borehole emplaced containers in the UF vault. However, temperature levels even here are not anticipated to exceed 100°C.

The possible effect of differential heating in inducing growth of microcracks has been subject to a laboratory study (Ref. 79) in which it was found that there was an effect, which was first observable at temperatures from 76 to 160°C for several different Scottish granites. It should be pointed out that these were subjected to heating rates and thermal gradients much greater than would occur in the Canadian Concept repository. Furthermore, these tests were carried out under unconfined conditions and at a range of temperatures only likely to be reached in the very near field adjacent to the emplaced containers. Accordingly, no major extent of microfracture propagation or significant modifications of rock material properties is anticipated (Refs. 7, 31, 79).

Thermal induced stresses in the rock mass will increase in phase with temperature rise and in consequence, maximum stresses will develop around 50 years after waste emplacement. The influence of such stresses on the rock mass will likely be to compound the stress changes already induced in response to the original development of the excavation - i.e. the depth of any zones where potential compressive overstress or tensile loosening might be anticipated may well increase. This would tend to manifest itself as development of a pattern of microcracks oriented sympathetically to the dominating stress field. Computer analysis of the extent and magnitude of such stress changes (Ref. 31) suggest that any detrimental effects that might affect the rock mass are well within the scope of readily available rock support controls, (i.e. rock reinforcement - bolts, mesh, etc.). Accordingly, no generalized failure of the rock mass surrounding the vault would develop.

Minor changes in rock properties will, however, occur within the thermally perturbed area around the vault. A summary of the possible effects on primary rock properties was given on Table

10.1. In general, the effects of temperature are most marked on modulus and conductivity as shown on Table 12.1 (Ref. 30). Some influence also occurs on rock strength (Table 12.2, Ref. 20). The trend however is not totally clear as triaxial compressive strength has been found to increase with increasing confining pressure at a constant temperature, and decrease with increasing temperature at constant confining pressure.

Although there appears to be an overall trend of decreasing Young's modulus with increased temperature (Table 12.1), detailed variations of modulus with confining pressure and temperature appear irregular. No discernable changes have been noted with temperature in angles of internal friction, however, appreciable decreases in cohesion have been determined with increasing temperature at low confining pressures with almost no change at high confining pressures.

Significant changes also occur in thermal conductivity and thermal diffusivity as shown on Figure 12.2 and 12.3 (Ref. 20) respectively. As can be seen, both parameters decrease markedly with increased temperature, thermal diffusivity being most affected even in the relatively low temperature environments that might exist.

The thermal conductivity data on Figure 12.3 are for granitic rocks; information for more mafic rocks (gabbros for example) suggests that it decreases at a lesser rate, or in certain instances can actually increase due to the transparency of the mineralogical fabric to infrared radiation, which supplements lattice conductivity at higher temperatures.

Because of the very linear relationship for granitic rocks, the decrease in thermal conductivity can be readily approximated:

$$C_t = C_o - 0.0011\ (t_t - t_o)$$

where: C_o is the conductivity at the reference temperature
C_t is the conductivity at temperature "t"
$(t_t - t_o)$ is the difference in ^oC between the reference temperature and the design temperature

This relationship though cannot be applied consistently to more basic, gabbroic rocks.

12.5 Thermo-Chemical Effects on Rock Mass Mineralogy

The establishment of a temperature gradient from 100°C to ambient around the vault would have very little chemical effect on granitic or gabbroic rocks in the absence of groundwater as both rock types are stable under low-grade metamorphic conditions in the absence of a fluid (Ref. 26). The presence of groundwater, though, has a strong catalytic effect on mineral reactions, and reaction rates are controlled by access of fluid to the rock as is clearly illustrated by wall/rock alteration around hydrothermal veins.

Table 12.1: Variations of Rock Properties With Temperature (Ref. 30)

Temperature (^{o}C)	Thermal Conductivity (W/(m·°C))	Specific Heat (J/(kg·°C))	Linear Coeff of Thermal Expansion ($10^{-6}/^{o}$C)	Young's Modulus (GPa)	Poisson's Ratio --
15	3.00	800	8.0	40	0.20
25	2.86	814	9.1	39	0.20
50	2.74	827	10.2	38	0.19
100	2.51	855	12.4	34	0.17
150	2.31	881	14.6	30	0.13
200	2.14	910	16.8	25	0.10

Table 12.2: Comparative Ultimate Strength of High Silica and Low Silica Rocks (Ref. 20)

Material	Confining Pressure	Strength at Elevated Temperature (°C) 24°	150°	200°	300°	500°	800°
Olivine Basalt, Blairsden, California	5.0	15.4	--	--	13.8	10.3	2.6
Westerly Granite, Rhode	5.1	20.8	--	--	16.6	11.3	6.2
Peridotite,	5.1	22.5	--	--	15.5	10.8	8.5
Pyroxenite, California	5.1	17.4	--	--	12.5	9.3	6.7

Note: All stresses and strengths quoted are in units of 10^{3} psi

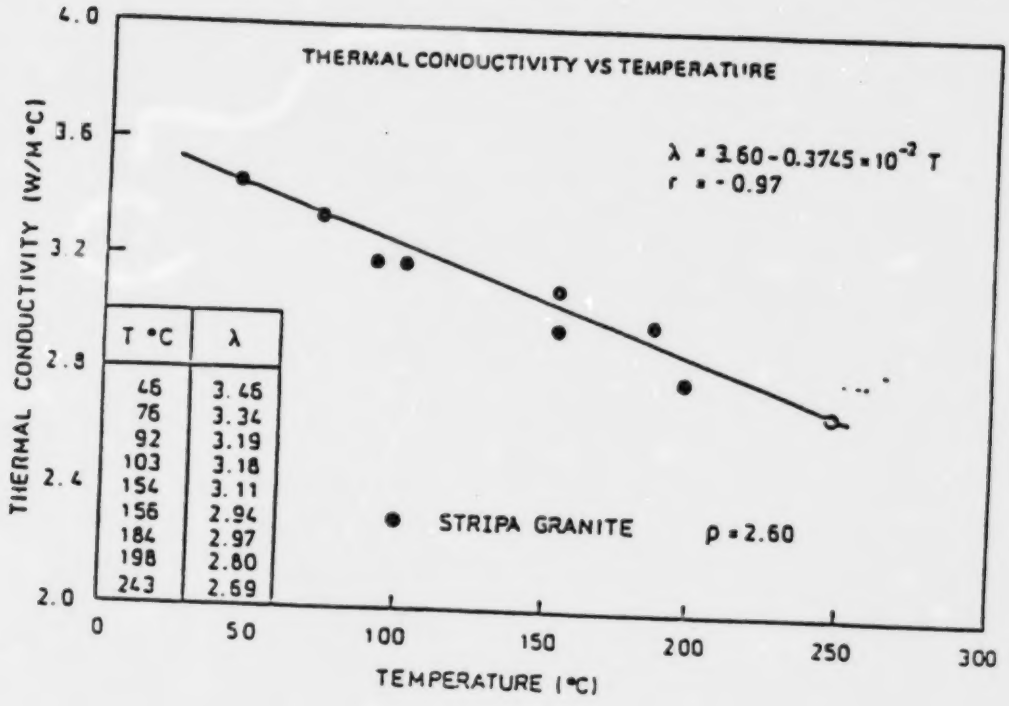

Figure 12.2: Thermal Conductivity VS Temp. of the Stripa Granite (Ref. 20)

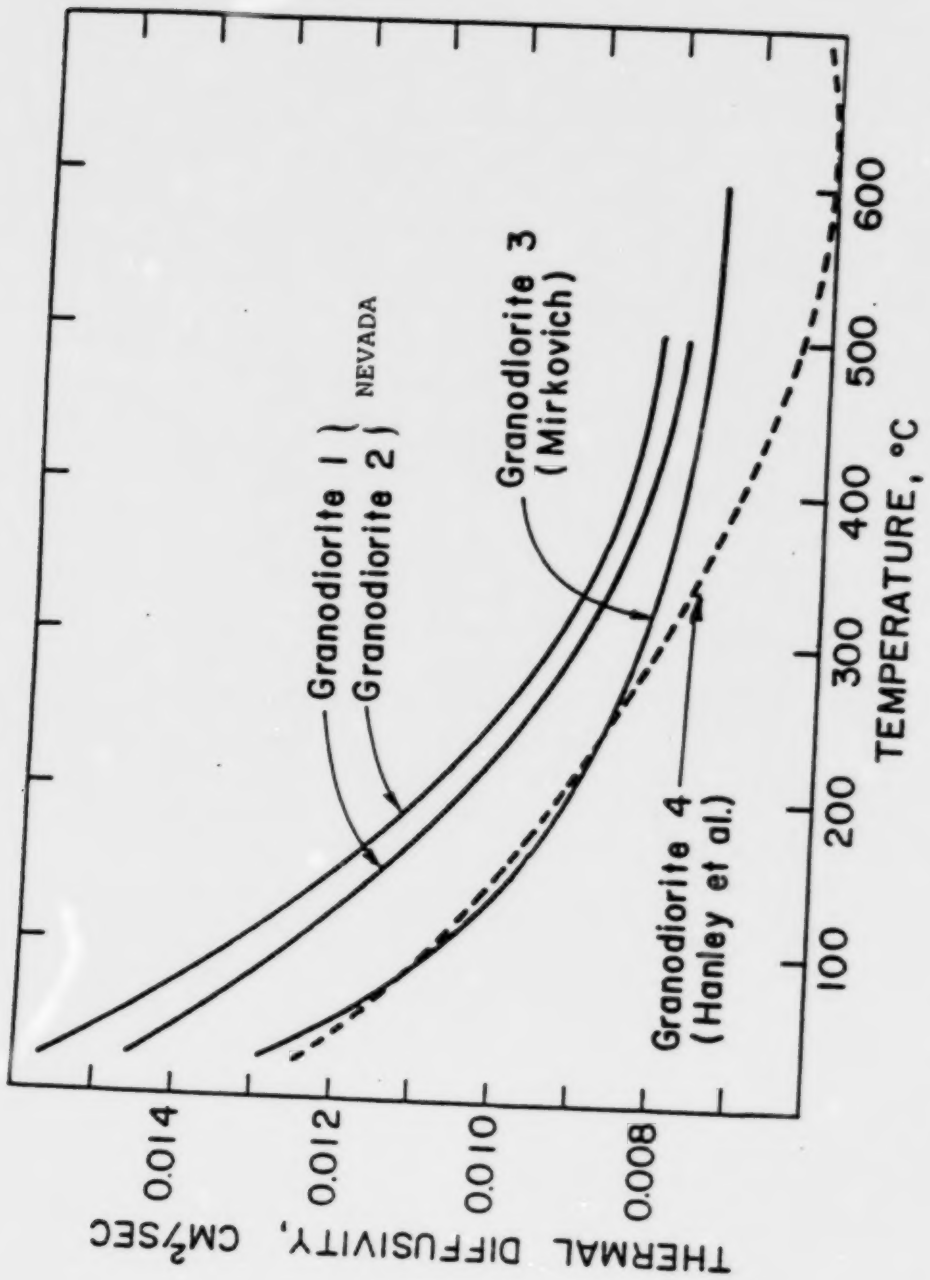

Figure 12.3: Comparison of Thermal Diffusivities of Granodiorite From Nevada Test Site and From Two Other Sources (Ref. 20)

In the low temperature vault environment (<150°C) some chemical alteration of the rock along a fracture could result in a net increase in fracture aperture, i.e. the dissolution of the major mineral phases (feldspars + ferromagnesian silicates) usually involves the removal of significant amounts of soluble species. However, incongruent dissolution may produce alteration products with a significantly higher specific volume, thus compensating for any volume decrease from the removal of soluble matter. Precipitation of insoluble phases could further reduce the aperture of specific fractures.

The rate of movement of water through crystalline rock masses is usually assumed to be very low or stagnant and, therefore, chemical equilibrium is also assumed. However, because of perturbations induced by the vault there may be regions where flow (induced thermally or otherwise) will be sufficient to make the kinetics of the nuclide chemistry important.

Some studies on passing granitic composition groundwater (simulating the vault environment) through a saline equilibrated fracture (simulating a natural fracture at depth in the granitic pluton) indicate that chemical equilibrium with the in situ fracture sidewall mineralogical composition is achieved after some 30 to 40 days, but that the composition of the porewater after this time still varies markedly from that of the original saline solution (Figure 12.4) (Ref. 33).

It currently appears that although minerals on the sidewalls of fractures exert some influence on migration of chemical constituents it is not at all certain how they will affect radionuclide migration.

Ongoing work (Ref. 21, 26, 32, 33, 99 etc.) points to the fact that little quantitative data is available on the exact chemical effects that warm groundwater circulation will exert on the mineralogy of the fracture fillings and host rock mass.

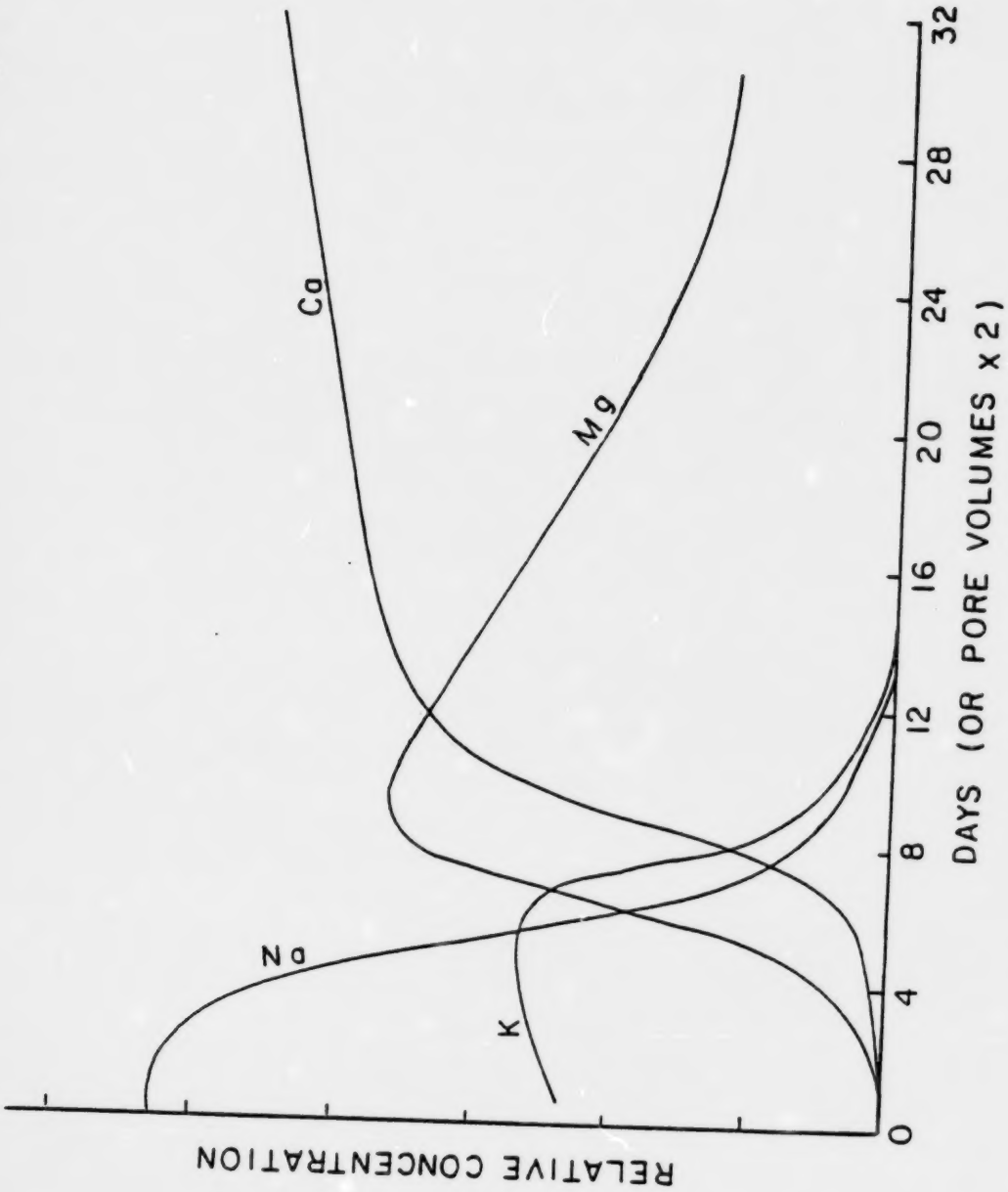

Figure 12.4: Results of Model Simulation to Predict Composition with Time During Flow Through a Fracture. Fracture Contains Calcite and an Unspecified Phyllosilicate with a Cation-Exchange Capacity of 5 meq/100g (Ref. 33)

13. Natural Analogues

Chapman and coworkers (Ref. 80) point out that, owing to the complexity of the phenomena being considered, the extrapolation from grams, centimetres and hours or weeks in laboratory experiments to tonnes, kilometres and many thousands of years for the disposal concept is enormous. It is highly desirable to seek natural analogues of the various processes by which by which the effectiveness of long term storage may be evaluated. For the same reason of complexity, it is unreasonable to expect that any one natural analogue will mirror all features of the concept. Many relevant phenomena in nature are being studied by various workers. Some of them mimic more than one feature. Some are processes now going on; some are fossils. These authors have examined the analogues from the points of view of the Swedish (KBS) and Swiss (Nagra) concepts, which, however, are each sufficiently similar to the Canadian concept to justify paying rather close attention to their findings.

13.1 Key Processes

Chapman et. al (Ref. 80) list nine key processes, and then consider each in turn, first in general terms, then looking at the relevant analogues, and finally recommending further study. Their nine processes form the titles of the following subsections.

As noted above, no analogues exist for the complete system. The most promising are ore deposits, and geochemical anomalies generally; dissimilar rocks in contact, moving porewater, etc. Many radionuclides cannot be observed in nature, but chemical analogues exist for most, i.e. elements with similar oxidation states, ionic radii and tendencies to complex formation. For example, among non-natural or rare elements, Tc is similar to the natural Re, Pa to Th, Np to U and Th, and Pu, Am and Cm to the Rare Earth elements.

13.1.1 Thermal/Chemical Breakdown of Buffer and Seal

Analogues are to be sought in examples of diagenesis and low-grade ($<100^{o}C$) metamorphism, thickly-bedded sediments, and igneous intrusions into clay.

Trials have shown that bentonite clays that have dried out resaturate smoothly on rewetting. The question is whether this will occur after temperatures in the vicinity of $100^{o}C$ have been reached. It is known that smectites, when exposed to higher temperature in the presence of abundant potassium ion can be transformed into illite, with reduced volume and reduced ion exchange capacity. Anderson (Ref. 81) has reviewed available data and concluded that while relatively rapid illitization occurred in a thick sediment, with adequate K^{+} supply and temperatures in excess of $100^{o}C$, more relevant examples in K^{+}-poor granite groundwater showed less than 0.3% transformation per million years. A possible high-temperature

example was studied by Altaner (Ref. 82), of an intrusion of a dyke at 800°C into clay. He found that the effect was confined to the 2m nearest the contact.

No models were found that are relevant to the use of plastic clay or for sand-clay mixtures as proposed for backfill and shaft sealing materials.

13.1.2 Waste Package Corrosion

Under this heading, Chapman et al (Ref. 80) considered only the copper (Swedish) and iron (Swiss) containers, so their analogues are only marginally relevant to the present study. We note briefly that archeological artifacts in copper and iron, native copper boulders and iron-nickel meteorites were examined, enabling predictions of 250,000 a lifetimes for the Nagra iron containers, and 80,000 - 400,000 a for the KBS copper containers. The observed pitting factors for copper were from 2 to 6. The extension of these results to titanium is difficult, but perhaps use of similar pitting factors would be justified.

13.1.3 Waste Forms

13.1.3.1 Borosilicate Glass Forms

No good analogue for borosilicate glass exists naturally. Some parallels do exist, however. The chief enemy is devitrification, which requires moisture, witness the ancient glass found on the Moon. The process of hydration and devitrification proceeds from the surface according to a parabolic time law, i.e. it is proportional to $t^{1/2}$. The products tend to retard the process. At modest temperatures it is slow, and Chapman et al. (Ref. 80) estimate the life of a glass block exposed to limited water at 10^7 to 10^8 years. They do not describe the block in detail. They suggest that more work is needed on the effects of radiolysis.

13.1.3.2 Spent Fuel

It is under this heading that the extensive study (Ref. 62) of the natural reactor at Oklo, Republic of Gabon, finds its chief application.

For present purposes, two aspects of the phenomenon are important. The first, historically, was the transport of uranium by groundwater to the site of the reactor. The host rock is a relatively porous sedimentary formation, with a low natural content of uranium. What appears to have happened is that well oxygenated water has oxidized uraninite to uranate ion, which, being more mobile, was transported to a region where organic remains or Fe(II) created reducing conditions. There uraninite was redeposited. The second aspect relates to the period during and after the activity of the reactor, when temperatures were elevated and hydrothermal conditions would be

expected to accelerate both chemical change and transport of fission products.

What is extraordinary is the degree to which these expectations were not realized. The uraninite grains within the reactor zone are intact except for the outermost micrometre (Ref. 83). Smellie and Rasholt (Ref. 84) mention that uraninite is not subject to metamictization, and that ore bodies at 50 - 130 m depth have remained texturally stable for as long as 1750 Ma. The loss of fission products that has taken place apparently occurred by diffusion rather than by dissolution of the grains, which would take more than 10^8 years.

Even diffusion escape has occurred only to a limited extent. Walton and Cowan (Ref. 61) tentatively conclude that virtually the only radioactive products that moved during criticality were ^{85}Kr, ^{137}Cs and ^{90}Sr. Later on some movement of Xe, Rb, Ba, Mo and I occurred. Brookins (Ref. 85) reports studies of the Rb/Sr and Cs/Ba isotope distributions that suggest that while some migration has occurred, cesium was retained in the overall system until at least 26 million years after reactor shutdown. The Rb/Sr data are not as clear, but seem similar. This is encouraging, because the Oklo formations are much more permeable than the granite of plutons.

Oklo is not totally comparable to the spent-fuel storage situation, but it is useful because of

(a) the long time scale, approaching 2×10^9 years
(b) the high temperatures reached, above 400°C, greater than in any storage concept
(c) the geology of the site, characterized by high porosity and liberal access of groundwater. Thus Oklo represents something like a "worst case". Nevertheless, the movement of fission products and of actinides away from the site has been very limited, being confined to the few noted above. The chief negative feature is that the burnup ratio is very modest, though Cowan reports one drill core in which the ^{235}U content has declined to 0.44% of the total uranium (Ref. 86).

13.1.4 Solution and Speciation

Under this heading Chapman's group found little that was considered relevant. The chief difficulty with the one natural analogue, the near-surface deposits at Morro do Ferro, Brazil (Ref. 87, 88) and also with various studies of mine and mill tailings (Ref. 89) is that both were characterized by high organic carbon contents in the groundwater, which is not expected in any of the Swedish, Swiss or Canadian sites. They were helpful to a limited extent in confirming some theoretical predictions concerning transport of certain nuclides as complexes.

13.1.5 Mineralogical Fixation at High Temperatures

Here Chapman and coworkers (Ref. 80) concluded that the higher temperature examples, e.g. the Eldorado stock (Ref. 90) and hydrothermal vein filling (Ref. 91) were inappropriate owing to too high temperatures and wrong chemistry. The lower-temperature examples (50-150°C) considered by Apps et. al. (Ref. 92), of development of clays (kaolin) may be relevant, but it is hard to find cases where the groundwater composition is appropriate.

13.1.6 Radiolysis

Oklo was considered most likely to yield evidence of a "redox front" and possible enhanced transport as a consequence. Curtis and Gancarz (Ref. 93) found evidence of local radiolytic redox activity, but the hydrogen produced was not lost by diffusion as has been predicted. Rather it actively reduced iron in the neighbouring rocks, and to a lesser extent in an aureole. They found that 80% of the Mo produced in the reactor, 35% of the Tc and 25% of the Ru were missing from the reactor zone, together with a small amount of U. The amount of hydrogen that had to be lost to effect this amount of oxidation agreed with estimates based on the calculations of Christensen and Bjergbakke (Ref. 94). The oxidized and reduced zones were not well separated, and were distributed in a complicated way. The "redox front" idea is clearly oversimplified.

An unanswered question remains: would the reduction of iron by the escaping hydrogen happen at the lower temperatures of the Canadian concept? If not, more migration of oxidized species would be expected, but even then it would be confined to the zone of oxidation, and not reach far into the rock mass.

13.1.7 Redox Equilibration

Ore deposition is an analogue of redox deposition, but usually poor because of elevated temperatures. A class of exceptions is found in "roll-front" deposits, which are products of "redox traps". Oklo is an example. They result from migration of a tongue of oxygenated water through a sandstone aquifer into a reducing zone. The conclusion is inescapable that redox changes certainly influence radionuclide migration. Oklo provides evidence for redox transport of uranium to the reactor site before (and perhaps during) the active phase, and of Mo, Tc and Ru and their reprecipitation afterwards. The applicability to the concept is limited, however, because as noted above

(a) the sandstone is too porous compared to granite
(b) organic and microbiological activity were important factors

Chapman and coworkers (Ref. 80) mention studies in progress of Eh, pH, pS^{2-}, Fe^{2+}/Fe^{3+}, etc. in the groundwater at Oklo that may be helpful in the future.

13.1.8 Retardation

This is a particularly fertile field for natural analogue studies, as laboratory data do not extrapolate well to the natural world. The multiple processes involved - physical adsorption, chemisorption of several kinds, ion exchange, ion exclusion, ultra-filtration - have different scaling laws. Brookins (Ref. 95) in studies at Oklo, notes that the source term is appropriate, but that conditions were uncertain and variable, and that interpretation in quantitative form is difficult. Qualitatively, he lists the following:

Most migrated	- Kr, Mo, Cd, I, Xe, Cs
Variable, or locally redistributed	- Rb, Sr, Tc*, Ru*, Ba, Pb*, U*
Most retained	- Y, Zr*, Nb, Rh, Pd, Ag, In, REE, Bi*, Po, Th, Np, Pu
Not measured	- Sn, Sb*, Te, Am

(Elements marked with the asterisk* are predicted from known Eh-pH properties to show some migration, especially at higher temperatures).

Krishnaswami et al. (Ref. 96) and Hussain and Krishnaswami (Ref. 97) by means of multiple isotope-ratio studies on the transport of members of natural radioactive series have shown that retardation by large factors does occur.

Perhaps the most interesting study, especially in its relevance to the buffer and backfill and their ability to retain certain elements, is the one discussed above (Sec. 11.1), by McKinley et. al. (Ref. 60) on the interbedded fresh water and marine deposits in Loch Lomond. The astonishing immobility of I and Br flies in the face of all predictions.

13.1.9 Matrix Diffusion

By this is meant diffusion of radionuclides from cracks in the rocks into the rock matrix itself. If it occurs, it might provide a powerful retarder of many elements, or even an effective sink. Laboratory studies by Birgerson and Neretniek, (Ref. 98) support the idea, even in "impermeable" granite. It is a phenomenon that is hard to extrapolate from the laboratory time scale to geological scales.

At the time of the Chapman report (Ref. 80) studies were in progress at Lac Du Bonnet by Cramer and Gascoyne, and elsewhere

by Shea, but Chapman et. al. conclude that the effect has not yet been evaluated.

13.2 Natural Analogues - Reassurances and Questions

The lessons from study of natural analogues so far carry a number of reassurances. Illitization of bentonite is not likely to be a problem. Long container lifetimes are possible, though perhaps not quite as long as assumed in the Second Interim Assessment. Devitrification and leaching of glass waste forms may be even slower than currently expected. Dissolution of irradiated fuel by groundwater will take a very long time, perhaps more than 10^8 years. Our ideas concerning retardation of ions by buffer, backfill and host rock seem basically correct, and largely our estimates of extent of retardation are conservative, especially as regards iodine.

There are some unanswered questions. Work is needed especially on:

(a) the development of redox fronts, and mobilities across them
(b) migration in veins, especially water-bearing fissures
(c) migration from geochemical anomalies (e.g. why is I so immobile in the Loch Lomond sediments?)
(d) migration of negative ions in geological formations (e.g. migration of Cl^- into rocks in contact with seawater)
(e) the reaction of hydrogen with iron-bearing rocks at moderate (30-100^{o}C) temperatures

The lessons of the natural analogues are, however, largely reassuring, and suggest that the design criteria at each stage in the Canadian concept are conservative.

14. Conclusion

14.1 Summary of Findings

This report has reviewed the design and the predicted consequences of the Canadian Concept for long-term waste storage in the light of information gleaned from the general literature as well from publications coming from other countries' nuclear waste management programmes. The properties of the important radionuclides, and the behaviour of the various component materials under the influences of stress changes, heat and radiation effects and due to chemical and physical changes as a result of groundwater migration were considered.

The Concept as currently envisaged has been documented and involves placing containers of wastes in mined vaults at approximately 1 km depth in plutons in the Canadian Shield. The wastes will consist of:

(a) used fuel (UF) from CANDU reactors, in bundles of zircaloy-clad elements, packed with glass beads in sealed titanium containers and

(b) wastes from fuel recycling operations of two kinds; highly active fuel recycle wastes (FRW), mainly fission products, cast as glass in stainless steel canisters and similarly enclosed in titanium containers, and less active transuranic wastes (TRUW) contaminated with transuranic elements, in drums.

Each will be placed in separate vaults, the UF and FRW in boreholes in the vault floor, the TRUW standing in the rooms. All will be packed round with buffer material (bentonite clay and sand, with additives) and the rooms backfilled and sealed.

The geometries and relative placing of the rooms making up each vault, and the several vaults, are still undergoing detailed design optimization which must take into account the thermal radiation and stress environments to ensure no detrimental stress fracturing develops and that the temperature in the neighbourhood of the emplacement chambers will not exceed 100°C. Temperatures close to this value however, are predicted to be maintained for more than 10,000 years for UF and 100 years for FRW.

The immediate surroundings of the containers (the buffer) will be subjected to radiation at dose rates initially reaching 20.4 SV h^{-1} for UF and 154 SV h^{-1} for FRW. Because the FRW contains mainly relatively short-lived radionuclides the ultimate total dose to the buffer at the container surface will be higher for the UF (> 3×10^8 Sv at 1 Ma) than for the FRW (approx. 1.5×10^8 Sv). Damage to minerals (see above Sec. 10.3), except for certain sensitive ones such as calcite, appears to require absorbed doses in excess of 10^{10} Gy, and at the same time dose

rates in excess of 10^3 Gy h^{-1}. In consequence, there appears to be little danger of direct radiation damage occurring to the buffer. This applies a fortiori to the backfill and host rock, for the radiation dose rate declines one hundredfold less than one-third of a metre into the clay. In the granite rock mass it is even lower; at 1.5 m from the centre of a single container (FRW or UF) it will be close to the surface natural background dose rate.

Potentially more serious is the micro and macrofracturing likely to develop due to stress changes and blasting effects associated with vault and shaft excavation. The stress changes in the host rock adjacent to the excavations that develop as a consequence of blasting out the vaults will likely be compounded by stress redistribution as a result of differential heating of the adjacent rock mass, owing to the release of radiogenic heat from the stored wastes. Interconnection of such local fracturing with natural rock fractures could allow unwanted pathways to the surface to develop. No plutons are entirely free from fractures, which may include microscopic local cracks, more systematic sets of joints or even faults and complex fracture or shear zones. Many of these are narrow, and thus permit only very slow flow of groundwater. However, certain of the younger fractures and fracture zones, (and notably some of the subhorizontal features such as seen at Lac du Bonnet) are sufficiently permeable that they may provide preferential pathways for more rapid flow.

The combined effects of vault excavation, stress changes and thermal stress redistribution mentioned above will develop new fractures in the rock mass as well as increasing the amount of fracturing in the neighbourhood of existing natural fracture systems. These effects are strictly local in scale and therefore are of concern only as they may create pathways through the rock along vault walls, drifts, and shafts to the surface. Although the geometry of the envisaged vault arrangement is such that these paths will be very long, greater than 1 km, because of the dramatic contrast in permeability that can occur adjacent to underground excavations when compared to the typical bulk permeability of the rock mass, very careful control of the excavation methods and final sealing (grouting) is essential.

For the Candian Concept, there are five barriers to the escape of radionuclides, to the point where they might affect man's environment. They are (in space sequence) the waste form itself, the canister or cladding, the container, the buffer and the host rock. We consider them in time sequence, beginning with the titanium container, which must resist both mechanical stresses due to the environment in which it is placed, and corrosion by groundwater.

Since the location of the vault is to be within a stable pluton in the Shield, which has not suffered tectonically for many

millions of years, the insitu stress state of the rock mass can likely be predicted with reasonable accuracy and the potential stresses that might develop on the container due to thermal and other effects computed.

As the vault will be designed to be completely backfilled with relatively low modulus materials (clays essentially) all major stresses will be borne by the rock and no significant stresses will be taken by the emplaced canisters other than that imposed by the pore pressures built up in the resaturated buffer and backfill. Such pressures are themselves unlikely to exceed full hydrostatic for which the containers are currently being designed, and thus the risk of rupture of the containers from this cause is low.

Corrosion of the containers will be more important. It is neverthless expected to be slow. Estimates of container lifetime were made for the Second Interim Assessment (Ref. 11) by extrapolating laboratory experiments on uniform corrosion, with allowance being made for accelerated corrosion by pitting. Since titanium is protected by an adhering film of corrosion products, the rate of corrosion is governed by diffusion through the adhering layer, which leads to the extent of corrosion being proportional to the square root of exposure time, making linear extrapolation for the rate of corrosion yield pessimistic estimates of container lifetimes.

Once the container is pierced, access of groundwater to the waste form will soon follow, for the inner metal layer (cladding or canister) is relatively thin. The radionuclides in the waste are not all of equal concern. Among fission products, those which have relatively long lifetimes, and are present in appreciable amounts in the waste, and have been deemed most likely to be readily transported by groundwater have attracted most attention. These include isotopes of Se, Tc, I and Cs. The most worrisome radionuclide is ^{129}I, which has a half-life of 2×10^7 years, and is present in used fuel at about 40 mg/kg of uranium.

The reason for this concern is discussed below. This and several other more soluble elements are likely to be present to a limited extent in the intergranular spaces in used fuel, and therefore instantly accessible to the groundwater. The remainder (85% or more) will be bound within the UO_2 grains. All the radionuclides in the vitrified FRW will, at least in principle, be bound. Since neither the UO_2 grains nor the FRW glass are expected to be rapidly dissolved by groundwater, their burden of soluble radionuclides must escape by diffusion, a slow process. There is some concern that locally oxidizing conditions could allow recrystallization of UO_2 and consequent escape of impurities, but the observation that the uraninite grains at Oklo were hardly touched in 10^9 years, and the long life of volcanic and man-made glass (Refs. 62, 80) suggest that

this escape will not be much accomplished in the 10^7 years of the planned containment.

The diffusible or soluble radionuclides that do escape immediate containment are then exposed to groundwater that may contain complexing agents (ligands) such as carbonate, bicarbonate and chloride, and may be locally oxygenated, at least during the early stages of the burial period, through radiolysis of water. Oxidation and complexation by anions can cause other elements than those listed above to be present as negative ions (anions). This is seen as a problem because most minerals, while they tend to have cations (positively charged) that are exchangeable for cations in solution, they do not have exchangeable anions. The anions in most minerals are bound into the framework of the crystal, while free cations occupy interstitial positions. The particular concern for iodine is that it exists in ordinary circumstances only in anionic forms. It appears to have been assumed by Wuschke *et al.* (Ref. 11) that it would not be retarded at all by the geologic formations though which it was being carried by flowing groundwater. In consequence, it was the first radionuclide to reach the biosphere in their computer simulations, and it did so at times less than its half-life.

This and almost all reviewed simulations appear to have been done assuming that the groundwater circulation patterns remain essentially unperturbed by the excavation of the vaults and the emplacement of the wastes. This is probably a fair assumption on a gross scale, except for the few years immediately after the vault closure, after which time the initial perturbations at the vault site would have likely disappeared. The groundwater patterns that would be established for the next ten thousand years or so might, however, be perturbed by thermal effects arising from the stored wastes. Computer simulation (Ref. 73) and geological study (Refs. 74, 35) have shown that perturbations are likely. The results of such perturbations on radionuclide transport are unclear, for the simulations led, depending on the choice of initial parameters, either to accelerated or retarded "escape" of radionuclides. The water-rock interactions are complex, and depend in detail on the chemical history of the groundwater, the nature of the rock, the pattern of joints and microcracks, the minerals filling or lining these joints, etc. This requires further study, and at present is probably best handled, in future simulations of radionuclide transport by groundwater, by increasing the assumed uncertainty of the groundwater transit times.

The effect on groundwater flow from the thermal gradient may be significant locally to the vault in that, because of preferential fracturing developed around the openings due to excavation and stress related effects, a more permeable zone will exist than likely occurs deeper into the rock mass (except in proximity to major natural fracture systems). Groundwater movement due to thermal conduction and convection effects within this more fractured zone may mirror that seen in the

Empire Creek stock in Montana where significant groundwater movement and high thermal gradients occur within the geothermally active fracture zones. Such thermally induced groundwater movement could give rise to upwelling of warmer water in the immediate vicinity of the original vault access excavations, (e.g. shafts and the like).

Detailed study of the influence of local and large scale excavation-induced fracturing and of zones of increased hydraulic conductivity on thermally induced groundwater flow obviously require addressing. Data from natural analogues such as the Empire Creek stock and the Nevada springs and other data from the hot-dry rock programs of Los Alamos in the States and the Carnmanelis granite program in Cornwall in the UK may provide significant information relevant both to the optimization of access methods (i.e. shafts and ramp systems) and to the design of effective vault sealing systems sufficient to minimize the develop of a potential thermal plume.

By contrast, the assumption that iodine is not retarded in the groundwater system is probably too stringent and could conceivably be relaxed, for observations at Oklo (Refs. 61, 62) imply only very limited movements of iodine isotopes away from the reactor site. The discovery of the interbedded iodine-rich (marine) and iodine-poor (freshwater) sediments in Loch Lomond (Ref. 60) in which iodine and some other supposedly mobile elements have hardly moved in nearly 40,000 years reinforces this suggestion. It is probable that ways of binding many substances to a variety of minerals exist that are not foreseeable at present. Nothing can make a nuclide move faster than the groundwater, but there are many ways in which it can be retarded. Ways that have been considered include ion exchange, precipitation and adsorption by minerals. Some of these processes that in particular cases have not been observable in the laboratory may yet occur given the long times available for slow reactions in the real case.

The conclusions that the present authors have reached from this review suggest that the Canadian Concept as presented to them seems to be essentially sound, and is in most respects probably conservative.

There are some unanswered questions, some of which have been already posed in the earlier chapters of this Report. The main topics for further examination however are reiterated in Section 14.2.

14.2 Recommendations

The following are listed in no particular order, but are numbered for reference only. It is RECOMMENDED:

1. That the Canadian Concept be proceeded with in the confidence that it is essentially sound, and that minor

adjustments can be made as they appear appropriate or necessary.

2. That evaluations of radiation dose rates and integrated doses to the near field components of the repository be prepared, including maximum doses to the inner walls of containers, the buffer, backfill and rock components. Geometry factors reflecting the placement of multiple containers should be included. The resulting data will provide a consistent basis for evalutions of radiation effects during the assessment of the waste repository concept.

3. That further studies be conducted on the transport of certain radionuclides by groundwater (I, especially, but also Cl, Cd, Sr and Cs) through study of natural analogues, through laboratory experiments and by computer simulation.

4. That further study of corrosion of titanium be done, to determine whether pitting can be easily induced, and with what result.

5. That the reality of the "redox front" be further investigated, in view of the findings at Oklo (Ref. 93), that the reduced and oxidized regions were not well separated.

6. That the effect of reducing agents in the buffer and host rock, especially iron sulphides, on the results of radiolysis of water be further studied to resolve the apparent contradiction between different workers' conclusions (Refs. 31, 68).

7. That thermally induced groundwater convection, in undisturbed rock and in the fracture zone that develops around the vault and around the shafts be studied with further reference being made to natural geothermal systems to quantify governing processes.*

8. That study of all available natural analogues be continued, as these are the most fruitful sources of information that reflect the complexity and long time scale of the phenomena upon which the design of the disposal system depends.

*[A modelling study is underway of coupled thermal and hydrological of the vault. The effects of fracturing are not included, but significant acceleration of groundwater movement to the surface is predicted (Ref. 101)

REFERENCES

1. Baumgartner et. al. (1986), Technical Specifications for a Concept Assessment Engineering Study of Nuclear Fuel Waste Disposal Centres, Atomic Energy of Canada unpublished report.

2. W.L. Wardrop and Associates Ltd. (1978), Buffer and Backfill Engineering Study, Interim Report No.4: Materials Handling, Atomic Energy of Canada Ltd. Technical Record 273.

3. Atomic Energy of Canada Ltd. (1982), Geotechnical Research: Proceedings of the Seventh Nuclear Fuel Waste Management Information Meeting, Ottawa, Ontario, AECL TR-190.

4. Radhakrishna, H.S. (1982), Evaluation of the Thermal Properties of Buffer Materials for a Deep Underground Nuclear Waste Disposal Vault, AECL TR-183.

5. Atomic Energy of Canada Ltd. (1981), Waste Forms and Engineered Barriers: Proceedings of the Tenth Information Meeting of the Nuclear Fuel Waste Management Program, Whiteshell, Pinawa, Manitoba TR-166.

6. Atomic Energy on Canada Ltd. (1982), Proceedings of the Fourteenth Information Meeting of the Nuclear Fuel Waste Management Program, Winnipeg, Manitoba, AECL TR-207.

7. Hood, Michael (1979), Some Results from a Field Investigation of Thermo-Mechanical Loading of a Rock Mass when Heaters are Emplaced in the Rock, Technical Information Report No. 26, Swedish American Cooperative Program (LBL-9392).

8. ONWI (1980), Proceedings: Workshop on Thermo-Mechanical - Hydrochemical Modelling for a Hardrock Waste Repository, Berkeley, California (LBL-11204).

9. Mayman, S.A., Charlwood, R.G., and Ratigan, J.L. (1980), Long-Term Thermal Response of a Candu Fuel Disposal Vault (TR-134).

10. Gillespie, P.A., Wuschke, D.M., Guvanasen, V.M., Mehta, K.K., McConnell, D.B., Tanim, J.A., and Lyon, R.B., 1985, Second Interim Assessment of the Canadian Concept for Nuclear Fuel Waste Disposal, Vol. 2: Background, AECL-8373-2.

11. Wuschke, D.M., Gillespie, P.A., Mehta, K.K., Heinrich, W.F., LeNeveu, D.M., Guvanasen, V.M., Sherman, G.R., Donahue, D.C., Goodwin, B.W., Andres, T.H. and Lyon, R.B., (1985), Second Interim Assessment of the Canadian Concept for Nuclear Fuel Waste Disposal, Volume 4: Post-Closure Assessment, AECL TR-8373-4.

12. Crosthwaite, J.L., 1985, Metal-Matrix Used-Fuel Disposal Container Development Program, Proceedings of the Nineteenth Information of the Nuclear Fuel Waste Management Program, Toronto, 1985 May 14-16, AECL TR-350.

13. Hosaluk, L.J. and Teper, B. (1985), Status of Alternative Container Designs for Fuel Waste Disposal, Proceedings of the Nineteenth Information Meeting of the Nuclear Fuel Waste Management Program, Volume 1, AECL TR-350, p. 65.

14. Bird, G.W. (1979), Possible Buffer Materials for Use in a Nuclear Waste Vault, AECL TR-72.

15. Dixon, D.A. and Gray, M.N. (1985), The Engineering Properties of Buffer Material, in Proc. 19th Information Meeting, AECL TR-350.

16. Yong, R.N., Boonsinuk, P. and Wong, G. (1985), Formulation of Backfill Materials for a Nuclear Waste Disposal Vault, in Proc. of 19th Information Meeting, AECL TR-350.

17. Sargent, F.P. (1982), Applied Chemistry and Geochemistry Research for the Canadian Nuclear Fuel Waste Management Program, AECL TR-149.

18. Hyndman, D.W. (1972), Petrology of Igneous and Metamorphic Rocks, McGraw Hill Book Company, New York.

19. Carmichael, I.S.E., Turner, F.J. and Verhoogen, J. (1974), Igneous Petrology, McGraw Hill Book Company, New York.

20. Golder Associates (1979), Geologic, Structural, Thermal and Mechanical Factors which Influence Repository Design in Granitic and Basaltic Rocks, Report to Lawrence Livermore Laboratories.

21. Cramer, J.J. (1984), Effects of Rock-Water Interaction on Radionuclide Transport, AECL TR-201.

22. Golder Associates (1983), Report to Atomic Energy of Canada Ltd. on a Stiff Packer System for Monitoring Groundwater Pressures.

23. Stone, D. and Kamineni, D.C. (1981), Fractures and Fracture in Fillings of the Eye-Dashwa Lakes Pluton, Atikokan, Ontario, Can. J. Earth Sci.19, 789-803.

24. Kamineni, D.C., Brown, P.A. and Stone, D. (1980), Fracture-filling Materials in the Atikokan Area, Northwestern Ontario, AECL TR-109.

25. Dugal, J.J.B., Hillary, E., Kamineni, D.C., Flindall, R.N., Ejeckam, R. and Sikorsky, R. (1985), Well History Report for Borehole ATK-1 in the Atikokan Research Area, AECL TR-292-1.

26. Fleer, W.N., and Johnston, R.M. (1985), The Dissolution Behaviour of Minerals in Granitic and Gabbroic Systems, AECL TR-328.

27. Garrels, R.M. and Mackenzie, F.T. (1967), Origin of the Chemical Composition of Some Springs and Lakes, In Equilibrium Concepts in National Water Systems, Am. Chem. Soc. Adv. Ser. 67, 222-242.

28. Rose, A.W. and Burt, D.M. (1979), Hydrothermal Alteration, In Barnes, H.L. (ed.) Geochemistry of Hydrothermal Ore Deposits, 2nd ed., Wiley-Interscience, New York, pp. 173-235.

29. Ellis, A.J. (1979), Explored Geothermal Systems, In Barnes, H.L. (ed.) Geochemistry of Hydrothermal Ore Deposits, 2nd ed., Wiley-Interscience, New York, pp. 632-683.

30. Atomic Energy of Canada Ltd. (1981), Proceedings of the Eleventh Information Meeting of the Nuclear Fuel Waste Management Program, AECL TR-180.

31. Chan, T. (1979), Thermal and Stress Analyses for a High-Level Radioactive Waste in Crystalline Rock, Whiteshell, Pinawa, Manitoba, TR-69.

32. Ticknor, K.V., Vandergraaf, T.T., and Kamineni, D.C. (1985), Radionuclide Sorption on Mineral and Rock Thin Sections, Part I: Sorption on Selected Minerals, AECL TR-365.

33. Reardon, E.J. and Reimer, J.D. (1982), A Laboratory Investigation of Crystalline Rock-Water Interactions, University of Waterloo, AECL TR-137.

34. Johnston, L.M. (1983), A Review of the Geochemistry of Groundwater in Crystalline Rocks, AECL TR-154.

35. Haverslew, B., and Tammemagi, H.Y., (1985). Geochemical Analysis of Core From a Geothermal Anamaly. Atomic Energy Control Board Research Report #INFO-0155, Ottawa.

36. Burgess, A.S. (1979), Pluton Hydrogeology, AECL TR-73.

37. Isherwood, D., Raber, E. and Stone, R., 1981; in Topp, 1981, pp. 199 - 206 (Ref. 19).

38. White, D.E., Hem, J.D. and Waring, G.A. (1963), Chemical Composition of Subsurface Groundwaters, USGS Prof. Pap. 440-F.

39. Fritz, P. and Frape, S.K. (1982), Saline Groundwaters on the Canadian Shield - a First Overview, Chem. Geol. 36 - 179-190.

40. Bottomley, D., Graham, B., and Ross, J. (1980), Investigations into the Geochemistry of Groundwater in PreCambrian Crystalline Rocks, AECL TR-122.

41. Mirkovich, V.V. (1979), Some Thermophysical Properties of a Granodiorite Rock from Nevada Test Site, AECL TR-18.

42. Hamstra, J., Ed., 1982, Geological Disposal of Radioactive Waste: Geochemical Processes, O.E.C.D., Paris.

43. Chapman, N.A., McKinley, I.G., Savage, D. and West, J.M., 1981; in Topp, 1981, pp. 347 - 354 (Ref. 19).

44. Topp, S.V., Ed., 1981, Materials Research Society Symposia Proceedings, Vol. 6, Scientific Basis for Nuclear Waste Management, North-Holland, New York, etc.

45. Black, J.H. and Barker, J.A., 1981; in Topp, 1981, pp. 223 - 230 (Ref. 19).

46. Petit, J.C., Langevin, Y. and Dran, J.C. 1985, Geochim et Cosmochim Acta, 49, 871 - 876.

47. Tait, J.C. (1985), Radiolysis in Waste Form Interaction Tests, Geochemistry and Applied Chemistry Branch, Whiteshell Nuclear Research Establishment, Pinawa, Manitoba, AECL TR-350.

48. SKBF Technical Report on Final Storage of Spent Nuclear Fuel - Report #KBS-3, Section III, Subsection 13.3.

49. Greagor, R.G., Lytle, F.W., Ewing, R.C. and Waaker, R.F. (1984), Exaps Studies of Metamict Materials, Third International Exaps Conference, Palo Alto, California.

50. Tait, J.C. (1982), Radiation Effects in Nuclear Waste Forms, in Chemistry and Geochemistry - Proceedings of the Thirteenth Information meeting of the Nuclear Fuel Waste Management Program, AECL TR-201, V.1. pp. 176-184.

51. Koplik, C.M., Oston, S.G., Pentz, D.L. and Talbot, R. (1985), Information Base for Waste Repository Design, Volume 3 Waste/Rock Interactions, U.S. Nuclear Regulatory Commission, NUREG/CR-0495 TR-1210-1.

52. Van Konynenburg, R.A., 1984, Radiation Doses in Granite Around Emplacement Holes in the Spent Fuel Test - Climax (Final Report), UCRL 53580.

53. Jenks, G.H. (1975), Gamma-Radiation Effects in Geologic Formations of Interest in Waste Disposal: A Review and Analysis of Available Information and Suggestions for Additional Experimentation, Oak Ridge National Laboratory, TR TM-4827.

54. Corbett, W.J., Burson, J.H. and Young, R.A., 1963, in, Swineford, A. and Franks, P.C. Eds., Clay and Clay Minerals, Macmillan, N.Y., pp. 344 - 355.

55. Komarneni, S., Palau, G.L. and Pillay, K.K.S., 1983, Nuclear and Chemical Waste Management, 4, 335 - 338.

56. Haire, R.G. and Beall, G.W., 1979; in, Radioactive Waste in Geological Storage, Amer. Chem. Soc., Washington, pp. 291 - 295.

57. Soo, P., Ed., (1983), Review of DOE Waste Package Program, NUREG/CR-2482-BNL-NUREG 51494 v. 4.

58. KBS Ann. Rep. (1983), citing SKBF KBS TR 83 - 38.

59. Lee, S.Y. and E.A. Bondietti, (1982); in Brookins, D.G., Ed., Materials Research Society Symposia Proceedings, Vol. 15, Scientific Basis for Nuclear Waste Management VI, North-Holland, New York, etc., pp. 315 - 322.

60. McKinley, I.G., Mackenzie, A.B., West, J.M., Scott, R.D., (1983), Scientific Basis for Nuclear Waste Management VII, pp. 851-857, McVay, G.L. Ed., North-Holland, New York

61. Walton, R.D. Jr., and Cowan, G.A. (1975), Relevance of Nuclide Migration at Oklo to the Problem of Geologic Storage of Radioactive Waste, in ref. 60, pp. 499-507.

62. Davies, M., Ed. (1975), Le Phenomene d'Oklo, I.A.E.A., Vienna.

63. Breck, W.G., (1972), Journal of Marine Research, 30, 121 - 39.

64. Torstenfelt, B., Anderson, K., Kipatsi, H., Allard, B. and Olofsson, V., (1981); in Topp, 1981, (Ref. 19) pp. 295 - 310.

65. Beall, G.W., Ketelle, B.H., Haire, R.G. and O'Kelley, G.D. (1979); in Fried, S., Ed., Radioactive Waste in Geological Storage, Amer. Chem. Soc., Washington, pp. 201 - 213.

66. Christensen, H., (1978), SKBF KBS TR 78.

67. Erikson, T. and Lind, J. (1983), DE 83 - 0177 BNL-TR-1000.

68. Christensen, H. and Bjergbakke, E., (1982); in Brookins, D.G.,Ed., Scientific Basis for Nuclear Waste Management VI, North-Holland, New York, etc., pp. 429 - 436.

69. Neretnieks, I. and Åslund, B. (1983), SKBF KBS TR 83 - 66.

70. Eriksen, T., (1983), SKBF KBS TR 83 - 27.

71. Moore, D.W., Morrow, C.A., and Byerlee, J.D., 1983, Chemical Reactions Accompanying Fluid Flow through Granite Held at a Temperature Gradient, Geochim. Cosmochim. Acta 47, 445-453.

72. Claesson, T. and Ronge, B., 1983, Water-Rock Interaction when Heated Water is Stored in Unlined Rock Caverns, In 4th Int. Symp. Water-Rock Int., Misasu, Japan, pp 90-93.

73. Beddoes, R.J., and Tammemagi, H.Y., (1986). The Effects of Radiogenic Heat on Groundwater Flow. Atomic Energy Control Board Research Report #INFO-0194, Ottawa.

74. Tammemagi, H.Y., Grisak, G.E., and Parrish, D.K. (1983). A Case History of the Marysville Geothermal Anomaly from a Nuclear Waste Disposal Perspective. Atomic Energy Control Board Research Report #INFO-0092, Ottawa.

75. Pusch,R. and Bergström, A. (1981); in Moore, J.G. Ed., Scientific Basis for Nuclear Waste Management 3, Plenum, New York and London.

76. Head, C.M., Moody, W.E., Mitchell, L. and Young, R.A., (1963), in, Swineford, A., and Franks, P.C. Eds., Clay and Clay Minerals, Macmillan, N.Y., pp. 356 - 364.

77. Westsik, J.H. Jr., Bray, L.A., Hodges, F.N. and Wheelwright, E.J., (1981); in Topp 1981, (Ref. 44) pp. 329 - 336.

78. Radhakrishna, H.D. (1985), Near Field Thermal Analysis of the Nuclear Waste Disposal Vault, AECL TR-350.

79. MacLaren, J.R., Davidge, R.W., Titchell, I., Sincock, K., and Bromley, A., (1981); in Topp, S.V., Ed., (1981), (Ref. 44), Materials Research Society Symposia Proceedings, Vol. 6, Scientific Basis for Nuclear Waste Management, North Holland, New York, pp 355-362.

80. Chapman, N.A., McKinley, I.G. and Smellie, J.A.T. (1984) EIR-Bericht Nr. 545, Eidgenoessisches Inst. fur Reaktonforschung, CH 5303, Wurenlingen, Switz.

81. Anderson, D.M., KBS R83-03, Stockholm, (1983).

82. Altaner, S., Whitney, G. and Hower, J. Abstr. (1981), Clay Mineral Conf. No. 30, Urbana Il. p 4 (1981).

83. Duffy, C.J., (1978), STI/PUB/475 pp. 229-234, IAEA Vienna.

84. Smellie, J.A.T. and Rasholt, J.N., Lithos 17 pp. 215-225 (1984).

85. Brookins, D.G., (1981); in Moore, J.G., Ed., Scientific Basis for Nuclear Waste Management 3, Plenum, New York and London, pp. 275 - 282.

86. Cowan, G.A. (1976), Scientific American, v. 235 (1), 36-47.

87. Eisenbud, M., Lei, W., Ballad, R., Kranokopf, K., Penna Franca, E., Callen, T.L. and Freeborn, P. (1982), STI/PVB/997 pp 739-755 IAEA, Vienna.

88. Miekley, N., Vale, M.G.R., Tavares, T.M. and Lei, W.,(1982), Scientific Basis for Nuclear Waste Management V pp. 725-733, Lutze, W. Ed. Elsevier, New York.

89. Benes, P., (1980), STI/PUB/597 pp. 3-23, IAEA, Vienna.

90. Brookins, D.G., Abashim, M.S., Cohen, L.H. and Wallenburg, H.A. (Jr.), Scientific Basis for Nuclear Waste Management IV p. 231 Topp SV Ed. N-H, NY (1982).

91. Shea, M. (1984), Scientific Basis for Nuclear Waste Management VII pp. 227-238, McVay, G.L. (Ed.), North-Holland, New York.

92. Apps, J.A., Carnahan, C.L., Lichtner, P.C., Michel, M.C., Perry, D., Seloa, R.J., Weres, O. and White, A.F., US NRC NUREG/CR-3062 Wash., p 365, (1983).

93. Curtis, D.B. and Gancarz, A.J., KBS TR 83-10, Stockholm, (1983).

94. Christensen, H. and Bjergbakke, E., KBS TR 82-18 Stockholm, (1982).

95. Brookins, D.G., Geochemical Aspects of Radioactive Waste Disposal, Springer-Verlay, New York, (1984).

96. Krishnaswami, S., Granstein, W.C., Turekian, K.K. and Dows, J.F., Wat. Res. 18 1663-75, (1982).

97. Hussain, N. and Krishnaswami, S., Earth Planet Sci. Lett. 58, 430-438, (1982).

98. Birgerson, I., and Neretnieks, I., KBS R82-08, 83-89, Stockholm, (1982, 1983).

99. Ticknor, K.V., Vandergraaf, T.T., and Juhnke, D.G. (1986). The Effect of Laboratory Time-Scale Hypothermal Alteration on Igneous Rock Coupon Radionuclide Sorption/Desorption. AECL TR-376.

100. Headley, T.J., Ewing, R.C., Haaker, R.F., Bailey, G.W. (1981). High-Resolution Study of the Metamict State in Zircon. Electron Microscopy Soc. of America, No. 39, pp. 112-113.

101. Wai, R.S.C., 1983. Coupled Thermal-Hydrological Modelling of a Nuclear Waste Disposal Vault. Unpublished draft report, Ontario Hydro/AECL.

APPENDIX A

AECB STATEMENT OF WORK

APPENDIX A

DSS SERIAL: 05SB4-00198 DSS FILE: 5SSS.87055-4-4058

PAGE 1 of 2

STATEMENT OF WORK

Work Statement

1) Background Information: There are many factors which must be considered in order to properly assess the risk, to people and the environment, of the deep disposal of radioactive waste. The response of the individual components of a deep geological waste disposal system to imposed conditions, such as radiation, is one such factor. If radiation does produce any effects they will probably be most apparent on the engineered and natural components of the disposal system in and near the waste repository. Thus, the components most likely to be affected would be the canisters, buffer, backfill and sealant. The wallrock adjacent to the repository and the groundwater anticipated to eventually enter the repository may also be affected.

2) Objectives:

To evaluate the response to radiation of the near-field components of a deep disposal system in plutonic rock on the Canadian Shield.

3) Range, extent and bounds of the work (scope):

The information from this study is to come from published and unpublished reports, notes, and personal communications pertaining to field, laboratory and theoretical studies that have been undertaken to investigate and evaluate the effects of radiation.

4) Tasks to be Performed:

a) Acquire the most up-to-date information on repository design, including the design of engineered components, for the Canadian Nuclear Fuel Waste Management Program.

b) Acquire information, from international as well as Canadian sources, which is relevant to the effects of irradiation on the materials and designed components of the repository currently being considered for the Canadian Nuclear Fuel Waste Management Program.

c) Acquire information on the type and intensity of the radiation fields produced by irradiated CANDU fuel.

d) Estimate the effects of α, β, γ and neutron irradiation on the engineered components of a Canadian deep geological repository according to their anticipated design, construction and emplacement. In so doing:

1. Consider irradiated CANDU fuel as the radiation source

2. Identify the effects of radiation on all materials being considered for buffer and backfill, canisters, waste-form matrices, overpack, etc. given the radiation fields likely to occur according to the latest Canadian design

3. Pay attention to the effects of temperature, dose and dose rate

4. Estimate the length of time required for irradiation to result in significant effects which may lead to fracturing, dissolution, etc.

DSS SERIAL:OSS84-00198 DSS FILE: 55SS.87055-4-4058

e) Obtain information on the physical and chemical properties of the common plutonic rocks (granite, granodiorite, diorite and gabbro), and vein-filling minerals, dike rocks and groundwater likely to be found in the aforementioned plutonic rocks on the Canadian Shield.

f) Estimate the effects of irradiation on the items identified in Task e). Pay particular attention to the possibility of changing the oxidation potential of the groundwater.

g) Write a report in which all information and impressions, inferences and conclusions which arise from tasks a) to f) are described in detail and thoroughly documented. The impressions, inferences and conclusions should be those arrived at by the contractor as well as those garnered from the literature.

5) Deliverables:

a) Progress or milestone reports

i)	frequency:	to accompany milestone claims
ii)	no. of copies:	3
iii)	contents instructions:	An indication of progress to date and future scheduling

b) Draft final report(s): (note iterations of the draft final report will be submitted as required)

i)	delivery date:	July 19, 1985
ii)	no. of copies:	3
iii)	bilingual requirements:	Abstract in French and English
iv)	format instructions:	The format is to be compatible with AECB published reports. A style guide will be provided by the AECB.
v)	contents instructions:	The final report must contain a disclaimer (to be supplied by the AECB). The final report must bear AECB research report covers and an AECB code number, both of which will be supplied by the AECB.

c) Final report:

i)	delivery date:	August 30, 1985
ii)	no. of copies:	one unbound, unpunched reproducible master and one copy thereof
iii)	bilingual requirements:	See 5 b) above
iv)	format instructions:	See 5 b) above
v)	contents instructions:	See 5 b), (v) above

APPENDIX B

PHYSICAL PROPERTIES OF GRANITIC ROCKS

PHYSICAL PROPERTIES OF GRANITIC ROCKS

APPENDIX B

ROCK TYPE	DENSITY (lbs/ft^3)	UNAXIAL COMPRESSIV STRENGTH (10^3 PSI)	TRIAXIAL COMPRESSI STRENGTH (10^3 PSI)	YOUNG'S MODULUS (10^6 PSI)	POISSON'S RATIO	SHEAR MODULUS (10^6 PSI)	V_p COMPRESSIONAL VELOCITY (10^3 ft/sec)	V_s SHEAR WAVE VELOCITY (10^3 ft/sec)	COEFFICIENT OF THERMAL EXPANSION ($10^{-6}{}^oF^{-1}$)	THERMAL CONDUCTIVITY (BTU/hr-ft^{o}F) X 1	REFERENCE
Stripa Granite Sweden	162.2	30.108	44.741	10.06	0.21	4.16*	17.089 17.934*	10.866*	____	0.77	
Quartz Monzonite California	164.7	____	____	____	____	____	____	11.906	____	1.76	
Schus Granite	162.2	22.769	____	7.73	0.20	3.22*	15.619*	9.564*	____	____	
Silver Flume Granite, Colorado	____	____	3.290 @ 150°C	____	____	____	____	____	____	____	
St. Cloud Granodiorite, Minn.	169.7	40.900	8.220 @ 150°C	10.3	0.25	4.12*	18.318*	10.576*	____	____	
Monzonite Colorado	____	____	6.400 @ 150°C	____	____	____	____	____	____	____	
Obsidian (glass) Modoc, California	152.6	____	____	9.51	0.08	4.40*	17.065*	11.530*	____	____	
Tonalite Bonsal, California	170.98	____	____	____	____	____	20.762	____	____	1.52	
Diorite Mineville, N.Y.	188.0	____	____	10.29	____	____	____	____	____	____	
Quartz Diorite Dedham, Mass.	186.9	____	____	____	____	____	21.189	12.103	____	____	
Quartz Diorite Amchitka Island, Alaska	169.1	33.280	____	7.15	0.28	2.79	16.603	9.507	____	____	

ROCK TYPE	DENSITY (lbs/ft^3)	UNAXIAL COMPRESSIVE STRENGTH (10^3 PSI)	TRIAXIAL COMPRESSIVE STRENGTH (10^3 PSI)	YOUNG'S MODULUS (10^6 PSI)	POISSON'S RATIO	SHEAR MODULUS (10^6 PSI)	V_P COMPRESSIONAL VELOCITY (10^3 ft/sec)	V_S SHEAR WAVE VELOCITY (10^3 ft/sec)	COEFFICIENT OF THERMAL EXPANSION (10^{-6}°F^{-1})	THERMAL CONDUCTIVITY (BTU/hr-ft°F) X 1	REFERENCE
ALFALIC (FOID) ROCKS											
Shonkinite Lyon Mountain, N.Y.	209.0	———	———	5.08	0.27**	2.0*	11.829*	6.640*	———	———	
Nepheline Syenite Montreal, Quebec	206.0	———	———	9.12	0.26	3.62*	15.799*	8,997*	———	———	
Syenite Dresden, Germany	———	———	———	9.73	———	———	———	———	———	———	
Syenite Freital, Germany	———	———	———	9.83	———	———	———	———	———	———	
Syenite Riesa-Groba, Germany	———	———	———	12.52	———	———	———	———	———	———	
Syenite #1 Ontario, Canada	174.1	———	———	———	———	———	———	———	———	1.29	
Syenite Porphyry Noranda Mines, Ont.	165.4	———	———	10.95	0.18	4.64*	18.202*	11.371	———	———	
Syenite Porphyry Kirkland Lake, Ont.	168.5	———	———	10.29	0.18	4.36*	17.481	10.920	———	———	
Mafic Syenite Kirkland Lake, Ont.	176.0	———	———	10.73	0.20	4.47*	17.669*	10.820*	———	———	
Vistor Syenite Colorado	———	———	5.320 @ 150°C	———	———	———	———	———	———	———	

ROCK TYPE	DENSITY (lbs/ft^3)	UNAXIAL COMPRESSIVE STRENGTH (10^3 PSI)	TRIAXIAL COMPRESSIVE STRENGTH (10^3 PSI)	YOUNG'S MODULUS (10^6 PSI)	POISSON'S RATIO	SHEAR MODULUS (10^6 PSI)	V_p COMPRESSIONAL VELOCITY (10^3 ft/sec)	V_s SHEAR WAVE VELOCITY (10^3 ft/sec)	COEFFICIENT OF THERMAL EXPANSION (10^{-6} °F^{-1})	THERMAL CONDUCTIVITY (BTU/hr-ft°F) X 1	REFERENCE
GRANITIC GNEISS											
Syenite Gneiss Mineville, N.Y.	175.3	____	____	7.97	0.25**	3.19*	15.854*	9.153*	____	____	____
Granitic Gneiss Star Lake, N.Y.	164.7	____	____	7.97	0.18**	3.38*	15.538*	9.719*	____	____	____
Diorite Gneiss Montezuma, Colordo	179.1	____	____	10.01	0.10	4.55*	16.230*	10.820*	____	____	____
Gneiss Hell Gate, N.Y.	165.4	____	____	____	____	____	20.106	____	____	____	____
Biotite Granite Peterhead, Scotland	163.0**	____	____	8.28	0.211	3.42*	16.145*	0.772*	____	____	____
Biotite Granite Lily Lake, N.B.	163**	____	____	8.17	0.198	3.41*	15.902*	9.758*	____	____	____
Quart monzonite Westerly, R.I.	163.4	____	____	7.38	0.220	3.02*	15.321*	9.130*	____	____	____
Biotite Granite Savenoe, Italy	165.0**	____	____	6.83	0.253	2.73*	15.172*	8.724*	____	____	____
Coarse Gray Granite; Quincy Mass. I	166.0	____	____	6.73	0.215	2.77*	14.553*	8.769*	____	____	____
Biotite-Muscovite Granite; Stanstead Quebec	165.0	____	____	5.69	0.259	2.26*	13.930*	7.945*	____	____	____
Granite Jancwitz, Germany	____	____	____	6.02	____	____	____	____	____	____	____

ROCK TYPE	DENSITY (lbs/ft^3)	UNAXIAL COMPRESSIVE STRENGTH (10^3 PSI)	TRIAXIAL COMPRESSIV STRENGTH (10^3 PSI)	YOUNG'S MODULUS (10^6 PSI)	POISSON'S RATIO	SHEAR MODULUS (10^6 PSI)	V_p COMPRESSIONAL VELOCITY (10^3 ft/sec)	V_s SHEAR WAVE VELOCITY (10^3 ft/sec)	COEFFICIENT OF THERMAL EXPANSION ($10^{-6}{}^{o}F^{-1}$)	THERMAL CONDUCTIVITY (BTU/hr-ft^{o}F) X 1	REFERENCE
Granite Dresden, Germany	———	———	———	6.31	———	———	———	———	———	———	
Granite Rock Port, Mass.	165.4	———	———	5.87	0.25**	2.48	20.270	11.611	———	1.96	
Quartz Monzonite Westerly, Mass.	165.4	———	———	7.38	0.22	3.02#	15.321#	9.180#	———	———	
Granite Westerly, R.I.	165.4	———	20,800 @ 24°C	5.79	0.065	2.72#	19.155 12.758#	11.021 8.702#	———	1.38	
Iron Granite	149.6	29.320	———	7.64	0.25	3.06#	16.805#	9.702#	———	———	
Granite, Fine Grain; Texas	164.5	———	———	11.32	0.312	4.31#	21.030#	10.993#	———	———	
Gray Granite Texas	162.5	———	———	12.12	0.24	4.89#	20.108#	11.761#	———	———	
Raymond Granite	165.0	26.084	———	5.33	0.25	2.13#	13.365#	7.716#	———	———	
Granite ConEdison, New York	166.6	33.282	———	9.12	0.192	3.83#	16.641#	10.295#	———	———	
Sherman Granite Tie Siding, Wyoming	169.4	———	———	———	———	———	———	———	———	———	
Granite Arbuckle Mountains	165.4	———	———	6.59	0.18	2.79#	14.119#	8.820#	———	———	
Barre Granite Vermont Perpendicular to Foliation	166.0	25.390	6.080 @ 24°C	4.41	-0.04	2.33#	11.063#	7.762#	0.22	1.56	

ROCK TYPE	DENSITY (lbs/ft^3)	UNAXIAL COMPRESSIVE STRENGTH (10^3 PSI)	TRIAXIAL COMPRESSIV STRENGTH (10^3 PSI)	YOUNG'S MODULUS (10^6 PSI)	POISSON'S RATIO	SHEAR MODULUS (10^6 PSI)	V_P COMPRESSIONAL VELOCITY (10^3 ft/sec)	V_S SHEAR WAVE VELOCITY (10^3 ft/sec)	COEFFICIENT OF THERMAL EXPANSION ($10^{-6}{}^oF^{-1}$)	THERMAL CONDUCTIVITY (BTU/hr-ft^{o}F) X 1	REFERENCE
Parallel to Foliation	166.0	___	___	5.18	0.11	2.33*	12.158*	8.048*	___	___	
Stone Mountain Granite, Georgia	164.7	___	___	8.95	0.16	3.79*	19.483	11.578	___	___	
Granodiorite Westoc, Mass.	164.1	___	___	8.70	0.187	3.66*	16.489*	10.300*	___	___	
Coarse Granite Big Thompson, Co.	164.1	10.460	___	3.9	0.12	1.74*	16.349*	10.144*	___	___	
Pegmatite Granite Big Thompson, Co.	163.5	8.440	___	3.0	0.11	1.35*	10.640*	6.992*	___	___	
Biotite Gneiss Fordham, N.Y.	___	___	7.650 e	___	___	___	9.323*	6.171*	___	___	
Biotite Gneiss St. Lawrence, N.Y.	___	___	5.890 e	___	___	___	___	___	___	___	
Diana Gneiss New York	___	___	6.320 e	___	___	___	___	___	___	___	
Magmatite New York	___	___	7.250 e	___	___	___	___	___	___	___	
PLAGIOCLASE ROCKS											
Albitite Sylmar, Pa.	162.9	___	___	10.01	0.29	3.88*	21.714	11.709	___	1.17	
Anorthosite Quebec	168.5	___	___	___	___	___	19.263*	10.476*	___	___	1.01

ROCK TYPE	Anorthosite Montana	Anorthosite Marcy, N.Y.	Anorthosite Transvaal
DENSITY (lbs/ft^3)	171.0		171.0
UNAXIAL COMPRESSIVE STRENGTH (10^3 PSI)			
TRIAXIAL COMPRESSIV STRENGTH (10^3 PSI)		5.940 @	
YOUNG'S MODULUS (10^6 PSI)			
POISSON'S RATIO			
SHEAR MODULUS (10^6 PSI)			
V_P COMPRESSIONAL VELOCITY (10^3 ft/sec)	22.862		22.763
V_S SHEAR WAVE VELOCITY (10^3 ft/sec)	12.103		
COEFFICIENT OF THERMAL EXPANSION ($10^{-6\,o}F^{-1}$)			
THERMAL CONDUCTIVITY (BTU/hr-ft^{o}F) X 1	0.98		1.08
REFERENCE			

APPENDIX C

GLOSSARY OF GEOLOGICAL TERMS

APPENDIX C

Glossary of Geological Terms

C.1 General Terms

Alteration,	n., (of mineral) the result of action of groundwater, with or without elevated temperature, replacing a mineral with the products of a chemical reaction, usually incongruent dissolution
Assemblage,	n., a group of minerals that characteristically occur together
Atterberg limits,	n.pl., the moisture contents above which a soil is liquid and below which it is not plastic
Aureole,	n., the portion of pre-existing rock around a pluton that is changed by the high temperatures due to the intruding magma (showing contact metamorphism)
Batholith,	n., a very large pluton
Calcic,	a., (of a mineral) containing much calcium
Deuteric,	a., characteristic of the second phase of cooling of a pluton
Diagenetic,	a., relating to diagenesis, the process by which sediments are consolidated into rock. (Characteristically by moderate heat, $\leq 300^{\circ}C$, and pressure)
Dyke,	n., a later rock that has intruded into a fissure in pre-existing rock
Essential,	a., (of a mineral) always present in at least moderate proportion in a particular rock type
Fabric,	n., (of jointing) the pattern of subparallel joints that show the direction of the principal stress that caused the rock to fracture
Fault,	n., a fracture that has slipped, grinding or polishing the fractured surface. Faults are classified according to the direction of slippage
Felsic,	a., (of rock) high in feldspars and silica; acidic (antonym; mafic)

Fissure, n., fracture (fault or joint) that has opened by movement or weathering, to more than microscopic width

Flowbanding, n., a pattern of parallel bands in an igneous intrusion near a boundary, showing that laminar flow has occurred

Fracture, n., (of a rock) a surface along which a rock has broken with (fault) or without (joint) slippage

Geothermal, a., related to the high temperatures of the Earth's interior. G. gradient n., the increase of temperature with depth

Groundwater, n., the water saturating the soil and rock below the water table

Hydrothermal, a., resulting from the presence of hot aqueous solutions under pressure

Incongruent dissolution, n. phr., the reaction of a solid with a liquid to give a solution and leave a solid residue of different composition from the original solid. (A principal mode of alteration of minerals)

Joint, n., a fracture in rock that has not slipped

Kinematic, a., related to movement, usually the emplacement of a pluton. Syn-,pre-, post-kinematic, during, before or after emplacement

Lineament, n., a linear feature seen on a surface, from which is inferred a planar structure in the body

Mafic, a., characterized by much magnesium and iron; basic (antonym: felsic)

Magma, n., rock in a molten or highly plastic state underground

Massif, n., core of a mountainous region made up of one or more batholiths

Metamict, a., (of mineral) altered without change of composition, usually to amorphous state

Metamorphic,	a., relating to the process (-ism) in which rocks are subjected to great heat (short of melting) and high pressure. Grades of metamorphism can be recognized by the presence of certain minerals. Regional metamorphism is recognized by large bodies of rock with evidences of plastic deformation. See also aureole
Orogenic,	a., related to the processes of mountain-building
Outcrop,	n., the portion of a rock mass visible at the surface
Plug,	n., a small pluton
Pluton,	n., a mass of igneous rock that has apparently intruded into overlying rock as magma from below
Porphyry,	n., rock having a texture of large crystals embedded in a microcrystalline ground-mass; a dyke-filling rock of syenite composition and porphyritic texture
Precambrian,	a., and n., (formed during) the period of Earth's history before about 600 Ma ago
Roll-front deposit,	n. phr., an ore deposit transported by moving groundwater to a region where it is precipitated by a change of conditions, chiefly to a more reducing Eh level
Shear zone,	n. phr., a layer or rocks between two bodies that have moved laterally, in which are multiple faults and plastically deformed rock
Slickensides,	n., the polished surfaces at a fault where the two bodies of rock have slipped
Sodic,	a., (of a mineral) high in sodium
Tectonic,	a., related to large movements of portions of the Earth's crust relative to one another
Vein,	n., fracture filled with material, like a dyke, but smaller and irregular, running in any direction

Weathering, n., the collection of processes whereby a rock is broken into fragments (physical weathering) by the action of windblown sand, wave action or frost, or dissolved, totally or incongruently (chemical weathering) by water, usually with the help of acidic dissolved substances, especially CO_2

C.2 Rocks

Andesite, a fine-grained, volcanic rock of intermediate composition (moderate SiO_2 content)

Anorthosite, an igneous or metamorphic rock containing large amounts of calcic plagioclase

Aplite, fine-grained light-coloured rock found in small dykes and veins around granites

Argillite, a sedimentary rock of ultrafine grain size, formed from clays

Arkose, a sedimentary rock containing sand-sized grains of feldspar and quartz

Bauxite, the chief aluminium ore, containing gibbsite and related minerals. Final alteration product of feldspars, especially in the tropics

Diorite, a coarse-grained, plutonic rock, of intermediate composition (moderate SiO_2 content)

Gabbro, a coarse-grained, mafic (basic) plutonic rock with low SiO_2 content and little or no free quartz

Gneiss, a banded rock of granitoid composition, indicative of rather high-grade metamorphism

Granite, the type of coarse-grained, plutonic rock of highest SiO_2 content, containing substantial free quartz, potassium and sodium feldspars, and usually accessory mica and small amounts of iron minerals. "Granitoid" includes all the plutonic rocks with notable free quartz

Limestone, sedimentary rock composed largely of calcite. Some are abundant in fossils

Monzonite,	an igneous rock of moderate silica content
Pegmatite,	a very coarse-grained vein-and dyke-filling rock, formed from late-stage magma. Single crystals over a metre in length have been found in large pegmatite dykes
Rhyolite,	the fine-grained, volcanic equivalent of granite
Sandstone,	sedimentary rock, the sand-sized grains of which are chiefly quartz, usually cemented together with calcite or haematite
Shale,	sedimentary rock with silt-sized grains, intermediate between sandstone and argillite
Silt,	water-borne sediment, between clay and sand in grain size
Syenite,	coarse-grained, plutonic rock containing feldspathoids and no free quartz
Till,	the very heterogeneous deposits, containing all sizes of material from clay to boulders, left by retreating ice

C.3 Minerals

Adularia,	see Feldspar
Albite,	see Feldspar
Amphibolite,	a class of silicate minerals of chain structure, including hornblende
Anhydrite,	$CaSO_4$ (without water of crystallization)
Attapulgite,	see clay
Bentonite,	a clay-like mixture of colloidal silica, montmorillonite and beidellite, derived from wind-blown deposits of volcanic ash in seawater, capable of absorbing large quantities of water
Biotite,	a variety of mica, usually dark in colour
Calcite,	the common variety of $CaCO_3$

Chlorite, a sheet silicate mineral, resembling mica

Clay, a class of minerals, mostly of sheet silicate type, usually occurring in mixtures or even interlayered crystals. Always microcrystalline, with platy habit. Clay minerals include the following subgroups:

kaolinites - kaolinite $Al_2Si_2O_5(OH)_4$
halloysite $Al_2Si_2O_5(OH_4 \cdot 2H_2O$

smectites - montmorillonite (complex formula)

illites - hydromuscovite (compex)
beidellite (complex)

palygorskites - attapulgite $Al_2Si_5O_{13} \cdot 6H_2O$
(not a sheet silicate)

Clinozoisite, $Ca_2Al_2(SiO_4)_3OH$. With substitution of Fe for Al, c. grades over into epidote

Epidote, an orthosilicate mineral (i.e., characterized by the presence of the SiO_4 group) common and widespread in metamorphic and hydrothermally altered rocks. $Ca_2(Al, Fe^{3+})_3(SiO_4)_3OH$

Feldspar, a class of minerals with a three-dimensional alumino-silicate framework, characterized by the group $AlSi_3O_8^-$ or $Al_2Si_2O_8^{2-}$ or mixtures of the two. They include:
- adularia, $KAlSi_3O_8$
- orthoclase and microline $(K,Na)AlSi_3O_8$
and the plagioclase series, ranging in composition from albite $NaAlSi_3O_8$ to anorthite $CaAl_2Si_2O_8$, of which oligoclase and labradorite are intermediate members

Feldspathoid, a group of minerals resembling the feldspars, but containing less silica, found in a number of igneous rocks

Ferromagnesian, (of a mineral) containing iron and magnesium as the main cations

Fluorite, CaF_2

Gibbsite, $Al(OH)_3$, one of the principal components of bauxite

Geothite, see iron oxides

Gypsum,	$CaSO_4 \cdot 2H_2O$ (Cf. anhydrite)
Haematite,	(=hematite) see iron oxides
Illite,	see clays
Ilmenite,	$FeTiO_3$, a widespread accessory mineral of mafic and ultramafic igneous rocks
Iron Oxides,	include haematite Fe_2O_3, goethite $Fe_2O_3.H_2O$, limonite $Fe_2O_3.xH_2O$ (indefinite), magnetite Fe_3O_4, maghemite (intermediate between Fe_3O_4 and Fe_2O_3)
Kaolinite,	see clays
Labradorite,	see feldspars
Limonite,	see iron oxides
Maghemite,	see iron oxides
Magnetite,	see iron oxides
Mica,	a class of layer silicate minerals easily cleaved into thin, flexible sheets
Microcline,	see feldspars
Mullite,	a rare aluminum silicate, Al_4SiO_8 to $Al_6Si_2O_{13}$
Muscovite,	a variety of mica, usually light-coloured
Oligoclase,	see feldspars
Olivine,	a class of ferromagnesian silicates $(Fe,Mg)_2SiO_4$, found in gabbro and other mafic and ultramafic igneous rocks
Orthoclase,	see feldspars
Plagioclase,	see feldspars
Pollucite,	a rather rare cesium bearing mineral, $Cs_3Al_4Si_9O_{26}.H_2O$ found in certain granites and pegmatites
Prehnite,	a "brittle mica"
Pyrite,	FeS_2, "Fool's gold"
Pyroxene,	a class of ferromagnesian chain silicates, $(Fe,Mg)SiO_3$, found in basic (mafic) to intermediate igneous rocks

Quartz,	a crystalline variety of silica, SiO_2
Rutile,	one form of TiO_2
Sericite,	secondary muscovite, resulting from alteration of orthoclase or diagenesis of clays
Silica,	a group of minerals of composition SiO_2 (some may be hydrated). Quartz is the most familiar example
Smectite,	see clays
Sphene,	$CaTiSiO_5$, a widespread accessory mineral in igneous rocks
Titanite,	sphene
Uraninite,	a uranium-bearing mineral of complex formula ($UO_2.xUO_3$ + minor constituents), an important uranium ore
Vermiculite,	a hydrated alteration product of biotite or other micas
Zeolite,	a class of framework silicate minerals characterized by channels which are occupied by readily-exchangeable cations
Zircon,	$ZrSiO_4$, a common accessory mineral in granites. Interesting because it is subject to metamictization, but it is also found in a metamict state in nature, apparently not from radiation but from hydrothermal alteration